Regulation of the transition between motile planktonic and sessile biofilm-associated lifestyles in *Pseudomonas aeruginosa*

Von der Fakultät für Lebenswissenschaften

der Technischen Universität Carolo-Wilhelmina

zu Braunschweig

zur Erlangung des Grades einer

Doktorin der Naturwissenschaften

(Dr. rer. nat.)

genehmigte

D i s s e r t a t i o n

von Juliane Schmidt
aus Zeitz

1. Referentin: Professor Dr. Katharina Riedel
2. Referentin: Professor Dr. Susanne Häußler
eingereicht am: 28.04.2011
mündliche Prüfung (Disputation) am: 22.06.2011

Druckjahr 2011

Vorveröffentlichungen der Dissertation

Teilergebnisse aus dieser Arbeit wurden mit Genehmigung der Fakultät für Lebenswissenschaften, vertreten durch die Mentorin der Arbeit, in folgenden Beiträgen vorab veröffentlicht:

Publikationen

Juliane Schmidt, Mathias Müsken, Tanja Becker, Zofia Magnowska, Daniela Bertinetti, Stefan Möller, Bastian Zimmermann, Friedrich W. Herberg, Lothar Jänsch, Susanne Häussler (2011). The *Pseudomonas aeruginosa* chemotaxis methyltransferase CheR1 impacts on bacterial surface sampling. *PloS ONE 6(3):e18184*.

Juliane Schmidt, Daniela Bertinetti, Stefan Möller, Frank Schwede, Michael Morr, Josef Wissing, Lena Radamm, Bastian Zimmermann, Hans-Gottfried Genieser, Lothar Jänsch, Friedrich W. Herberg, Susanne Häussler (submitted). A chemical proteomics approach to identify c-di-GMP binding proteins in *Pseudomonas aeruginosa*. Eingereicht bei *Analytical Biochemistry*.

Vanessa Jensen, Juliane Schmidt, Sebastian Bruchmann, Andreas Dötsch, Robert Geffers, Susanne Häussler. A ChIP-chip approach uncovers co-operative target binding of *Pseudomonas aeruginosa* RpoS and the quorum sensing regulators. Eingereicht bei *PLoS Pathogens* am 06.03.2009, abgelehnt am 17.04.2009. Wiedereinreichung nach abschließenden Experimenten geplant.

Tagungsbeiträge

Juliane Schmidt, Daniela Bertinetti, Tanja Becker, Michael Morr, Frank Schwede, Josef Wissing, Zofia Magnowska, Lothar Jänsch, Susanne Häussler. Signal transduction of c-di-GMP in *Pseudomonas aeruginosa*. *Vortrag*. Dritte gemeinsame Tagung der Deutschen Gesellschaft für Hygiene und Mikrobiologie und der Vereinigung für Allgemeine und Angewandte Mikrobiologie, Hannover, 2010.

Juliane Schmidt, Daniela Bertinetti, Tanja Becker, Michael Morr, Frank Schwede, Josef Wissing, Zofia Magnowska, Lothar Jänsch, Susanne Häussler. Signal transduction of c-di-GMP in *Pseudomonas aeruginosa*. *Vortrag*. 5th ASM Conference on Biofilms, Cancun, 2009.

Juliane Schmidt, Daniela Bertinetti, Michael Morr, Frank Schwede, Josef Wissing, Lothar Jänsch, Susanne Häussler. Isolation and identification of c-di-GMP binding proteins in *Pseudomonas aeruginosa*. *Poster*. 61. Jahrestagung der Deutschen Gesellschaft für Hygiene und Mikrobiologie, Göttingen, 2009.

Vanessa Jensen, Juliane Schmidt, Sebastian Bruchmann, Andreas Dötsch, Robert Geffers, Susanne Häussler. A ChIP-chip approach uncovers co-operative target binding of *Pseudomonas aeruginosa* RpoS and the quorum sensing regulators LasR and RhlR. *Vortrag*. 61. Jahrestagung der Deutschen Gesellschaft für Hygiene und Mikrobiologie, Göttingen, 2009.

Juliane Schmidt, Daniela Bertinetti, Michael Morr, Frank Schwede, Josef Wissing, Lothar Jänsch, Susanne Häussler. Isolation and identification of c-di-GMP binding proteins in *Pseudomonas aeruginosa*. *Vortrag*. First European Congress on Microbial Biofilms, Rom, 2009.

Juliane Schmidt, Daniela Bertinetti, Michael Morr, Frank Schwede, Josef Wissing, Lothar Jänsch, Susanne Häussler. Isolation and identification of c-di-GMP binding proteins in *Pseudomonas aeruginosa*. *Poster*. XII. International Conference on *Pseudomonas*, Hannover, 2009.

Susanne Häussler, Vanessa Jensen, Juliane Schmidt, Sebastian Bruchmann, Andreas Dötsch, Giuliano Degrassi, Robert Geffers, Vittorio Venturi. A ChIP-chip approach uncovers co-operative target binding of *Pseudomonas aeruginosa* RpoS and the quorum sensing regulators LasR and RhlR. *Poster*. XII. International Conference on *Pseudomonas*, Hannover, 2009.

Juliane Schmidt, Daniela Moll, Michael Morr, Frank Schwede, Josef Wissing, Lothar Jänsch, Susanne Häussler. Isolation and identification of c-di-GMP binding proteins in *Pseudomonas aeruginosa*. *Poster*. 60. Jahrestagung der Deutschen Gesellschaft für Hygiene und Mikrobiologie, Dresden, 2008.

Abstract

Regulation of the transition between motile planktonic and sessile biofilm-associated lifestyles in *Pseudomonas aeruginosa*

Many bacteria are able to adopt two fundamentally different lifestyles. While the planktonic mode of growth enables dissemination and exploration of novel niches, growing within multicellular, matrix-encased biofilms offers protection and survival in unfavorable environments.

The aim of this thesis was to elucidate how the opportunistic pathogen *Pseudomonas aeruginosa* integrates and translates extra- and intracellular signals to regulate the transition between motile and sessile lifestyles in order to give an appropriate response to a changing environment. In this context, we characterized the chemotaxis methyltransferase CheR1 and demonstrated that its activity is not only essential for flagella-mediated chemotaxis but that it is also important for the formation and maintenance of biofilm structures. Another aim of this thesis was the identification of proteins that bind the small di-nucleotide c-di-GMP – an important bacterial second messenger which governs the switch between motility and sessility. We used immobilized c-di-GMP to perform affinity pull down experiments in which isolated proteins were identified by high-resolution mass spectrometry. This chemical proteomics approach proved to be sufficient for the isolation of c-di-GMP binding proteins harboring known but also novel c-di-GMP binding motifs in the model organism *P. aeruginosa*. To understand how environmental cues can influence bacterial behavior at the level of transcription, we identified the global regulon of the stationary phase sigma factor RpoS by performing chromatin immunoprecipitation experiments in combination with DNA-microarray analysis. Our results provide evidence that RpoS controls transcription of genes directly linked to biofilm formation but also of genes encoding components of other regulatory systems that trigger the formation of biofilms. Overall, this thesis contributes to our understanding of adaptive pathways leading to the development and maintenance of bacterial biofilms.

Zusammenfassung

Regulierung des Übergangs zwischen motilen planktonischen und sessilen Biofilm-assoziierten Lebensweisen in *Pseudomonas aeruginosa*

Viele Bakterien können zwei völlig verschiedene Lebensweisen annehmen. Während planktonisches Wachstum die Ausbreitung in neue Nischen ermöglicht, bietet Wachstum in multizellulären, matrixumhüllten Biofilmen Überlebensvorteile in widrigen Umgebungen.
Ziel dieser Arbeit war es zu erforschen, wie der opportunistische Krankheitserreger *Pseudomonas aeruginosa* extra- und intrazelluläre Signale übersetzt, um den Übergang zwischen motilen und sessilen Lebensstilen zu regulieren und besser auf eine sich verändernde Umgebung zu reagieren. In diesem Zusammenhang haben wir die Chemotaxismethyltransferase CheR1 charakterisiert und konnten zeigen, dass ihre Aktivität nicht nur wichtig für flagellenvermittelte Chemotaxis ist, sondern auch für die Ausbildung und Strukturierung von Biofilmen. Ein weiteres Ziel dieser Arbeit war es, Proteine zu identifizieren, die c-di-GMP binden – einen wichtigen bakteriellen sekundären Botenstoff, der den Übergang zwischen Motilität und Sessilität steuert. Immobilisiertes c-di-GMP wurde als Affinitätsmatrix genutzt, um aus komplexen Proteingemischen c-di-GMP-Bindepartner zu isolieren. Die sich anschließende Massenspektrometrieanalyse zur Identifizierung der angereicherten Proteine ergab, dass nicht nur Proteine mit bereits bekannten sondern auch mit neuartigen c-di-GMP-Bindemotiven erfolgreich isoliert wurden. Mit dem Ziel zu verstehen, wie Umweltsignale bakterielles Verhalten auf der Ebene der Transkription beeinflussen, haben wir das globale Regulon des alternativen Sigmafaktors RpoS mit Hilfe von Immunopräzipitationsexperimenten in Verbindung mit DNA-Microarray-Analysen aufgeklärt. Unsere Ergebnisse zeigten, dass RpoS nicht nur die Transkription von Genen kontrolliert, die direkt mit der Bildung von Biofilmen zusammenhängen, sondern auch von Genen die Bestandteil anderer Biofilm-regulierender Systeme sind. Insgesamt trägt diese Arbeit zu unserem Verständnis bei, auf welchen Wegen Biofilme gebildet und erhalten werden.

Dass ich erkenne, was die Welt
im Innersten zusammen hält.

- Faust -
(J. W. v. Goethe)

Table of Contents

List of Figures

List of Tables

Abbreviations

$A_{280\ nm}/A_{550\ nm}$	absorbance at 280 nm/550 nm
2'-AHC-c-di-GMP	2'-O-(6-aminohexylcarbamoyl)-cyclic dimeric guanosine monophosphate
AHT	anhydrotetracycline
ATP	adenosine triphosphate
B. subtilis	*Bacillus subtilis*
BSA	bovine serum albumin
C. crescentus	*Caulobacter crescentus*
ChIP	chromatin immunoprecipitation
ChIP-chip	chromatin immunoprecipitation in conjunction with DNA microarray
CHO cells	Chinese hamster ovary cells
CLSM	confocal laser scanning microscopy
CV	crystal violet
cAMP	cyclic adenosine monophosphate
c-di-GMP	cyclic dimeric guanosine monophosphate
cGMP	cyclic guanosine monophosphate
dATP	deoxyadenosine triphosphate
dCTP	deoxycytidine triphosphate
DGC	diguanylate cyclase
dGTP	deoxyguanosine triphosphate
dH_2O	deionized water
DNA	deoxyribonucleic acid
dNTP	deoxynucleotide triphosphate
ds	double-stranded DNA
DTT	dithiothreitol
dTTP	deoxythymidine triphosphate
dUTP	deoxyuridine triphosphate
E. coli	*Escherichia coli*
EC_{50}	half maximal effective concentration
EDC	*N*-ethyl-*N'*-(3-dimethylaminopropyl)carbodiimide
EDTA	ethylenediaminetetraacetic acid
EMSA	electrophoretic mobility shift assay
EPS	extracellular polymeric substances
et al.	et alii
FAD	flavin adenine dinucleotide
GFP	green fluorescent protein
GMP	guanosine monophosphate
GTP	guanosine triphosphate
HEPES	4-(2-hydroxyethyl)-1-piperazineethanesulfonic acid
HPLC	high-performance liquid chromatography
igr	intergenic region
IP	immunoprecipitation
IPTG	isopropyl 1-thio-β-D-galactopyranoside
K_D	dissociation constant
LB	Luria-Bertani
LC-MS/MS	liquid chromatography - tandem mass spectrometry
MCP	methyl-accepting chemotaxis protein
MCS	multiple cloning site

MS	mass spectrometry
MWCO	molecular weight cut off
NAD	nicotinamide adenine dinucleotide
NB	Nutrient broth
n.d.	not determined
NHS	*N*-hydroxysuccinimide
Ni-NTA	nickel-nitrilotriacetic acid
nl	non-labeled
NMR	nuclear magnetic resonance
OD_{600}	optical density at 600 nm
ON	overnight
ORF	open reading frame
P. aeruginosa	*Pseudomonas aeruginosa*
P. fluorescens	*Pseudomonas fluorescens*
PAGE	polyacrylamide gel electrophoresis
PBS	phosphate buffered saline
PCR	polymerase chain reaction
PDE	phosphodiesterase
pGpG	linear dimeric guanosine monophosphate
PMSF	phenylmethylsulfonyl fluoride
poly(dIdC)	poly-(deoxyinosinic-deoxycytidylic) acid
psi	pound-force per square inch
REC	response regulator receiver domain
RNA	ribonucleic acid
RU	resonance unit
***S.* Typhimurium**	*Salmonella enterica* serovar Typhimurium
SAM	*S*-adenosylmethionine
SDS	sodium dodecyl sulfate
SOE	gene splicing by overlap extension
SPR	surface plasmon resonance
ss for	single-stranded forward (template) DNA
ss rev	single-stranded reverse (non-template) DNA
TM	transmembrane
TOF	time-of-flight
Tris	tris(hydroxymethyl)aminomethane
UV	ultraviolet
V. cholerae	*Vibrio cholerae*
v/v	volume per volume
w/v	weight per volume
X. axonopodis* pv. *citri	*Xanthomonas axonopodis* pathovar *citri*
X. campestris* pv. *campestris	*Xanthomonas campestris* pathovar *campestris*

Three letter and single letter abbreviation for the amino acids

Ala	A	alanine
Arg	R	arginine
Asn	N	asparagine
Asp	D	aspartic acid (aspartate)
Cys	C	cysteine
Gln	Q	glutamine
Glu	E	glutamic acid (glutamate)
Gly	G	glycine
His	H	histidine
Ile	I	isoleucine
Leu	L	leucine
Lys	K	lysine
Met	M	methionine
Phe	F	phenylalanine
Pro	P	proline
Ser	S	serine
Thr	T	threonine
Trp	W	tryptophan
Tyr	Y	tyrosine
Val	V	valine
-	X	any amino acid

1 Introduction

1.1 The bacterial way of life

More than 300 years ago, the fabrication and use of microscopes enabled the discovery of the microbial universe. One of the major discoverers was the Dutch draper Antoni van Leeuwenhoek who observed swimming bacteria – which he called animalcules – by the use of a simple single-lens microscope [1]. In the following centuries, extensive studies were carried out with regards to how bacteria move and how they are able to respond to chemical stimuli in their environment (reviewed by H. C. Berg, 1975 [2]). However, in the second half of the 20th century, it became evident that bacteria can adopt a lifestyle that is profoundly distinct from the planktonic, free-living lifestyle studied so far: that is growth within structured, surface-associated bacterial communities commonly known as biofilms. In fact, biofilm communities represent not only the predominant mode of bacterial growth in the environment [3], but largely impact industry and human health as well [4, 5]. It has been estimated that up to 80% of the bacterial infections in industrialized countries are biofilm-associated infections, refractory to antimicrobial therapy [6]. In order to develop novel strategies for biofilm control, it is critical to understand the adaptive pathways leading to the development and maintenance of bacterial biofilms.

1.2 *Pseudomonas aeruginosa* as a model organism

The gram-negative γ-proteobacterium *Pseudomonas aeruginosa* has become one of the most-studied model organisms in biofilm research. This ubiquitous environmental bacterium is able to thrive in a wide variety of natural habitats. Moreover, it is an opportunistic human pathogen and a significant source of life-threatening nosocomial infections [7]. *P. aeruginosa* can cause severe acute infections which are characterized by the use of a large arsenal of virulence factors [8]. On the other hand, *P. aeruginosa* is able to produce chronic infections, in which bacteria adapt to their environment, survive within biofilms, and persist in their host for years [9, 10]. The remarkable adaptability of *P. aeruginosa* is enabled by its large genetic diversity. Analysis of the complete genome sequence of the *P. aeruginosa* strain PA01 (6.3 million base pairs) revealed 5570 predicted open reading frames (ORFs) [11]. Approximately 10% of the identified genes are encoding for transcriptional regulators, sigma factors or two-component regulatory systems [11] allowing *P. aeruginosa* to respond to a wide range of environmental conditions.

1.3 Principles of motility and chemotaxis

P. aeruginosa is capable to explore its environment by three types of motility. Swimming in aqueous surroundings is enabled by the rotation of a single, polar flagellum. Twitching motility allows the translocation over wet surfaces in a flagellum-independent way by using polar type IV pili which extend, attach and retract [12, 13]. In addition, *P. aeruginosa* is capable of swarming, which is a rapid and coordinated group movement over semisolid surfaces and requires both, flagella and type IV pili [14, 15].

Motile bacteria can sense changes in the concentration of chemicals in their surroundings and are able to bias their movement towards a more favorable environment. This chemotactic response is achieved by modulating the frequency of changes in swimming direction. While peritrichously flagellated bacteria, such as *Escherichia coli* and *Salmonella enterica* serovar Typhimurium, move by “running” and active “tumbling” that reorients the cells, monotrichous bacteria exhibit a run/short back-up/run mode of swimming [2, 16, 17]. The two behaviors “run” and “tumble/back-up” are caused by the direction of flagellar rotation switching between clockwise (tumble/back-up) and counterclockwise (run) rotation.

1.3.1 The chemotaxis system of *E. coli*

The molecular mechanisms underlying bacterial chemotaxis have been studied most extensively in *E. coli* and *S.* Typhimurium [18, 19]. Chemotactic ligands are detected by cell surface chemoreceptors called methyl-accepting chemotaxis proteins (MCPs). Several homologous transmembrane receptors (MCPs) sense extracellular stimuli and produce signals that are transmitted to their cytoplasmic domains. This signal transduction impacts via the adaptor protein CheW on the associated CheA/CheY two-component system, in which CheA is the sensor kinase that phosphorylates the response regulator CheY. Activated CheY-P localizes to flagellar motor complexes and, upon interaction with the rotational switch protein FliM, causes a switch from counterclockwise rotation (run) to clockwise rotation (tumble) [20, 21]. The phosphorylation status of CheY is also controlled by the protein phosphatase CheZ, which enhances dephosphorylation of CheY-P. Upon binding of attractants, the kinase activity of CheA is reduced, which promotes the bacterial running mode, whereas the binding of repellents increases CheA activity - hence tumbling. The effect of ligand binding is counterbalanced by reversible MCP methylation, providing the ability to detect chemical changes over time. Thereby, the opposing activities of two specific enzymes, CheR, a methyltransferase, and CheB, a methylesterase, control the MCP methylation level. CheR

converts specific glutamic acid residues in the MCP cytoplasmic domain to glutamyl methyl esters, using *S*-adenosylmethionine (SAM) as the methyl donor [22]. CheB hydrolyses those methylated residues, releasing methanol and restoring glutamic acid [23]. CheR activity is unregulated, whereas CheB is another response regulator that becomes phosphorylated by CheA [24].

1.3.2 *P. aeruginosa* has multiple chemotaxis systems

Studies of chemotaxis and MCP methylation in other organisms have revealed both similarities and differences to the *E. coli*/*S.* Typhimurium chemotaxis pathway [25-30]. Whole genome sequencing has demonstrated that many bacteria possess multiple paralogs of chemotaxis (*che*) genes which are often organized into independent systems [31]. Sequence analysis of the *P. aeruginosa* PA01 genome revealed a very complex chemosensory system with more than 20 *che* genes in five distinct clusters and 26 *mcp*-like genes (Figure 1.1) [11].
Cluster I and V (Che1 system) and cluster II (Che2 system) have been implicated in flagella-mediated chemotaxis [32-35]. Each of those *che* gene products is homologous to an *E. coli* Che protein [33], with the exception of CheD (encoded in cluster II) and CheV (encoded in cluster V), that cannot be found in *E. coli* but e.g. in *Bacillus subtilis*. In this organism, CheD is a receptor deamidase that converts specific glutamines to glutamates, but also regulates the kinase activity of CheA [26]. The *B. subtilis* CheV protein is, like CheW, an adaptor protein that is additionally involved in the adaptation process [26].
The two remaining *P. aeruginosa che* clusters encode chemotaxis systems that are unrelated to flagellar motility. The Pil-Chp system (encoded by cluster IV) has been shown to regulate type IV pili biosynthesis and twitching motility [36-38], whereas the Wsp system (encoded by cluster III) is involved in biofilm formation [39, 40].
Among the 26 MCPs of *P. aeruginosa*, nine have been identified as MCPs for amino acids, inorganic phosphate, oxygen, ethylene and volatile chlorinated aliphatic hydrocarbons [41], whereas 3 MCPs were demonstrated to be involved in type IV pili production and function, [42] and in biofilm formation [39, 43].

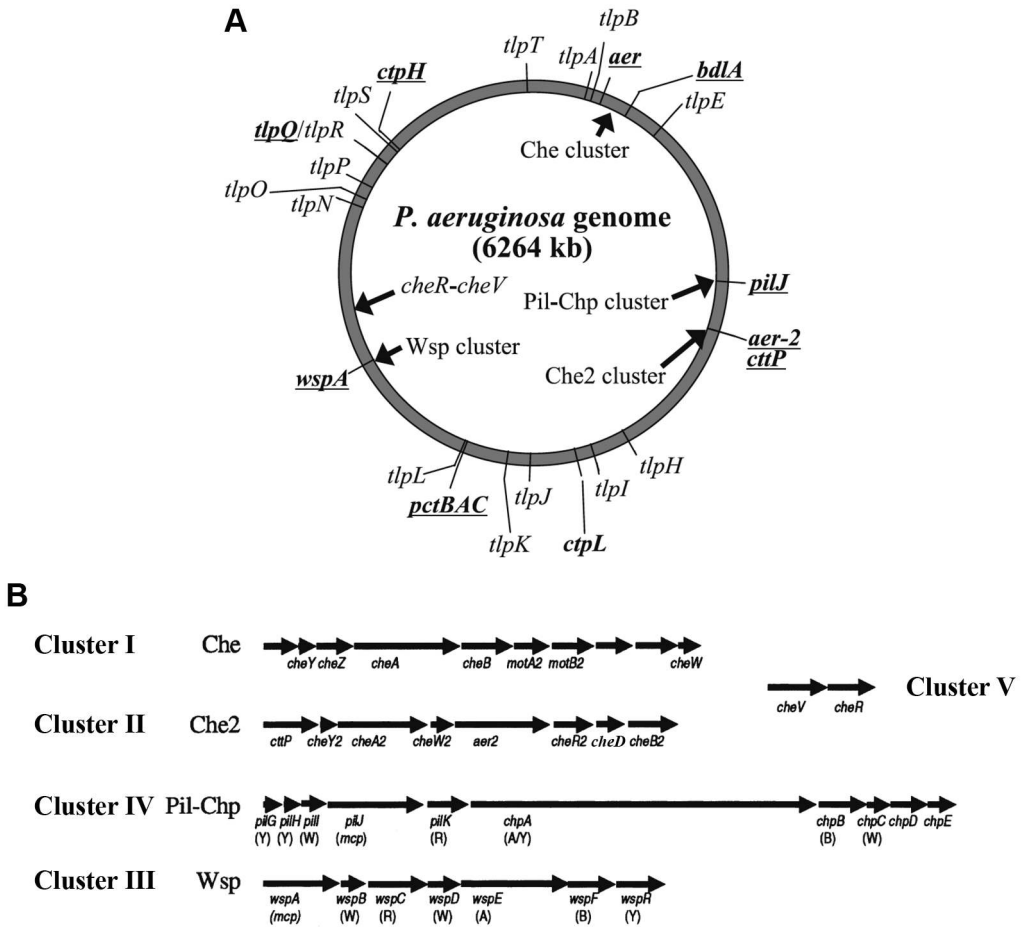

Figure 1.1. Overview of the complex chemotaxis systems of *P. aeruginosa*.
(A) Distribution of putative *mcp* genes (outside the circle) and *che* gene clusters (inside the circle) on the genome of *P. aeruginosa* PA01. The *mcp* genes which have been characterized are underlined. (B) Genetic organization of the five distinct Che clusters. A, B, R, W, and Y in parentheses denote homologs of *cheA*, *cheB*, *cheR*, *cheW* and *cheY*, respectively. Modified from Kato *et al.* [41].

1.4 Living within biofilms

In environments that provide a little moisture and some nutrients, *P. aeruginosa* readily adheres to available surfaces to form sessile, matrix-enclosed biofilm communities. The biofilm mode of growth offers a competitive advantage over free-swimming individual cells, as the bacteria are protected from environmental stress (e.g. UV radiation [44], heavy metal toxicity [45], dehydration [46]) and from biological and chemical antibacterial agents [4, 47]. One key feature of the biofilm community is the self-produced, heterogeneous matrix which facilitates adhesion to the surface, forms the scaffold for the three dimensional architecture of the biofilm and acts as a protective shield. It consists of extracellular polymeric substances (referred to as EPS) including polysaccharides, proteins, lipids and extracellular DNA [48]. The structure of mature biofilms is not only determined by the composition of the EPS matrix,

but also depends on hydrodynamic conditions, nutrient conditions and cell-to-cell communication (“quorum sensing”). The resulting biofilm architecture can be filamentous, or smooth and flat or highly structured with mushroom-like macrocolonies that are separated by open water channels [5, 48, 49].

The formation of complex biofilm structures is a sequential process and involves several stages [50]. In the beginning, individual cells reversibly attach to a surface, followed by robust adhesion. Then cells aggregate to form microcolonies and further mature into complex biofilm structures, in which bacteria adapt to the conditions in their particular niches. From the established biofilm, individual cells are released and return to the planktonic mode of growth so that new habitats can be colonized with new biofilms.

So far, research on global gene or protein biofilm expression patterns has not succeeded in the identification of a specific developmental biofilm program. New knowledge about mechanisms involved in biofilm formation has recently been obtained by the use of optical tools to monitor *in vitro* grown biofilms. From these studies, it has become evident that motility can have a profound impact on the colonization of surfaces [51-55]. However, the impact of chemotaxis on the formation of biofilms has been less intensively studied. While in *E. coli* chemotaxis seems to be dispensable for biofilm formation, there is evidence for the impact of chemotaxis on surface interactions and biofilm formation in other bacterial species [53, 56-58]. Given the different nature of the chemotactic system in the enteric bacteria and other environmental motile bacteria, it is not surprising that the role chemotaxis plays in biofilm development is quite distinct.

1.5 C-di-GMP: the lifestyle switch

The choice to settle down or move away is an important decision to be made by microorganisms, and requires the integration of many environmental cues into a sophisticated regulatory network. One key regulator for the switch between the motile planktonic and the sessile biofilm-associated lifestyle is the bacterial second messenger bis-(3'-5')-cyclic di-GMP (c-di-GMP) [59-61] (Figure 1.2). While low levels of this intracellular signaling molecule are known to promote motility, high c-di-GMP levels trigger the production of exopoly-saccharides and biofilm formation. The intracellular c-di-GMP level is thereby tightly controlled by the opposing activities of two classes of enzymes, diguanylate cyclases (DGCs) and phosphodiesterases (PDEs) [62-67]. DGCs contain a conserved GGDEF domain and convert two molecules of GTP into a single c-di-GMP molecule. A common feature of most

DGCs is an allosteric feedback inhibition, as binding of c-di-GMP to an I-site motif within the GGDEF domain inhibits enzymatic activity [68, 69]. The break down of c-di-GMP to pGpG or two molecules GMP is mediated by PDEs harboring an EAL or, less common, an HD-GYP domain.

In many cases, GGDEF and EAL/HD-GYP domains are fused to transmembrane or signal-sensing partner domains which enables post-translational regulation of the enzymatic activity by environmental or cellular cues [71, 72]. Common partner domains are the small molecule-binding PAS domain [73], the two-component receiver (REC) domain, the HAMP domain which is commonly found in signal-sensing histidine kinases [74] and the GAF domain which may bind nucleotides [75]. Until now, only a few signals which are sensed by these domains

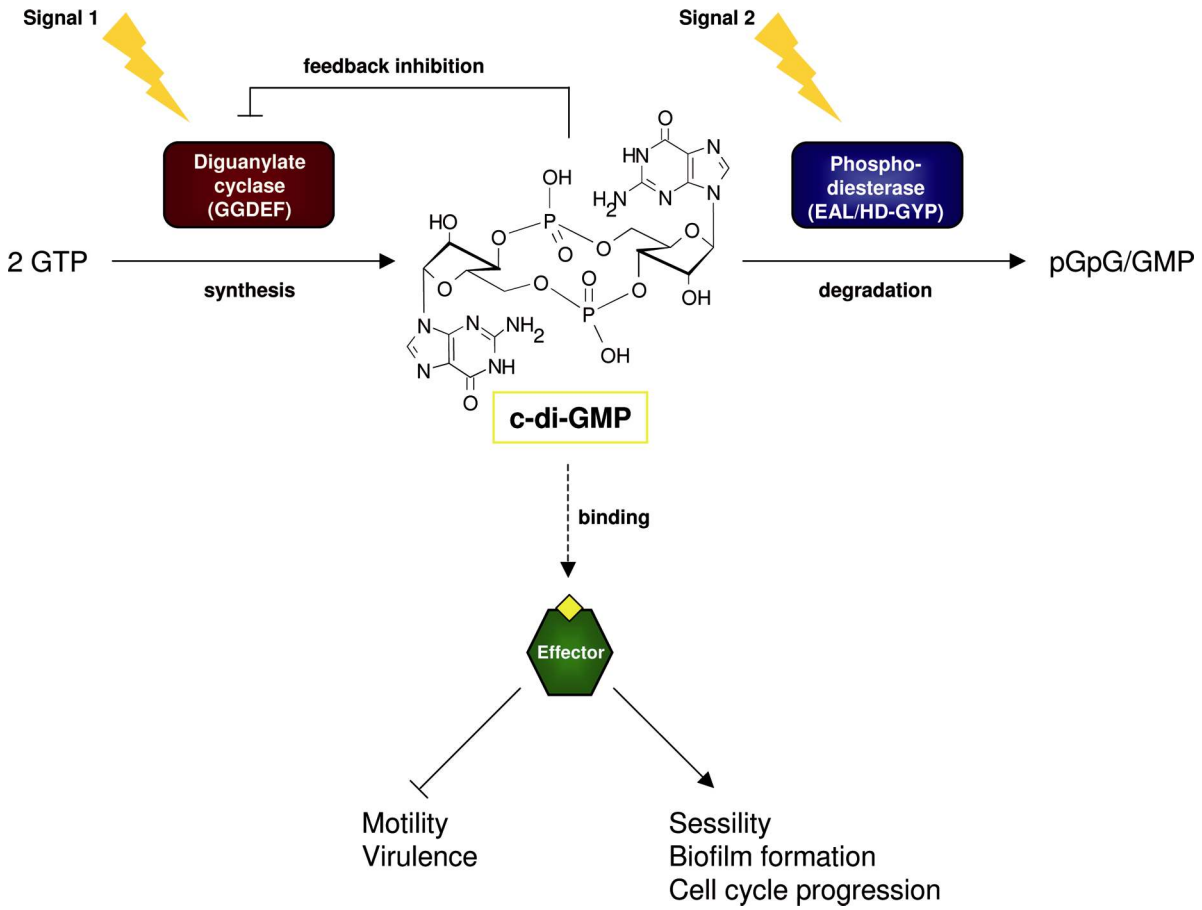

Figure 1.2. Components of c-di-GMP signaling pathways.
C-di-GMP is synthesized from 2 GTP by diguanylate cyclases (DGC) which carry catalytic GGDEF domains. C-di-GMP is hydrolyzed to pGpG and/or GMP by phosphodiesterases (PDE) which carry catalytic EAL or HD-GYP domains. DGC and PDE activity is influenced by cellular and environmental signals that are sensed by associated partner domains (not shown). Most DGCs are prone to allosteric feedback inhibition which involves binding of c-di-GMP to a secondary site (I-site) within the GGDEF domain. By binding to diverse effector molecules, c-di-GMP inhibits cell motility and traits associated with bacterial virulence while sessility and biofilm formation is promoted. This figure is based on previous published models [59, 70].

and which affect DGC or PDE activity have been identified, for example, oxygen, blue light and antibiotics [60, 76].

Additionally, knowledge of factors involved in the translation of intracellular c-di-GMP levels into bacterial behavior on the single cell level, still remains limited. So far, only few classes of c-di-GMP effectors are known. The best-studied class are proteins harboring a PilZ domain [59, 70]. Initially discovered by an bioinformatic approach [77], the PilZ domain is known to bind c-di-GMP and to impact virulence [78], flagellar motility [79-81] and the production of exopolysaccharides [82, 83]. Another class of c-di-GMP binding proteins are proteins that contain degenerate GGDEF or EAL domains, which have lost their enzymatic activity. For example, the PopA protein from *Caulobacter crescentus* has a catalytically inert GGDEF domain with an intact secondary c-di-GMP binding motif (I-site). Upon c-di-GMP binding, PopA localizes to the cell pole where it facilitates the degradation of the master cell cycle regulator CtrA [84]. In *P. fluorescence*, the catalytically inactive GGDEF-EAL hybrid protein LapD communicates intracellular c-di-GMP levels to the membrane-localized attachment machinery upon binding of c-di-GMP to its degenerate EAL domain [85-87]. The third class of c-di-GMP effector molecules are transcriptional regulators, including FleQ from *P. aeruginosa* [88], Clp from *Xanthomonas axonopodis* pv. *citri* and *X. campestris* pv. *campestris* [89-91], and VpsT from *Vibrio cholerae* [92]. However, these transcription factors do not share a common domain organization or c-di-GMP binding motif. Finally, conserved RNA domains (GEMM), which reside in 5'-untranslated regions of different mRNAs, have been shown to be c-di-GMP targets and to affect gene expression by functioning as riboswitches [93, 94]. Although c-di-GMP controlled riboswitches were found in several organisms, for example in *V. cholerae*, *Bacillus cereus* and *Clostridium difficile*, the conserved GEMM RNA binding motifs are absent in most species. In addition, there are many bacterial species, which encode functional GGDEF and EAL proteins but no proteins harboring PilZ domains.

1.5.1 C-di-GMP signaling in *P. aeruginosa*

GGDEF, EAL and PilZ domain proteins are widely distributed across the prokaryotic kingdom [71, 72, 77]. While some organisms tend to have only a few or no GGDEF or EAL proteins, other organisms encode multiple copies of those c-di-GMP metabolizing enzymes. The genome of *P. aeruginosa* strain PA01 encodes 17 proteins with a GGDEF domain, 5 proteins with an EAL domain and 16 “hybrid” proteins that contain both a GGDEF and an EAL domain (listed in the appendix, Table 5.1) [62]. Furthermore, three genes encode

proteins with an HD-GYP domain [95]. Some of these proteins have been shown to be enzymatically active, while others seem to be degenerate or are still uncharacterized (for references see Table 5.1). One of the best characterized examples is the diguanylate cyclase WspR. In addition to its conserved GGDEF domain, WspR carries an N-terminal receiver domain and is part of the above mentioned Wsp chemotaxis-like system (see chapter 1.3.2). Upon phosphorylation by the WspE histidine kinase, WspR becomes active and produces a localized pool of c-di-GMP that triggers the production of the Pel and Psl exopolysaccharides and biofilm formation [32, 39].

One possibility of how the c-di-GMP level produced by WspR might be translated into an enhanced expression of the *psl* and *pel* genes is via the transcriptional regulator FleQ. Recently, Hickman and Harwood [88] demonstrated that c-di-GMP binds to FleQ and causes a derepression of *pel* and *psl* transcription. However, the exact FleQ binding site of c-di-GMP has not yet been identified.

P. aeruginosa encodes a total of eight PilZ domain containing proteins (listed in Table 1.1). All but one of them, PA2960 (PilZ), were shown to bind c-di-GMP [82]. The PilZ domain protein Alg44 is involved in the biosynthesis of the exopolysaccharide alginate [82], but the molecular function of the remaining c-di-GMP binding PilZ domain proteins is still unknown. Two other proteins of *P. aeruginosa* have been demonstrated to bind c-di-GMP: the PelD protein is required for Pel exopolysaccharide production and exhibits secondary structure similarities to the I-site of DGCs [98]. FimX is a protein that governs twitching motility and

Table 1.1. C-di-GMP binding proteins of *P. aeruginosa*.

PA number	Gene name	Domains[a]	C-di-GMP binding site	Selected references
PA0012		PilZ	PilZ domain	[82]
PA2799		PilZ	PilZ domain	[82]
PA2960	*pilZ*	PilZ	-[b]	[82, 96]
PA2989		PilZ	PilZ domain	[82]
PA3353		YcgR, PilZ	PilZ domain	[82]
PA3542	*alg44*	TM, PilZ	PilZ domain	[82]
PA4324		PilZ	PilZ domain	[82]
PA4608		PilZ	PilZ domain	[82, 97]
PA1097	*fleQ*	FleQ, AAA σ^{54} interaction domain, HTH	unknown	[88]
PA3061	*pelD*	TM	I-site like	[98]
PA4959	*fimX*	REC, degenerate GGDEF, degenerate EAL	EAL domain	[99]

[a] TM, transmembrane; HTH, helix-turn-helix; REC, receiver
[b] no c-di-GMP binding demonstrated so far

that has lost enzymatic activity of its degenerate GGDEF and EAL domains, however, the inactive EAL domain has retained its c-di-GMP binding ability [99].

Overall, the c-di-GMP signaling network of *P. aeruginosa* and many other bacterial organisms is highly complex. As many genomes encode numerous c-di-GMP metabolizing and binding proteins, the question arises of how specificity within the signaling system is achieved. One answer might be the spatial separation of multiple c-di-GMP pathways by sequestration of c-di-GMP modulating proteins to different subcellular localizations where they create and respond to discrete, localized c-di-GMP pools. Thereby, some c-di-GMP metabolizing proteins might first require the perception of certain environmental signals via associated partner domains, before any c-di-GMP synthesizing or degrading activity is conducted. Furthermore, the separation of distinct c-di-GMP signaling systems can be achieved by tightly controlling the expression of subsets of c-di-GMP related genes in response to different environmental conditions. For example, a recent study by Weber *et al.* demonstrated that seven of the 29 GGDEF/EAL genes in *E. coli* depend on the alternative sigma factor RpoS – the master regulator of the general stress response [100]. Systematic approaches need to be applied in order to understand how environmental signals and global regulators control the c-di-GMP signaling network enabling a specific output response of the bacterial cell.

1.6 Aims of the thesis

Biofilms constitute the predominant mode of bacterial growth and allow survival in hostile environments such as the human host. They have been associated with chronic and device-related infections, and are a major challenge for clinicians due to their inherent resistance to antibiotic therapy and host defense mechanisms. In order to control such biofilm infections, it is important to understand the genetic and molecular basis of this bacterial community behavior.

Various studies have demonstrated that motility, including swimming, swarming and twitching, seems to play an important role in the surface colonization and establishment of structured biofilms. Thereby, the impact of chemotaxis on biofilm formation has been less intensively studied. Another important factor for the transition between motile and sessile lifestyles is the bacterial second messenger c-di-GMP. Despite extensive research, many details of the complex c-di-GMP signaling network are still uncharacterized. One major area of interest is understanding the mechanisms by which c-di-GMP exerts its effects. Although some protein and RNA-based c-di-GMP targets have been identified, the fact that numerous cellular functions are regulated by c-di-GMP, calls for further classes of c-di-GMP effectors.

In this thesis, we aimed at the characterization of the *P. aeruginosa* chemotaxis methyltransferase CheR1, and the investigation of a potential role in biofilm formation. Another main focus was to identify novel c-di-GMP binding proteins by applying a chemical proteomics approach using a c-di-GMP affinity resin as an enrichment tool in combination with high-resolution mass spectrometry. To understand how environmental signals can impact c-di-GMP signaling at the level of transcription, we furthermore aimed at the elucidation of the regulon of the alternative stationary phase sigma factor RpoS by performing chromatin immunoprecipitation experiments in conjunction with DNA-microarray analysis (ChIP-chip). The overall aim was to increase knowledge of how *P. aeruginosa* regulates the transition between motile planktonic and sessile biofilm-associated lifestyles in response to growth conditions and the sensing of diverse signals from the environment.

2 Materials and Methods

2.1 Bacterial strains, plasmids and growth conditions

The bacterial strains and plasmids used in this study are listed Table 2.1 and Table 2.2, respectively. All strains were maintained at -70°C as 15% (v/v) glycerol stocks. *Escherichia coli* strain DH5α was used for all cloning steps, strain BL21 (DE3) for protein overexpression and strain S17-1 for conjugative DNA transfer.

Research on *Pseudomonas aeruginosa* was carried out using the well-established and sequenced PA01 and PA14 strains. *P. aeruginosa* transposon mutants were purchased from the Washington Genome Center PA01 mutant library [101] and the NR PA14 transposon mutant library [102], respectively. Of note, world-wide, diverse PA01 sublines have evolved from the original PA01 strain, displaying different pheno- and genotypes [103]. For example, the PA01 wild-type delivered together with the "Washington" transposon mutants is impaired in its twitching motility (own observations). Thus, we chose the transposon mutant *P. aeruginosa* PA01 PA4684, ID 8031, as wild-type control (PA01 wt control) in phenotypic characterization assays. The open reading frame (ORF) PA4684 is most likely coding for a non-functional gene product due to a large gene deletion [103, 104]. The respective transposon mutant is proficient in swimming, swarming and twitching motility (see chapter 3.2.7).

For all transposon mutants, correct insertion of the transposon into the respective gene was verified by PCR using gene-specific primers (as listed in Table 2.3). In case of the PA01 "Washington" transposon mutants PA3740 (mutant ID 21422 and 55385) and PA4396 (mutant ID 35076 and 36991), correct transposon insertion could not be confirmed. Instead, PA3740 and PA4396 transposon mutants from a distinct PA01 mutant library (Tn5 *lux* transposon library, [105]) were used (kindly provided by Robert E. Hancock, University of British Columbia, Canada). The PA01 strain used for the generation of this mutant library is termed H103 and exhibits all three types of motility (swimming, swarming and twitching).

All *P. aeruginosa* and *E. coli* strains were cultured at 37°C in Luria-Bertani (LB) broth with shaking (180 rpm), unless otherwise indicated. When required for plasmid or transposon selection, 100 μg/ml ampicillin and 50 μg/ml kanamycin were used for *E. coli* and 400 μg/ml carbenicillin, 15 μg/ml gentamycin, 150 μg/ml streptomycin and 25 μg/ml tetracycline respectively for the selection in *P. aeruginosa*. For the growth of cells on agar plates, the LB medium was solidified by addition of 1.6% (w/v) agar.

Table 2.1. Strains used in this thesis.

Strains	Relevant characteristics[a]	Source or reference
E. coli		
DH5α	F⁻ endA1 glnV44 thi-1 recA1 relA1 gyrA96 deoR nupG Φ80d*lacZ*ΔM15 Δ(*lacZYA-argF*)U169, hsdR17(r_K^- m_K^+), λ–	[106]
BL21 (DE3)	F⁻ ompT $hsdS_B$($r_B^-m_B^-$) gal dcm	Stratagene
S17-1	C600::RP-4 2-(Tc::Mu) (Kn::Tn7) *thi pro hsdR hsdM+recA*	[107]
HCB721	Δ(*tsr*)7021 *trg*::Tn*10* Δ(*cheA-cheY*)::XhoI(Tn*5*), Km^r, Tc^r	[108]
BL21 (DE3) pRP89	Strain carrying pET11:*pleD** for overexpression of PleD*-His_6 for the purpose of protein purification, Ap^r	[109]
M15 pREP4 pQERpoS	Strain overexpressing His_6-RpoS for the purpose of protein purification, Ap^r, Km^r	[110]
P. aeruginosa		
PA01 wt	Wild-type	Lab collection
PA01 wt control	PA4684 transposon mutant from the Washington Genome Center PA01 mutant library, ID 8031, Tc^r	[101]
PA01 *cheR1*	*cheR1* transposon mutant from the Washington Genome Center PA01 mutant library, ID 47867, Tc^r	[101]
PA01 PA3353	PA3353 transposon mutant from the Washington Genome Center PA01 mutant library, ID 37088, Tc^r	[101]
PA01 PA5017	PA5017 transposon mutant from the Washington Genome Center PA01 mutant library, ID 33729, Tc^r	[101]
PA01 wt control_PA3353	PA3353 knockout mutant constructed in the PA01 wild-type control background, Gm^r, Tc^r	This study
PA01 wt control_PA3740	PA3740 knockout mutant constructed in the PA01 wild-type control background, Gm^r, Tc^r	This study
PA01 PA5017_PA3353	PA3353 knockout mutant constructed in the PA01 PA5017 background, Gm^r, Tc^r	This study
PA01 PA5017_PA3740	PA3740 knockout mutant constructed in the PA01 PA5017 background, Gm^r, Tc^r	This study
PA01 H103 wt	Wild-type	R. E. Hancock
PA01 H103 PA3740	PA3740 transposon mutant from the PA01 mini-Tn5 *lux* transposon mutant library, ID PA01_lux_19_F11 and PA01_lux_51_E2, Tc^r	[105]
PA01 H103 PA4396	PA4396 transposon mutant from the PA01 mini-Tn5 *lux* transposon mutant library, ID PA01_lux_25_C8, Tc^r	[105]
PA14 wt	Wild-type	[102]
PA14 *cheR1*	*cheR1* transposon mutant from the NR PA14 transposon mutant library, ID 36949, Gm^r	[102]

[a] Ap^r, ampicillin resistant; Gm^r, gentamycin resistant; Km^r, kanamycin resistant; Tc^r, tetracycline resistant

2.2 Plasmid and strain construction

Isolation and manipulation of recombinant DNA molecules was performed in accordance with standard molecular cloning techniques or as indicated by the product manufacturers instructions.

Table 2.2. Plasmids used in this thesis.

Plasmid	Relevant characteristics[a]	Source or reference
pUCP20	Shuttle vector, Ap^r/Cb^r	[111]
pUCP20:*cheR1*	*cheR1* (promoter region and gene) cloned into *Bam*HI-*Xba*I in MCS, Ap^r/Cb^r	This study
pUCP20:PA3353	PA3353 (promoter region and gene) cloned into *Bam*HI-*Xba*I in MCS, Ap^r/Cb^r	This study
pUCP20:PA3740	PA3740 (promoter region and gene) cloned into *Bam*HI-*Xba*I in MCS, Ap^r/Cb^r	This study
pUCP20:PA4396	PA4396 (promoter region and gene) cloned into *Bam*HI-*Xba*I in MCS, Ap^r/Cb^r	This study
pET21a(+)	Plasmid for overexpression of proteins with C-terminal His_6-tag, Ap^r	Novagen
pET21a(+):*cheR1*	*cheR1* gene without stop codon cloned into *Nde*I-*Hin*dIII in MCS, Ap^r	This study
pET21a(+):PA3353	PA3353 gene without stop codon cloned into *Nde*I-*Xho*I in MCS, Ap^r	This study
pET21a(+):PA3740	PA3740 gene without stop codon cloned into *Nde*I-*Hin*dIII in MCS, Ap^r	This study
pASK-IBA7(+)	Plasmid for overexpression of proteins with N-terminal Strep-tag, Ap^r	IBA
pASK-IBA7(+):PA4396	PA4396 gene without start codon cloned into *Eco*RI-*Bam*HI in MCS, Ap^r	This study
pSunny	GFP expressing plasmid, Km^r, Sm^r	[112]
pHSe5:*tsr*	Plasmid expressing the *E. coli* MCP Tsr, inducible with IPTG, Ap^r	[113, 114]
pHSe5:*pctA*	Plasmid expressing the *P. aeruginosa* MCP PctA, inducible with IPTG, Ap^r	This study
pPS856	Source of Gm^r cassette, Ap^r, Gm^r	[115]
pEX18Ap	Gene replacement vector; $oriT^+$ $sacB^+$, Ap^r/Cb^r	[115]
pCR-Blunt II-Topo	*E. coli* cloning vector, Km^r	Invitrogen
pTopo:PA3353	*Bam*HI-*Xba*I fragment of pUCP20:PA3353 subcloned into pCR-Blunt II-Topo, Km^r	This study
pTopo:PA3353ΩGm	Gm-cassette from pPS856 (cut with *Pst*I) subcloned into pTopo:PA3353 cut with the same enzyme, Gm^r, Km^r	This study
pEX18Ap:PA3353ΩGm	PCR amplified PA3353ΩGm fragment (blunt end) cloned into *Sma*I site of pEX18Ap, Ap^r/Cb^r, Gm^r	This study
pEX18Ap:PA3740	PA3740 mutant allele constructed by SOE-PCR[b] and cloned into *Eco*RI-*Xba*I of pEX18Ap, Ap^r/Cb^r	This study
pEX18Ap:PA3740ΩGm	Gm-cassette from pPS856 (cut with *Bam*HI) subcloned into pEX18Ap:PA3740 cut with the same enzyme, Ap^r/Cb^r, Gm^r	This study

[a] Ap^r, ampicillin resistant; Cb^r, carbenicillin resistant; Km^r, kanamycin resistant; Sm^r, streptomycin resistant; IPTG, isopropyl 1-thio-β-D-galactopyranoside; GFP, green fluorescent protein; MCS, multiple cloning site
[b] SOE, gene splicing by overlap extension

Primers used for cloning (listed in Table 2.3) were ordered from Eurofins MWG Operon and are based on the PA01 genome sequence (www.pseudomonas.com) [11]. All PCR amplifications were performed with Pfu polymerase using PA01 genomic DNA as a template. The primer dependent annealing temperatures and target specific extension times used in the respective PCR reactions are depicted in Table 2.4. Purified PCR products were digested with appropriate restriction enzymes (Fermentas) and cloned into the target vector as indicated in Table 2.2 and Table 2.4. All obtained constructs were sequenced to rule out PCR errors.

For complementation studies, the individual ORFs including their promoter regions were cloned into the *E. coli - P. aeruginosa* shuttle vector pUCP20 [111] and introduced into *P. aeruginosa* by electroporation. For recombinant protein expression in *E. coli*, the respective genes were cloned into the expression vector pET21a(+) (Novagen) without their stop codon which led to a C-terminal His_6-tag fusion. Alternatively, the gene was cloned in frame with an N-terminal Strep-tag into the pASK-IBA7(+) vector. The obtained plasmids for

Table 2.3. Primers used for cloning strategies in this thesis.

Primer	Sequence[a]
PA3348 fPr1	5'-AAAACATATGGTGTCGGCAGCTAATGCG
PA3348 rPr2	5'-GATCAAGCTTCTTGGCCCGGTAGAT
PA3348 fPr3	5'-GATCGGATCCTTGCATACTTCGTTGTCC
PA3348 rPr3	5'-GATCTCTAGACTACTTGGCCCGGTAGATG
PA3353 fPr1	5'-AAAACATATGGTGCTATCATTGAGGCAT
PA3353 rPr1	5'-AAAACTCGAGGAACAGTTCGTCAAACTC
PA3353 fPr3	5'-GATCGGATCCGAACTGCTGGAGCGTTGCCA
PA3353 rPr3	5'-GATCTCTAGAGAGCATCACCTGTTGCCGGCG
PA3740 fPr1	5'-AAAACATATGATGACCATGTCCAATCAACAAC
PA3740 rPr2	5'-GATCAAGCTTGGGCCGCAGGCTGAT
PA3740 fPr3	5'-GATCGGATCCAACGACTACCAGGCGCTGCA
PA3740 rPr3	5'-GATCTCTAGAGGATCAGGGCCGCAGGCTGA
PA3740KO UP FEco	5'-GGAATTCCCAATCCCACCTCGCAGCACG
PA3740KO UP RBam	5'-CGGGATCCCGTGAAGTCTAGTCGGCGATTTCCGT
PA3740KO DOWN FBam[b]	5'-*ACGGAAATCGCCGACTAGACTTCACGGGATCCCG* GAAACCGGCAAGACGCAAAGCA
PA3740KO DOWN RXbaI	5'-GCTCTAGAGCGTGACCGTTTCCACCGATCG
PA4396 fPr3	5'-GATCGGATCCTTTGCCTTTCAGGTCGAA
PA4396 rPr3	5'-GATCTCTAGACTAGCGCAGTGCCGGTAG
PA4396 fPr4	5'-GATCGAATTCCCCGCCGGTGTGGCGGAGAC
PA4396 rPr4	5'-GATCGGATCCCTAGCGCAGTGCCGGTAGCC
pctA fPr2	5'-GATCGGATCCATGATCAAAAGTCTGAAGTTCAGC
pctA rPr2	5'-GATCAAGCTTTCAGATCTTGAAGCTGTCCAC

[a] engineered restriction sites are underlined

[b] the sequence which is complementary to the PA3740KO UP RBam primer is displayed in *italics*

Table 2.4. Cloning strategies for the construction of plasmids used in complementation studies and for protein overexpression.

Primer	PCR[a] T_a; t_{ex}; product length	Cut with	Clone into
PA3348 fPr1	63.1°C; 1 min 50 s 842 bp	*Nde*I *Hin*dIII	pET21a(+)
PA3348 rPr2			
PA3348 fPr3	63.1°C; 2 min 10 s 1059 bp	*Bam*HI *Xba*I	pUCP20
PA3348 rPr3			
PA3353 fPr1	61.1°C; 2 min 30 s 810 bp	*Nde*I *Xho*I	pET21a(+)
PA3353 rPr1			
PA3353 fPr3	66.7°C; 2 min 30 s 1104 bp	*Bam*HI *Xba*I	pUCP20
PA3353 rPr3			
PA3740 fPr1	63.4°C; 1 min 30 s 704 bp	*Nde*I *Hin*dIII	pET21a(+)
PA3740 rPr2			
PA3740 fPr3	65.9°C; 2 min 5 s 1005 bp	*Bam*HI *Xba*I	pUCP20
PA3740 rPr3			
PA4396 fPr3	64.2°C; 2 min 45 s 1329 bp	*Bam*HI *Xba*I	pUCP20
PA4396 rPr3			
PA4396 fPr4	63.7°C; 2 min 20 s 1118 bp	*Eco*RI *Bam*HI	pASK-IBA7(+)
PA4396 rPr4			
pctA fPr2	60°C; 4 min 20 s 1910 bp	*Bam*HI *Hin*dIII	pHSe5
pctA rPr2			

[a] T_a, annealing temperature; t_{ex}, extension time

protein overexpression were introduced into chemically competent *E. coli* BL21 (DE3) by transformation. An *E. coli* strain overexpressing the diguanylate cyclase PleD* [109] was kindly provided by Urs Jenal (University of Basel, Switzerland) and the *E. coli* strain used for overexpression of the stationary phase sigma factor RpoS [110] was a gift from Vittorio Venturi (International Center for Genetic Engineering and Biotechnology, Trieste, Italy).

The IPTG inducible *E. coli* Tsr expression plasmid pHSe5 [113, 114], kindly provided by Robert M. Weis (University of Massachusetts, Amherst, USA), was modified for expression of the *P. aeruginosa* MCP PctA. The *tsr* sequence was removed by digestion with *Bam*HI and *Hin*dIII yielding in a vector backbone (4.8 kb) and a *tsr* fragment (2.4 kb). The vector backbone was gel-purified and ligated to the PCR amplified and *Bam*HI/*Hin*dIII digested *pctA* gene. The resulting construct, pHSe5:*pctA*, was transformed into chemically competent *E. coli* HCB721 cells.

2.3 Construction of knockout mutants

Knockout mutants were created by gene disruption using the gene replacement vector pEX18Ap [115]. Thereby, the chromosomal wild-type allele of the respective gene was exchanged with a mutated, pEX18Ap-borne allele which carries a gentamycin cassette as selectable marker. The pEX18Ap vector and the plasmid pPS856 [115], source of the Gm-cassette, were kindly provided by Robert E. Hancock (University of British Columbia, Canada).

Different strategies were used to create the pEX18Ap knockout plasmids pEX18Ap:PA3353ΩGm and pEX18Ap:PA3740ΩGm. In the case of PA3353, the *Bam*HI-*Xba*I fragment of pUCP20:PA3353 was cloned into pCR-Blunt II-Topo to generate pTOPO:PA3353. An internal region of PA3353 (138 bp), flanked by two *Pst*I restriction sites, was removed by *Pst*I digestion and replaced with the gentamycin resistance cassette cut from pPS856 with the same enzyme. From the resulting vector, the PA3353ΩGm fragment was amplified using Pfu polymerase and primer pair PA3353 fPr3/rPr3. The blunt-ended PCR product was ligated into the *Sma*I site of pEX18Ap to create pEX18Ap:PA3353ΩGm.

To engineer an internal deletion in PA3740, the method of gene splicing by overlap extension (SOE) was used [116]. In brief, N-terminal (490 bp) and C-terminal (509 bp) regions flanking the PA3740 gene were amplified using the primer pairs PA3740KO UP F/R and DOWN F/R, respectively (Table 2.3). The primer sequence of PA3740KO DOWN F included nucleotides at the 5' end which were complementary to the PA3740KO UP R primer, so that the PCR products of the two separate reactions share homologous sequences. Both PCR products were mixed and employed in a second PCR reaction using the primer pair PA3740KO UP F/DOWN R. The obtained 1000 bp fragment resembles PA3740 but lacks a significant part of the coding sequence (495 of 687 bp) and has an engineered *Bam*HI restriction site in the middle. This fragment was ligated between the *Eco*RI and *Xba*I sites of pEX18Ap before the gentamycin resistance cassette of pPS856 was cloned into the PA3740 sequence via the introduced *Bam*HI site to generate the final pEX18Ap:PA3740ΩGm plasmid.

The generated gene replacement constructs were transformed into chemically competent *E. coli* S17-1 cells before being conjugated into *P. aeruginosa* PA01 wt control and PA01 PA5017, respectively. Double recombinants were identified by their resistance towards gentamycin (200 µg/ml) and tetracycline (25 µg/ml) combined with their sensitivity towards carbenicillin (400 µg/ml) upon growth on LB plates containing the indicated antibiotics. The loss of the vector backbone was additionally confirmed by their ability to grow on LB plates

containing 5% (w/v) sucrose. Chromosomal mutant candidates were analyzed by colony PCR to verify disruption of the designated gene.

2.4 DNA transfer techniques

2.4.1 Transformation of *E. coli*

Chemically competent *E. coli* DH5α, BL21 (DE3) and HCB721 cells were prepared as follows: an overnight culture of the respective strain was used to inoculate 25 ml fresh LB. This culture was grown to an OD_{600} of 0.3 at 37°C, before bacterial growth was stopped by cooling the culture on ice for 10 min. Cells were harvested by centrifugation at 4°C at 3,200×*g* for 15 min, resuspended in 5 ml ice-cold 0.1 M $CaCl_2$ and cooled on ice for 5 min. After a second centrifugation step, cells were resuspended in 1 ml ice-cold 0.1 M $CaCl_2$ containing 15% (v/v) glycerol and incubated on ice for 15 min. The competent cells were frozen as 100 µl aliquots in liquid nitrogen and stored at -70°C.

For transformation, competent cells were gently thawed on ice, mixed with the DNA of interest and kept on ice for 20 min. After a heat shock for 90 s at 42°C, cells were placed back on ice for 2 min before 800 µl LB were added and the cells were incubated at 37°C in a thermomixer for 1.5 h. Thereafter, 100 µl of the transformation reaction were plated on LB agar containing antibiotics for selection of transformants. The plates were incubated overnight at 37°C.

2.4.2 Electroporation of *P. aeruginosa*

Electrocompetent *P. aeruginosa* PA01 and PA14 cells were always prepared fresh directly before use. The respective strains were plated on LB agar plates (one plate per electroporation reaction) and incubated for 20 h at 37°C resulting in a thick cell lawn. Cells were collected with an inoculation loop and resuspended in 1 ml deionized water (dH_2O). The bacterial suspension was centrifuged at 18,000×*g* for 2 min and the cell pellet was repeatedly washed with dH_2O to remove components of the extracellular matrix produced by *P. aeruginosa* cells. The bacteria were finally resuspended in 45 µl dH_2O, mixed with 1 µl plasmid DNA and transferred to an electroporation cuvette (2 mm electrode gap). The electric pulse was delivered with a voltage of 2.45 kV, a capacitance of 25 µF and a resistance of 200 Ω (Gene Pulser II, Bio-Rad). The resulting time constant varied between 5-5.5 ms. Directly after the discharge, 1 ml LB was added and the suspension was transferred to a microcentrifuge tube.

The electroporation reaction was incubated for 1.5 h at 37°C in a thermomixer, before 100 µl were spread on selective LB agar. The plates were incubated overnight at 37°C.

2.4.3 Plasmid transfer by conjugation

In some cases, plasmids were introduced into *P. aeruginosa* by conjugation using *E. coli* S17-1 [107] as the donor strain. For conjugation experiments, *P. aeruginosa* was grown in 5 ml nutrient broth (NB, Difco) for 24 h at 37°C, while *E. coli* S17-1 carrying the plasmid of interest was grown in 5 ml LB for 7 h at 37°C. Bacterial cells were harvested by centrifugation at 3,200×*g* for 15 min, resuspended in 500 µl fresh NB medium and transferred into a microcentrifuge tube. The cells were centrifuged again at 6,000×*g* for 5 min and finally resuspended in 100 µl fresh NB.

Biparental mating mixtures of donor and recipient cells (1:1, 20 µl) were spotted on a fresh NB agar plate and incubated overnight at 37°C. The colony was resuspended in 1 ml phosphate buffered saline (PBS) and 100 µl of this bacterial suspension were plated on LB agar plates containing suitable antibiotics to positively select for *P. aeruginosa* transconjugants but to counterselect the *E. coli* donor cells.

2.5 Protein overexpression and purification

E. coli BL21 (DE3) and M15 cells carrying the respective expression plasmids were grown to an OD_{600} of 0.5-0.7 before inducing protein expression by adding 0.1-1 mM isopropyl 1-thio-β-D-galactopyranoside (IPTG; for pET and pQE based overexpression) or 200 ng/ml anhydrotetracycline (AHT; for pASK-IBA based overexpression). The cultures were further shaken at temperatures and incubation times indicated in Table 2.5.

Table 2.5. Culture conditions for heterologous overexpression of diverse proteins in *E. coli*.

***E. coli* host strain**	**Expression vector**	**Induction with[a]**	**Growth temperature and time following induction[b]**	**Resulting protein**
BL21 (DE3)	pET21a(+):*cheR1*	0.1 mM IPTG	20°C, ON	CheR1-His_6
BL21 (DE3)	pET21a(+):*PA3353*	0.1 mM IPTG	37°C, 6 h	PA3353-His_6
Cell-free expression	pET21a(+):*PA3740*	0.1 mM IPTG	30°C, 1.5 h	PA3740-His_6
BL21 (DE3)	pASK-IBA7(+):*PA4396*	200 ng/ml AHT	20°C, ON	Strep-PA4396
BL21 (DE3)	pET11:*pleD**	0.1 mM IPTG	20°C, ON	PleD*-His_6
M15	pQERpoS	1.0 mM IPTG	20°C, 4 h	His_6-RpoS

[a] IPTG, isopropyl 1-thio-β-D-galactopyranoside; AHT, anhydrotetracycline
[a] ON, overnight

Table 2.6. Buffers used for purification strategies of diverse proteins.

Protein	Lysis and washing buffer	Elution buffer	Dialysis buffer
CheR1-His_6	50 mM NaH_2PO_4, pH 8.0, 300 mM NaCl, 10 mM imidazole	50 mM NaH_2PO_4, pH 8.0, 300 mM NaCl, 250 mM imidazole	50 mM NaH_2PO_4, pH 8.0, 300 mM NaCl
PA3353-His_6	50 mM NaH_2PO_4, pH 8.0, 300 mM NaCl, 10 mM imidazole	50 mM NaH_2PO_4, pH 8.0, 300 mM NaCl, 250 mM imidazole	50 mM NaH_2PO_4, pH 8.0, 300 mM NaCl
PA3740-His_6	50 mM NaH_2PO_4, pH 8.0, 300 mM NaCl, 10 mM imidazole, 0.05% (v/v) Tween 20	50 mM NaH_2PO_4, pH 8.0, 300 mM NaCl, 250 mM imidazole, 0.05% (v/v) Tween 20	50 mM NaH_2PO_4, pH 8.0, 300 mM NaCl
Strep-PA4396	100 mM Tris·Cl, pH 8.0, 150 mM NaCl, 1 mM EDTA	100 mM Tris·Cl, pH 8.0, 150 mM NaCl, 1 mM EDTA, 2.5 mM desthiobiotin	100 mM Tris·Cl, pH 8.0, 150 mM NaCl
PleD*-His_6	50 mM Tris·Cl, pH 8.0, 300 mM NaCl, 10 mM imidazole	50 mM Tris·Cl, pH 8.0, 300 mM NaCl, 250 mM imidazole	50 mM Tris·Cl, pH 8.0, 300 mM NaCl
His_6-RpoS	50 mM Tris·Cl, pH 8.0, 300 mM NaCl, 10 mM imidazole	50 mM Tris·Cl, pH 8.0, 300 mM NaCl, 250 mM imidazole	50 mM Tris·Cl, pH 8.0, 300 mM NaCl

After harvesting cells by centrifugation, the pellets were resuspended in suitable lysis buffers (3 ml lysis buffer per mg of wet cell pellet) containing 1 mM dithiothreitol (DTT), 1 mg/ml lysozyme, protease inhibitors (Complete mini, ethylenediaminetetraacetic acid (EDTA) free, Roche) and Benzonase Nuclease (Novagen). Cells were lysed by passage through a French pressure cell (SLM-Aminco) at 16,000 psi at least twice and then centrifuged at 37,500×*g* for 45 min in order to remove unbroken cells. Proteins containing a C-terminal His_6-tag were purified by affinity chromatography using Ni-NTA resin (Quiagen) following standard protocols. Proteins containing an N-terminal StrepII-tag were purified using Strep-Tactin as affinity resin and eluted as recommended by the supplier (IBA). Eluted fractions were examined for the presence and purity of recombinant protein by SDS-PAGE analysis. Preparations of pure protein (> 90%) were pooled and dialyzed for 16 h at 4°C using Slide-A-Lyzer dialysis cassettes (Thermo Scientific) with a molecular weight cut off (MWCO) of 10 kDa. The buffers used for cell lysis, protein purification (washing and elution) and dialysis of pure proteins are listed in Table 2.6.

Due to an apparent toxicity of PA3740 towards the *E. coli* expression host, a cell-free expression system was used for biosynthesis of PA3740-His_6 (EasyXpress, Quiagen). For this purpose, *E. coli* extracts were mixed with 1.5 µg pET21:PA3740 and the *in vitro* translation process was started by the addition of 0.1 mM IPTG (final reaction volume: 50 µl). After incubation at 30°C for 1.5 h under gentle agitation, His-tagged PA3740 was purified from the reaction mixture using Ni-NTA magnetic agarose beads (Quiagen) as recommended by the supplier. Eluted proteins were dialyzed in Slide-A-Lyzer mini dialysis units (MWCO 10 kDa, Thermo Scientific) for 16 h at 4°C (see also Table 2.5 and Table 2.6).

Table 2.7. Characteristic protein properties.

Protein	MW[a]	pI[b]	$A_{280\ nm}$[c] of 1 corresponds to[d]
CheR1-His_6	32.2 kDa	9.3	1.06 mg/ml
PA3353-His_6	31.0 kDa	6.5	1.71 mg/ml
PA3740-His_6	26.4 kDa	9.2	20.61 mg/ml
Strep-PA4396	42.9 kDa	5.6	2.06 mg/ml
PleD*-His_6	50.4 kDa	6.3	6.17 mg/ml
His_6-RpoS	39.2 kDa	5.6	1.66 mg/ml

[a] molecular weight
[b] isoelectric point
[c] absorbance of the protein at 280 nm
[d] those values depend on the amino acid sequence of the respective protein and were determined using the Vector NTI software (version 8, InforMax)

Protein concentrations were determined by measuring their absorbance at 280 nm (Table 2.7) or by using a Bradford assay (Bio-Rad protein assay). Purified and dialyzed proteins were commonly stored at 4°C.

2.6 Protein assays

2.6.1 Surface plasmon resonance analysis

All surface plasmon resonance experiments were performed at the University of Kassel in co-operation with the group of Friedrich W. Herberg (Daniela Bertinetti, Stefan Möller) and Bastian Zimmermann (Biaffin GmbH & Co KG, Kassel).

SAM binding to CheR1-His_6

Surface plasmon resonance (SPR) was used to detect binding of *S*-adenosylmethionine (SAM) to immobilized CheR-His_6. The interaction analyses were performed in 10 mM tris(hydroxymethyl)aminomethane (Tris), 300 mM NaCl, pH 8.0 (buffer A) at 25°C using a Biacore S51 instrument (GE Healthcare, Biacore). For covalent coupling of CheR-His_6, carboxymethylated sensor chip surfaces (Series S CM5, Biacore GE Healthcare) were activated with a 1:1 ratio of 0.4 M EDC (*N*-ethyl-*N'*-(3-dimethylaminopropyl)carbodiimide) and 0.1 M NHS (*N*-hydroxysuccinimide) for 10 min and purified CheR-His_6 (40 µg/ml in 10 mM 4-(2-hydroxyethyl)-1-piperazineethanesulfonic acid (HEPES), pH 7.0) was injected for 20 min at a flow rate of 5 µl/min. Deactivation of the surface was performed using 1 M ethanolamine-HCl (pH 8.5) for 8 min.

Interaction analyses were performed in buffer A containing 0.005% (v/v) surfactant P20 by injection of increasing concentrations (500 nM-1 mM) of SAM at a flow rate of 30 µl/min.

Association and dissociation signals were monitored for 60 s and 200 s, respectively. After subtracting the reference spot signal, resulting binding signals were fitted. Data evaluation was performed using the Biacore S51 evaluation software version 1.2.1.

C-di-GMP binding studies

All SPR experiments analyzing the interaction of purified proteins with immobilized c-di-GMP were performed on a Biacore 3000 instrument (GE Healthcare, Biacore) at 20°C.

To generate a c-di-GMP sensor chip, 2'-AHC-c-di-GMP (obtained from F. Schwede, Biolog, Bremen, Germany) was dissolved in 150 mM NaCl, 20 mM 3-(N-morpholino)-propanesulfonic acid (MOPS), pH 7 (buffer B) in an ultrasonic bath and by heating at 50°C. The concentration of the analog solution was determined via the respective extinction coefficient (ε = 23,700 l/(mol·cm)) [117]. For covalent coupling of 2'-AHC-c-di-GMP, a carboxymethylated sensor chip surface (CM5, Biacore GE Healthcare) was activated with EDC/NHS for 10 min according to the instructions of the manufacturer (amine coupling kit, Biacore GE Healthcare). The c-di-GMP analog (1 mM in 100 mM borate running buffer, pH 8.5) was injected for 7 min at a flow rate of 10 µl/min. Deactivation of the surface was performed using 1 M ethanolamine-HCl, pH 8.5 for 10 min. A reference cell was activated accordingly and deactivated subsequently without ligand immobilization.

Binding analysis was performed in buffer B containing 0.005% (v/v) surfactant P20, 1 mg/ml CM dextran and 1 mM DTT. For some experiments, proteins were pre-incubated with a ten-fold concentration of free c-di-GMP prior to injection. Association and dissociation were monitored for 9 min and 3 min, respectively (flow rate 10 µl/min). Nonspecific binding was excluded by subtracting blank runs performed on the reference cell. Resulting binding signals were plotted using the Biacore 3000 evaluation software, version 4.0.1.

Protein/nucleotide interactions were monitored as solution competition experiments [118, 119] in buffer B plus 0.005% (v/v) surfactant P20. In brief, proteins (15 nM – 1 µM) were pre-incubated with varying amounts of free c-di-GMP using at least eleven different concentrations and injected over the 2'-AHC-c-di-GMP surface. The association was monitored for 3 min and at the end of the association phase the binding signal was collected. After subtracting the reference cell, the resulting binding signals were plotted against the logarithm of the free c-di-GMP concentration and EC_{50} values were calculated from the dose response curve using GraphPad Prism 5.01 (GraphPad Software, San Diego, USA).

After each binding experiment the sensor surfaces were regenerated by two injections of 3 M guanidinium HCl and one injection of 0.05% (sodium dodecyl sulfate) SDS and the drifting baseline was stabilized by one injection of 1 M NaCl.

2.6.2 CheR1 methyltransferase activity assay

Preparation of membranes containing PctA

E. coli strain HCB721 [108], kindly provided by Howard C. Berg (Harvard University), was used to prepare membranes enriched for the MCP PctA. HCB721 is deficient in all known *E. coli* MCPs and all cytoplasmic chemotaxis proteins except the CheZ phosphatase and thus ensures that the overexpressed PctA receptor does not undergo post-translational modification. Cells were grown at 30°C in 500 ml LB supplemented with 100 µg/ml ampicillin. At OD_{600} 0.5-0.7, PctA expression was induced with 1 mM IPTG. After 3 h of induction, cells were harvested by centrifugation and resuspended in buffer containing 100 mM potassium acetate, 50 mM HEPES, pH 7.5, 5 mM magnesium acetate, 0.05% (v/v) β-mercaptoethanol, protease inhibitors (Complete mini, EDTA free, Roche) and Benzonase Nuclease (Novagen). Cells were lysed by adding 1 mg/ml lysozyme and by passage through a French Pressure cell (16,000 psi) at least twice. After removing unbroken cells by centrifugation for 20 min at 7,000×*g*, the supernatant was loaded on a sucrose step gradient (0.5 M, 1.5 M and 2 M) and centrifuged at 100,000×*g* for 1 h at 4°C. The second band was removed, diluted 5 times with water containing protease inhibitors (Complete mini, with EDTA, Roche) and centrifuged for 1 h at 100,000×*g* at 4°C. The pellet was resuspended in a small amount of storage buffer (50 mM NaH_2PO_4, 1 mM EDTA, 10% (v/v) glycerol), analyzed on Coomassie-stained SDS-PAGE and the total amount of protein concentration was determined by scanning densitometry against the Low Molecular Weight Calibration Kit (GE Healthcare) as a reference. The membrane samples were adjusted to a final protein concentration of 2 mg protein/ml in storage buffer and stored as single-use aliquots at -70°C.

Receptor methylation assays

In vitro methylation assays were performed as previously described with slight modifications [120, 121]. In brief, the methylation reaction (final volume 100 µl) was carried out at 30°C in 50 mM NaH_2PO_4, pH 8.0, 300 mM NaCl containing 50 µl receptor-enriched membranes, 0.1 µM CheR1-His_6 and with or without 1 mM serine or glutamine. After a pre-incubation step of 5 min, the reaction was started by adding 0.625 µM [^{3}H-methyl]-*S*-adenosylmethionine (specific activity 80 Ci/mmol, Amersham). At indicated time points, 10 µl aliquots were removed, spotted on filter paper (1 cm^2, Rotilabo, Roth) and quenched with 10% (w/v) trichloroacetic acid. The filters were washed twice with 10% (w/v) trichloroacetic acid and once with ethanol, for 15 min with gentle shaking. Air-dried filters were transferred into a 24-well sample plate, covered with 1 ml scintillation fluid and

incubated over night before radioactivity was quantified using a microplate liquid scintillation counter (1450 MicroBeta TriLux, Wallac).

2.6.3 Diguanylate cyclase activity assay

Diguanylate cyclase (DGC) assays were carried out as previously described [109, 122] with the following modifications. DGC-reactions in a total volume of 50 µl were performed at 30°C in buffer containing 10 µM of purified protein, 50 mM Tris-HCl, pH 8.0, 300 mM NaCl, 10 mM $MgCl_2$ and [α-^{32}P]GTP (3.33 pmol, 3,000 Ci/mmol, Hartmann analytic). At several time points, 5 µl aliquots were removed and mixed with an equal volume of 0.5 M EDTA, pH 8.0, to stop the enzymatic reaction. Product formation was analyzed with thin layer chromatography by spotting 1 µl on Polygram® CEL 300 polyethyleneimine cellulose plates (Machery-Nagel) and developing the plates in 1:1.5 (v/v) saturated NH_4SO_4 and 1.5 M KH_2PO_4, pH 3.6, for 60 min. Dried plates were exposed to a film for at least 1 h and qualitatively analyzed using a phosphor imager. In a control reaction, [^{32}P]c-di-GMP was enzymatically synthesized by the DGC PleD*.

2.6.4 Electrophoretic mobility shift assays

Electrophoretic mobility shift assays (EMSAs) were conducted using purified His_6-RpoS and fluorescence-labeled DNA fragments. The sequences of specific DNA probes were chosen such that they overlap with the peak ChIP-chip signal and/or the RpoS consensus box (see chapter 2.9). Non-specific control DNA fragments represent regions that were not enriched by the ChIP-chip experiments, e.g. that are part of the coding region of the house-keeping gene *gltA* or part of the intergenic region (igr) between the *rsaL* and *lasI* open reading frames.

In the beginning, DNA probes ≈200 bp in length were generated by PCR amplification using primer pair cheY2 fPr2/rPr2 for a specific DNA probe and primer pair gltA F/R for a non-specific DNA probe (Table 2.8). The primers used for amplification were ordered from Metabion (Martinsried, Germany) and carried the IRDye700 (excitation wavelength λ_{ex}= 685 nm, emission wavelength λ_{em}= 705 nm) at their 5' end. As gel shift assays using those double-stranded, long DNA fragments failed, the procedure was changed and short, IRDye700-labeled oligos (≈30 bp, Metabion, Table 2.7) were directly used as single-stranded or double-stranded DNA probes. To obtain double-stranded, short DNA fragments, complementary primers (5 µM each) were annealed in buffer containing 20 mM Tris-HCl,

Table 2.8. Oligos used for electrophoretic mobility shift assays.

Oligo	Sequence	5' Modification[a]
cheY2 fPr2	5'-CGATAGCCAATCCGTCTAAC	IRDye700
cheY2 rPr2	5'-ATCAGAATCGGTTTGCCCAT	IRDye700
gltA F	5'-GAACGCAACCTGTACCCGAACG	IRDye700
gltA R	5'-TTGTAGGGGCCGGAGAGCATTT	IRDye700
cheY2 short F[b]	5'-ACCGGACATTGTCTTTACTGGAACTAGCAA	IRDye700
cheY2 short R[b]	5'-TTGCTAGTTCCAGTAAAGACAATGTCCGGT	IRDye700
igr short F[c]	5'-ACCGAAATCTATCTCATTTGCTAGTTATAAAAT	IRDye700
igr short R[c]	5'-ATTTTATAACTAGCAAATGAGATAGATTTCGGT	IRDye700
gltA short F	5'-TGTACAAGTACTCCAAGGGCGAGCCGATGA	IRDye700
gltA short R	5'-TCATCGGCTCGCCCTTGGAGTACTTGTACA	IRDye700
PA3353 short F	5'-CCTGAACCCGACCAGCACACGTATCAAGGCACA	IRDye700
PA3353 short R	5'-TGTGCCTTGATACGTGTGCTGGTCGGGTTCAGG	IRDye700
rsmA short F	5'-CCGGCGGGACTGGTCAATACTGGGTGAAGG	IRDye700
rsmA short R	5'-CCTTCACCCAGTATTGACCAGTCCCGCCGG	IRDye700
PA0861 short F	5'-GGCAAACAGCCACTAGACTCCTACTGTTTG	IRDye700
PA0861 short R	5'-CAAACAGTAGGAGTCTAGTGGCTGTTTGCC	IRDye700

[a] labeled oligos only
[b] originally termed rpoS box F/R
[c] igr, intergenic region; originally termed lasR box F/R

pH 8, 50 mM NaCl and 10 mM $MgCl_2$ using the following conditions: 5 min at 95°C, 10 min at 58°C, 10 min at 37°C, 10 min at 20°C, cool down to 4°C.

Binding reactions (final volume 15 µl) contained 0.33 µM (single-stranded) or 0.5 µM (double-stranded) DNA probes and 0.5 µg/µl purified His_6-RpoS in binding buffer (20 mM HEPES, pH 7.5, 50 mM NaCl, 1 mM EDTA, 200 µg/ml BSA, 0.83 ng/µl poly(dIdC), 5% glycerol). The reaction mixture was incubated in the dark at room temperature for 30 min before being electrophoresed on native 5% Tris-borate-EDTA polyacrylamide gels (Bio-Rad) in TBE buffer (89 mM Tris base, 89 mM boric acid, 2 mM EDTA) at 4°C at 90 V for 45 min. Gels were scanned at 100 µm resolution with a FLA-9000 Reader (Fujifilm Europe GmbH, Düsseldorf, Germany) using the BPFR700 filter and 689 nm as excitation wavelength. Emitted light was detected at a wavelength of 700 nm. Each experiment was performed at least twice.

For competition experiments, RpoS was incubated with an excess of non-labeled DNA probes (3.3 µM – 10 µM) in binding buffer for 10 min at room temperature, before labeled oligos were added and the samples were processed as described above. Supershifts were performed by adding rabbit polyclonal RpoS antibody (6.7 ng/µl, kindly provided by V. Venturi, International Center for Genetic Engineering and Biotechnology, Trieste, Italy) to RpoS in

binding buffer, followed by incubation at room temperature for 10 min and addition of labeled oligos. In some experiments, *E. coli* core RNA polymerase (1 U/µl, Epicentre Biotechnologies) was added to the EMSA reaction mixture to test for improved binding of RpoS to the target DNA.

2.7 Phenotypic characterization assays

2.7.1 Growth curves

Planktonic growth rates of diverse *P. aeruginosa* wild-type and mutant strains were monitored using an automated growth analysis system (Bioscreen C MBR, iLF bioserve, Langenau, Germany).

LB pre-cultures were grown overnight at 37°C, diluted to an OD_{600} of 0.02 in fresh LB and transferred into a 100-well honeycomb plate (iLF bioserve, 100 µl/well, three replicates per strain). The plates were covered with a lid and incubated at 37°C with continuous shaking in a computer-controlled Bioscreen incubator. Turbidity of the bacterial suspensions (OD_{600}) was automatically measured every 15 min for a period of 16 h.

2.7.2 Motility assays

Swimming and swarming motility assays were performed as previously described [123]. In brief, swimming was evaluated on BM2 glucose plates (40 mM K_2HPO_4, pH 7, 7 mM $(NH_4)_2SO_4$, 2 mM $MgSO_4$, 10 µM $FeSO_4$, 0.4% (w/v) glucose) containing 0.3% agar and swarming on modified BM2 glucose plates (40 mM K_2HPO_4, pH 7, 2 mM $MgSO_4$, 10 µM $FeSO_4$, 0.4% (w/v) glucose) containing 0.5% agar supplemented with 0.1% Casamino acids (Difco). Freshly prepared plates (25 ml motility agar per plate) were allowed to dry for 15 min (swimming plates) or 60 min (swarming plates) under laminar flow directly before use. Plates were inoculated with 1 µl of a LB pre-culture with $OD_{600} > 1.0$ and incubated overnight at 37°C. Due to the fast swarming motility of PA01 strains, the incubation temperature was reduced to 30°C in some cases. Swimming results were analyzed by measuring the diameter of the swimming zone, while swarming was evaluated photographically.

Twitching assays were performed on LB plates with 1% agar by stab inoculation of single colonies with a toothpick. After 24-48 h incubation at 37°C, the diameter of the twitching zone at the plastic-agar interface was measured. For non-circular zones, the longest and shortest dimensions were measured and averaged.

2.7.3 Motility tracking

Bacterial cells were grown to exponential phase (OD_{600} ~1.0) in LB, diluted 1:200-1:1000 in 0.9% NaCl containing 3% (v/v) Ficoll (Sigma) and transferred into a 96-well plate with a thin glass bottom. Cells were monitored with an inverted microscope (Axiovert 135TV, Zeiss), equipped with a 25×/0.80 oil objective and a CoolSnap HQ2 camera (Visitron Systems) and operated with the MetaMorph software (version 7.5.3, Molecular Devices Corporation). Phase-contrast images visualizing cells near the glass bottom were acquired for 30 s at 5 frames per second, imported as stacks into ImageJ 1.42, where trajectories of swimming bacteria were monitored by hand.

2.7.4 Biofilm and attachment assays

Crystal violet staining of adherent cells was adopted from O'Toole and Kolter [124] with the following modifications. Overnight LB cultures were diluted to an OD_{600} of 0.02 with fresh medium. The bacterial suspensions were inoculated in PVC (polyvinyl chloride) 96-well plates (Becton Dickinson Labware) with 100 µl per well (eight replicates per strain), sealed with an air-permeable BREATHseal cover foil (Greiner Bio-One) and grown under static conditions at 37°C in an incubator with humid atmosphere. After 24 h of incubation, planktonic cells were removed and wells were washed with water (200 µl/well) prior to staining with 0.1% (w/v) crystal violet for 30 min at room temperature (150 µl/well). Wells were carefully washed with water to remove excess staining solution, air-dried and the retained crystal violet was solubilized in 95% ethanol (200 µl/well) for 30 min at room temperature. For quantification, 125 µl of the resulting solution were transferred into a 96-well polystyrene microtiter plate (Nunc) and absorbance was measured at 550 nm using a Tecan Sunrise microplate reader.

Analysis of static biofilms grown at the bottom of 96-well plates was performed as previously described [125]. In brief, overnight LB cultures were adjusted to an OD_{600} of 0.02 with fresh medium and transferred into a half-area 96-well µClear plate (Greiner Bio-One, 100 µl/well, four replicates per strain). The plate was covered with an air-permeable foil and incubated at 37°C in an incubator with humid atmosphere. After 24 h, bacteria were stained with 50 µl diluted staining solution (LIVE/DEAD BacLight Bacterial Viability kit, Molecular Probes/Invitrogen, final concentration of 1.4 µM Syto9 and 8.3 µM propidium iodide) and further incubated for 48 h at 37°C. Microscopic analysis of biofilm formation on the bottom of microtiter plates was performed using an Olympus Fluoview 1000 confocal laser scanning

microscope equipped with a 40×/0.90 air objective. Image stacks were acquired in the center of each well with a step size of 2 µm. Images of each experiment were processed and analyzed as previously described [125] and visualized using the IMARIS software package (version 5.7.2, Bitplane).

To monitor biofilm formation in the microtiter plates over time, the constitutively GFP-expressing plasmid pSunny [112] was transferred into *P. aeruginosa* by conjugation and biofilms were grown, images acquired and data analyzed as described above except that the staining step was omitted. To determine the amount of bacteria attached to the substratum, single images at the bottom of the wells were acquired. The images were processed with a pseudo flat field filter to adjust uneven luminance. The filtered, gray-scale images were thresholded to segment objects' pixel area from background pixels. The percentage of attached bacteria was calculated by determining the ratio of object pixels to the total number of pixels. All processing steps were performed using ImageJ (version 1.43).

2.8 Identification of c-di-GMP binding proteins

2.8.1 Immobilization of c-di-GMP on Sepharose 6B

C-di-GMP was synthesized by Michael Morr (Helmholtz Center for Infection Research, Braunschweig, Germany) as specified before [126]. Preparation of c-di-GMP affinity resin was performed in co-operation with Frank Schwede (Biolog, Bremen, Germany) as described previously for the immobilization of cGMP [127] with some modifications: a total of 500 mg epoxy-activated Sepharose 6B (GE Healthcare) was treated ten times with 25 ml cold deionized water. The washed resin was resuspended in 3 ml coupling buffer (100 mM $Na_2B_4O_7$, 100 mM NaCl, pH 11) and incubated with 2.2 mg (3 µmol) c-di-GMP at 40°C in a thermomixer. Progress of immobilization was monitored by analytical high-performance liquid chromatography (HPLC) using a 5% acetonitrile/ 20 mM triethylammonium formate buffer, pH 6.8, as eluent. The HPLC-system consisted of a L 6200 pump, a L 4000 variable wavelength UV-detector, and a D 2500 GPC integrator (all Merck-Hitachi). The stationary phase was YMC ODS-A 120-10 (YMC, Kyoto, Japan) in a 250 x 4.6 mm stainless steel column. The coupling reaction was proceeded for 144 h and any unreacted epoxy groups were blocked with 100 µmoles ethanolamine in coupling buffer for 24 h. After filtration and multiple washing steps (2 x 25 ml 20% ethanol, 2 x 25 ml water, 2 x 25 ml 30 mM NaH_2PO_4, pH 7) the affinity resin was stored in 30 mM NaH_2PO_4, 1% NaN_3, pH 7, at 4°C. Ligand density was 0.45 µmoles/ 100 mg resin (dry basis), as determined by HPLC-analysis during

coupling. In a control experiment, c-di-GMP was incubated in coupling buffer without affinity resin at 40°C for 144 h. After this period less than 15% degradation of c-di-GMP was detected by analytical HPLC.

To identify functional groups that react with epoxy-activated sepharose, a model reaction was performed under the above mentioned coupling conditions using the related cyclic nucleotide cGMP (Biolog, Bremen, Germany) and (*S*)-(-)-1,2-epoxy-butane (Aldrich). Obtained reaction products were analyzed with HPLC, nuclear magnetic resonance (NMR) and mass spectrometry (MS).

A control affinity resin was prepared by incubating epoxy-activated Sepharose 6B with 100 µmoles ethanolamine in coupling buffer at 40°C for 48 h.

2.8.2 Affinity pull down protocol

Main cultures (500 ml) of *P. aeruginosa* PA14 and PA01 were inoculated with a pre-culture and grown to stationary phase at 37°C. Cells were harvested by centrifugation for 10 min at 4°C and 6,000×*g*, the pellet was washed once with ice-cold phosphate buffered saline (PBS), pH 7.4, followed by a second centrifugation step. The bacteria (3.5 - 4.5 g wet weight) were resuspended in 15 ml ice-cold PBS containing 1 mM DTT, protease inhibitors (Complete mini, EDTA free, Roche) and Benzonase Nuclease (Novagen). The cells were lysed by bead beating (3 x 20 s at 4.5 m/s, Hybaid ribolyser) or by passage through a French Pressure cell (at 16,000 psi, SLM-Aminco). After a centrifugation step at 4°C, at 37,500×*g* for 45 min, the supernatant was mixed with 200 µl sepharose slurry, which has been pre-equilibrated with PBS buffer. Binding of proteins to the affinity matrix was allowed to progress for 2 h at 4°C under gentle rotation in a batch format. Subsequently, the resin was washed six times with 10 ml ice-cold PBS, before transferring the resin into a small reaction tube. Nonspecific binding was tried to be further reduced by incubating the beads with 250 µl of 10 mM cGMP in PBS and/or 10 mM GTP in PBS for 20 min at 4°C, followed by two washing steps. C-di-GMP binding proteins were then eluted by incubating the resin with 100 – 500 µM c-di-GMP in PBS for 40 min at 4°C under gentle rotation. All eluates were finally precipitated with chloroform/ methanol according to Wessel and Fluegge [128] and subjected to SDS-PAGE analysis.

This standard protocol was slightly modified. In PA01 experiment A, proteins bound to the c-di-GMP affinity beads and the control resin were finally eluted by heat treatment (95°C, 10 min). In PA01 experiment B and C and PA14 experiment 1, 1% (w/v) SDS instead of

c-di-GMP was used for final elution of proteins bound to the control sepharose. To all buffers used in PA01 experiment C, 1% (v/v) Triton was added to improve solubility of membrane associated proteins. In PA14 experiment 2, BugBuster reagent (Novagen) in 10 mM Tris-HCl, 140 mM NaCl, pH 7.4, containing protease inhibitors was used for the chemical lysis of cells (10 min at room temperature). In PA14 experiment 3, a pull down was performed using a membrane fraction in addition to the pull down with the soluble cell lysate fraction. Therefore, the pellet obtained after cell lysis and the following centrifugation step was resuspended in PBS and membranes were solubilized by adding 0.5% β-dodecylmaltoside for 1 h at 4°C and 35 rpm. The sample was then centrifuged in an ultracentrifuge for 60 min at 100,000×*g*, 4°C and the supernatant was incubated with the affinity resin as described above except that all buffers and solutions contained 0.5% β-dodecylmaltoside.

2.8.3 Sample preparation for LC-MS/MS

Coomassie stained protein bands were excised and destained in a solution containing 30% acetonitrile and 50 mM NH_4HCO_3. Destained gel slices were reduced for 30 min at 56°C with 20 mM DTT in 50 mM NH_4HCO_3 and subsequently alkylated with 20 mM iodoacetamide in 50 mM NH_4HCO_3. Gel slices were cut in small pieces, washed twice in 50 mM NH_4HCO_3 and then dried after dehydration in acetonitrile. For all procedures the volume of the solutions was higher than 20 times the gel volume. Dried samples were reswollen in a solution containing 50 mM NH_4HCO_3, 10% acetonitrile and sequencing grade modified trypsin (Promega) in a ratio of about 1:20. Digestion of the protein was performed at 37°C overnight. Peptides were subsequently eluted with H_2O, 1% triflouroacetic acid and two times 30% acetonitrile containing 0.1% triflouroacetic acid and dried in a vacuum centrifuge (Jouan RC 1010). For LC-MS/MS the dried peptides were desalted using ZipTip RP18 Tips (Millipore), evaporated again and resolubilized in 3% acetonitrile with 0.5% formic acid and centrifuged for 20 min at 100,000×*g* at 20°C.

2.8.4 LC-MS/MS analysis and database searching

LC-MS/MS was performed at the Helmholtz Center for Infection Research (Josef Wissing, Lothar Jänsch) on an Acquity Ultra Performance LC-system (Waters Corp., USA) connected to a Q-TOFmicro mass spectrometer (Waters Corp., USA) or to an Orbitrap XL mass spectrometer (Thermo Scientific). Peptides were flushed onto a C_{18} precolumn (5 µm Symmetry C_{18}, 180 µm x 20 mm, Waters Corp.) with a flow rate of 15 µl/min and washed at

constant flow for 3 min. Peptides were then separated on an analytical column (1.7 µm BEH130, 75 µm x 150 mm, Waters Corp.) with UPLC buffer A (0.1% formic acid in water) and UPLC buffer B (0.1% formic acid in acetonitrile) via linear B gradients from 0 – 25% at a flow rate of 300 nl/min controlled with AcquityUPLC software V1.22. Data-dependent acquisition of MS and MS/MS data was under control of MassLynx (V4.1, Q-TOFmicro) or Xcalibur ™ software (V2.1, Orbitrap XL). Doubly and triply charged peptide ions were automatically selected and fragmented with m/z dependent collision energy settings. The peak lists (Q-TOFmicro) or raw data files (Orbitrap XL) were processed using the Mascot Deamon (V2.1). Database searches were carried out with a local Mascot server (V2.2) in a PA01 or PA14 database (NCBI) using the given settings (enzyme, trypsin; maximum missed cleavages, 1; fixed modification: carbamidomethyl (Cys), and variable oxidation (Met); peptide tolerance, 150 ppm (Q-TOFmicro) or 10 ppm (Orbitrap XL); MS/MS tolerance, 0.3 Da). Scaffold (version Scaffold_3_00_03, Proteome Software Inc.) was used to validate MS/MS based peptide and protein identifications. Proteins were only accepted as identified when at least 1 unique peptide showed 95% confidence and the total protein identification confidence was at least 95%. Peptide probabilities were specified by the Peptide Prophet algorithm [129] and protein probabilities were assigned by the Protein Prophet algorithm [130].

2.9 ChIP-chip

2.9.1 Chromatin immunoprecipitation

Chromatin immunoprecipitation (ChIP) was carried out based on previously described procedures [131, 132]. PA01 wild-type cells were grown in LB at 37°C to stationary phase (OD_{600} of 2.0). To cross-link protein to DNA, formaldehyde was added to 30 ml culture to a final concentration of 1%. After incubation at room temperature for 20 min with gentle agitation, the reaction was quenched by the addition of glycine (final concentration 0.5 M) followed by incubation for 5 min at room temperature. Cells were harvested by centrifugation at 2,500×*g* at 4°C for 10 min, washed once with cold Tris buffered saline (TBS), pH 7.6, and resuspended in 500 µl of lysis buffer (10 mM Tris-HCl, pH 8, 20% (w/v) sucrose, 50 mM NaCl, 10 mM EDTA) containing 4 mg/ml lysozyme. The bacterial cells were incubated for 30 min at 37°C, before 500 µl immunoprecipitation (IP) buffer (50 mM HEPES-KOH, pH 7.5, 150 mM NaCl, 1 mM EDTA, 1% (v/v) Triton, 0.1% (m/v) sodium deoxycholate) containing 1 mM phenylmethylsulfonyl fluoride (PMSF) was added. The lysates were chilled

on ice and then DNA was shared to an average fragment size of 50-500 bp using a Branson S250 sonicator with a 5 mm standard tip (settings: 8 x 60 s, 90% duty, output control: 6). Cell debris were removed by centrifugation at 18,000×*g* for 10 min and the supernatant was aliquoted and stored at –70°C until use.

For immunoprecipitation, 20 µl pre-equilibrated Protein A-sepharose 4B beads (Sigma) were coated with 10 µg rabbit polyclonal RpoS antibody (kindly provided by V. Venturi, International Center for Genetic Engineering and Biotechnology, Trieste, Italy) in IP buffer for 1 h at room temperature with gentle mixing. For control experiments, an irrelevant rabbit polyclonal antibody was coupled to the Protein A-beads under the same conditions. In parallel, chromosomal DNA of 100 µl cross-linked cell extracts was pre-cleared by incubation with 20 µl blank Protein A-beads in 700 µl IP buffer containing 1 mM PMSF. The samples were centrifuged for 2 min at 425×*g*, and the supernatant was then incubated with the antibody-coated Protein A-beads for 1.5 h at room temperature under gentle agitation. The beads were washed twice with IP buffer, once with IP buffer supplemented with 500 mM NaCl, once with wash buffer (10 mM Tris-HCl, pH 8, 250 mM LiCl, 1 mM EDTA, 0.5% (v/v) Nonidet-P40, 0.5% (m/v) sodium deoxycholate) and once with TE buffer (10 mM Tris-HCl, pH 7.5, 1 mM EDTA). Immunoprecipitated complexes were eluted by incubation of the beads with 60 µl elution buffer (50 mM Tris-HCl, pH 7.5, 10 mM EDTA, 1% (m/v) SDS) at 65°C for 10 min. Beads were removed by centrifugation and cross-links were reversed by the addition of protease (0.1 µg/µl, dissolved in deionized water, Sigma) and incubation for 2 h at 42°C and for 6 h at 65°C. DNA was purified using a PCR purification kit (Quiagen). All ChIPs were performed twice.

2.9.2 Amplification of immunoprecipitated DNA

ChIP DNA was amplified based on the Affymetrix chromatin immunoprecipitation assay protocol [133].

In an initial round of linear amplification, random primers (PrimerA: 5'-GTTTCCCAGTCACGGTC$(N)_9$) were incorporated into immunoprecipitated DNA. Briefly, 10 µl purified ChIP DNA were mixed with 4 µl random primers (200 µM) in Sequenase reaction buffer (USB Corporation, Cleveland, Ohio, USA) and incubated for 4 min at 95°C followed by rapid cooling on ice. To this mixture, 2.6 µl first cocktail (specified in Table 2.9) was added and linear amplification was performed as described in Table 2.10.

Table 2.9. First cocktail for linear amplification of ChIP DNA.

Component	Volume for 1 reaction
20 mg/ml BSA	0.1 µl
0.1 M DTT	1 µl
25 mM dNTPs	0.5 µl
Sequenase[a] 1.3 U/µl	1 µl
Total volume	*2.6 µl*

[a] purchased from USB Corporation, USA

Table 2.10. Reaction conditions for linear amplification of ChIP DNA.

Step	Conditions
1	10°C for 5 min
2	Ramp from 10°C to 37°C in 9 min
3	37°C for 8 min
4	95°C for 4 min
5	Rapid cooling on ice
6	10°C hold
7	Add 1 µl of 1.3 U/µl Sequenase to each sample
8	Repeat step 1-7 three times
9	4°C hold

After DNA purification (PCR purification kit, Quiagen), DNA was PCR amplified using the corresponding 5'-GTTTCCCAGTCACGGTC primer (PrimerB) and a dNTP/dUTP mix (10 mM dATP, 10 mM dCTP, 10 mM dGTP, 8 mM dTTP, 2 mM dUTP). The detailed reaction mixture and the PCR program are listed in Table 2.11 and Table 2.12. Amplified DNA was purified using a PCR purification kit (Quiagen).

Table 2.11. Reaction mixture for PCR amplification of ChIP DNA.

Component	Volume for 1 reaction
Purified DNA	10 µl
10 mM dNTPs+dUTP	3.75 µl
100 µM PrimerB[a]	4 µl
GoTaq (5 U/µl, Promega)	2 µl
5x PCR buffer	20 µl
25 mM $MgCl_2$	10 µl
Nuclease-free water	50.25 µl
Total volume	*100 µl*

[a] PrimerB: 5'-GTTTCCCAGTCACGGTC

Table 2.12. Reaction conditions for PCR amplification of ChIP DNA.

Step	Temperature	Time
1	95°C	5 min
2	95°C	30 s
3	45°C	30 s
4	55°C	30 s
5	72°C	1 min
6	step 2-5 repeated 15-30 times	
7	95°C	30 s
8	45°C	30 s
9	55°C	30 s
10	72°C	1 min, dt 5 s[a]
11	step 7-10 repeated 15-30 times	
12	4°C	hold

[a] add 5 s for each subsequent cycle

2.9.3 Microarray analysis

Approximately 7.5 µg of amplified DNA from the control and the RpoS IPs were fragmented to a fragment size of 50-500 bp and terminally labeled using the GeneChip WT double stranded DNA terminal labeling kit (Affymetrix) according to the instructions of the manufacturer. The biotin-labeled DNA was hybridized to an Affymetrix *P. aeruginosa* genome chip as described previously [104].

Enrichment of hybridization signals was calculated (by Andreas Dötsch, Helmholtz-Center for Infection Research) with the Tiling Analysis Software (TAS, Affymetrix) from two independent RpoS IPs compared to two independent control IPs (bandwidth parameter was set to 150 bp). For each gene (PA01 annotation taken from the *Pseudomonas* genome database, [134]), the promoter region was defined as the sequence from -300 to -1 bp, excluding overlap to upstream coding regions. Promoter enrichment was defined as the maximum enrichment found within the promoter region.

2.9.4 Identification of an RpoS consensus sequence

Promoter regions were scanned by Andreas Dötsch (Helmholtz Center for Infection Research) with the web-based programs CONSENSUS and PATSER [135] (available at http://rsat.ulb.ac.be/rsat/) to detect RpoS consensus sequences. Sequence logos were created with WebLogo (http://weblogo.berkeley.edu). The initial consensus sequence was derived from a set of 16 RpoS-regulated genes as described previously [136] and used for the pattern based search of the sequences from -300 to -1 bp upstream of each open reading frame,

excluding coding regions. A revised consensus sequence was derived analogously from a set of 32 genes that were positive in all three criteria (enriched by ChIP, differentially regulated, consensus sequence identified, see chapter 3.3.2). The detection of consensus sequences by PATSER was limited to a weight score of 6.0.

3 Results

3.1 Characterization of the chemotaxis methyltransferase CheR1 and its impact on biofilm formation

3.1.1 Objective

In *E. coli,* CheR methylation activity is strongly enhanced upon binding to a conserved pentapeptide sequence (NWETF) at the C-terminus of highly abundant methyl-accepting chemotaxis proteins [137, 138]. Homologous pentapeptide structures are present in *P. aeruginosa* in only 2 of the 26 MCPs (CttP and Aer2 [33]). These two are organized on the chromosome in the vicinity of the *che2* system, whose predicted gene products (including CheR2) exhibit an even higher overall sequence identity to orthologous *E. coli* chemotaxis proteins [33]. To test whether *P. aeruginosa* CheR1 methylates MCPs that lack the pentapeptide motif, methylation assays with the chemoreceptor PctA (PA4309) were established. Another aim was to elucidate the role that the Che1 chemotaxis system might play in biofilm formation of *P. aeruginosa.*

3.1.2 Methylase activity of CheR1

The PA01 PA3348 gene product is predicted to be a probable chemotaxis protein methyltransferase (CheR1, www.pseudomonas.com, [139]). This function was proposed based on limited amino acid identity (31%) to the experimentally studied CheR gene product in *E. coli* and a conserved domain for *S*-adenosylmethionine (SAM) binding.

To characterize *P. aeruginosa* receptor methylation and to gain insight into methylation of MCPs lacking the pentapeptide motif, CheR1 was expressed with a C-terminal His_6-tag and purified by affinity chromatography using Ni-NTA agarose resin. Since chemotaxis methyltransferases use SAM as a substrate for receptor methylation, interaction of this coenzyme with *P. aeruginosa* CheR1 was analyzed by surface plasmon resonance in co-operation with the group of F. W. Herberg (University of Kassel). Purified CheR1-His_6 was immobilized on a sensor chip and SAM was injected over the sensor surface as an analyte in the mobile phase. In general, complex formation on the sensor surface causes SPR signals that are displayed as resonance units (RU, 1000 RU corresponds to 1 ng/mm^2) [140]. Here, increasing concentrations of injected SAM resulted in increased binding signals (Figure 3.1A). The obtained binding signals were plotted against the employed SAM concentration

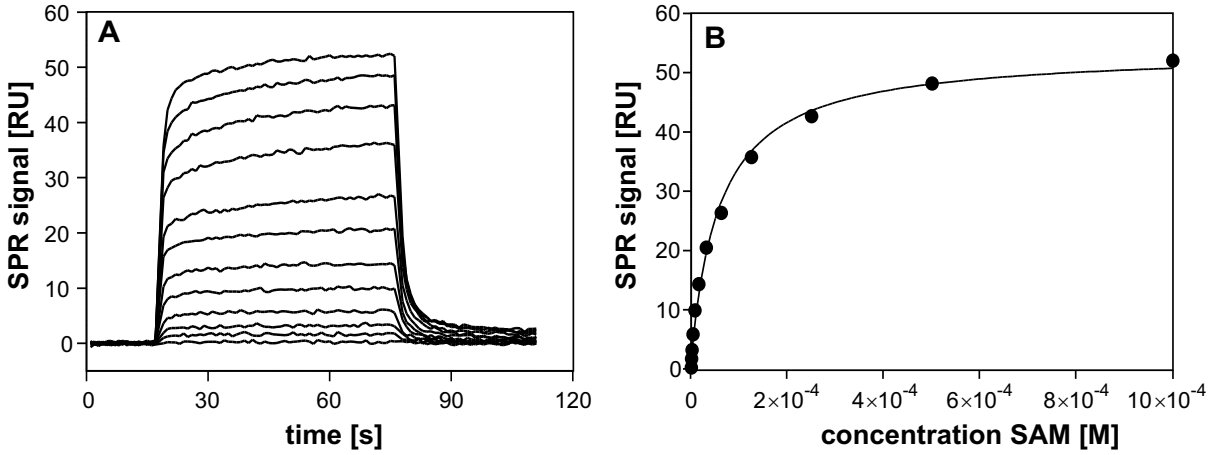

Figure 3.1. Surface plasmon resonance (SPR) analysis of the interaction of CheR1-His$_6$ and SAM using a Biacore S51.
CheR1 was immobilized on the sensor surface using standard amine coupling chemistry. The CheR1 interaction partner SAM was injected over the sensor surface. (A) SPR signals were detected for association (60 seconds) and dissociation (200 seconds) of SAM to CheR1. The graph shows the kinetic data for 12 SAM concentrations with data for the lowest (500 nM) to the highest (1 mM) SAM concentration displayed from bottom to top. (B) Data from (A) were analyzed with a steady state model. The resulting dissociation constant (K_D) was determined to be 61 µM.

and analyzed with a steady-state model (Figure 3.1B), revealing a binding constant (K_D) of 61 µM.

Next, *in vitro* methylation assays were performed by the utilization of purified *P. aeruginosa* His-tagged CheR1 protein, the methyl donor SAM and membranes from an *E. coli* strain (HCB721) effectively gutted of all the chemotaxis genes [108]. HCB721 cells were transformed with an IPTG inducible plasmid encoding the *P. aeruginosa* PctA receptor and membranes containing PctA were prepared as described under Materials and Methods (see chapter 2.6.2). Figure 3.2A depicts the initial methylation rate of the PctA receptor and demonstrates that PctA was methylated by the methyltransferase CheR1.

Previous studies have demonstrated, that PctA, in concert with the MCPs PctB and PctC, is responsible for the detection of amino acids in *P. aeruginosa* [141, 142]. Chemotactic assays of *pctA pctB pctC* triple mutants supplemented with either one of these MCP genes revealed that PctA, PctB and PctC detected 18 amino acids, 6 amino acids and 2 amino acids, respectively [142]. Among these amino acids, for example, serine was only detected by PctA, whereas glutamine was only detected by PctB. Therefore, the effect of these two amino acids on the methylation rate of PctA was tested. In accordance to the previous chemotactic experiments, the presence of serine, but not glutamine, increased the methylation rate of PctA by at least 1.2-fold ($p<0.001$, Figure 3.2B).

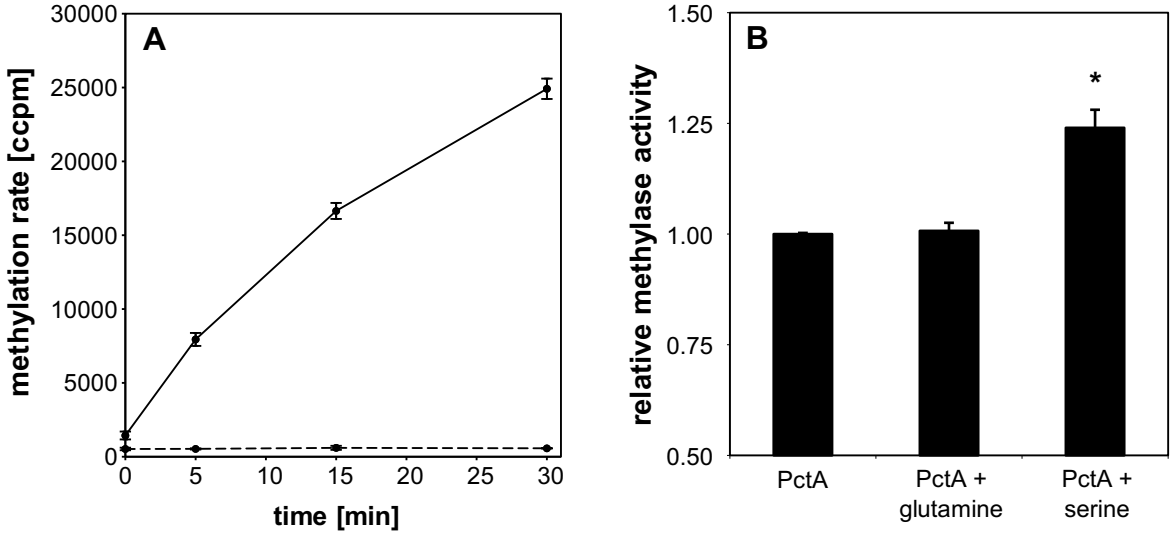

Figure 3.2. Methylation of the methyl-accepting chemotaxis protein PctA by CheR1-His$_6$ using [^{3}H-methyl]-SAM as the methyl donor.

(A) Methylation rate of *E. coli* HCB721 membranes containing no MCP (dashed line) or the *P. aeruginosa* MCP PctA (continuous line). (B) Methylation reactions carried out for 15 min in the presence of 1 mM serine resulted in a significantly increased methylation rate of the MCP PctA (* p<0.001, paired t-test), whereas the addition of glutamine had no effect.

Representative data from one experiment out of at least two are shown. Error bars are standard deviations of three replicates. ccpm – corrected counts per minute.

3.1.3 Motility defect of the *cheR1* mutant

In agreement with results described by Kato *et al.* [34], analysis of *cheR1* transposon mutants in the PA01 and PA14 strain background (correct insertion of transposon was confirmed by PCR) revealed a severely impaired swimming motility in minimal medium soft agar plates (Figure 3.3A and B). Both *cheR1* transposon mutants formed only small diameter swim rings in contrast to the diffuse large-diameter swim rings observed in the wild-type control and the complemented mutant strains. This phenotype defect is characteristic for mutants that cannot respond to a chemical gradient generated upon nutrient consumption, and was not due to a defect in the growth rate (data not shown). By contrast, the *cheR1* mutant and complemented mutant strain were positive in swarming (Figure 3.3C and D) and twitching (Figure 3.3E and F) in both the PA01 and PA14 strain background.

To characterize the swimming motility defect in more detail, the cells were observed by light microscopy. In general, *E. coli* bacteria move unidirectional with periodic pauses that involve active tumbling, which reorients the cell prior to continued forward motion. This essential random movement can be biased through taxis mechanisms that modify the frequency of reorientations [18, 19]. However, the mono-flagellated *P. aeruginosa* swims in a straight,

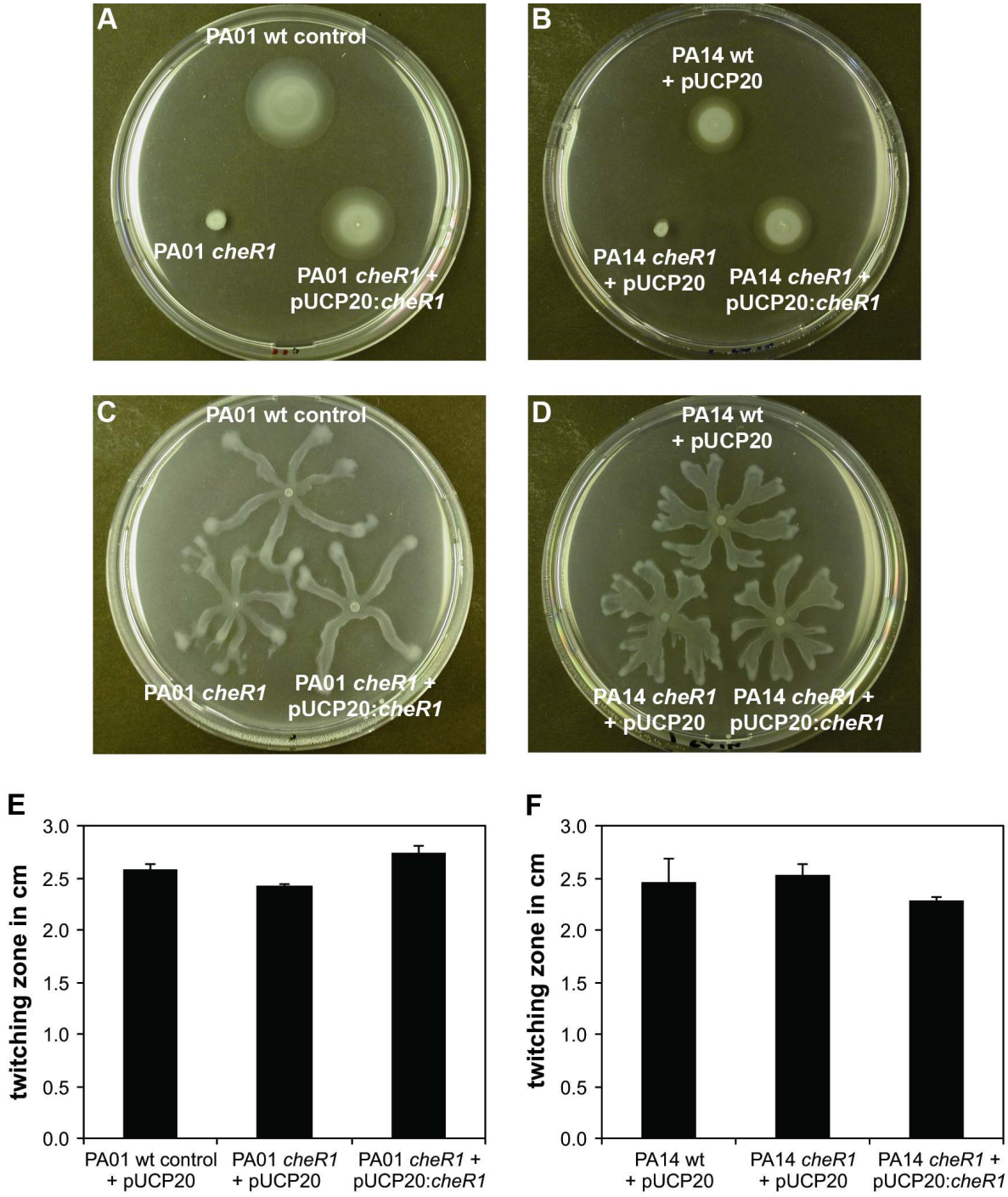

Figure 3.3. Motility phenotype of the *cheR1* mutant and the complemented strain of PA01 (A, C, E) and PA14 (B, D, F).

(A, B) Swimming assays were performed on minimal medium soft agar plates supplement with 0.3% agar. The impaired swimming motility of the *cheR1* mutant can be complemented by providing the *cheR1* gene *in trans*. (C, D) Swarming assays were performed on minimal medium plates supplemented with 0.5% agar. All strains, the wild-type/wild-type control, the *cheR1* mutant and the complemented *cheR1* mutant, were capable of swarming. (E, F) Twitching zones were measured at the plastic-agar (LB-agar, 1.5%) interface after 36 h. All strains, the wild-type/wild-type control, the *cheR1* mutant and the complemented *cheR1* mutant displayed similar twitching motility.

Representative data from one experiment out of at least three are shown. Error bars are standard deviations of three replicates.

back-up, turn mode (described by Pratt *et al.* [55]), driven by a (i) counter-clockwise rotation of the flagellum, (ii) brief reversal and (iii) reorientation. Both *P. aeruginosa* strains (PA01 and PA14) were motile and exhibited the run/back-up/run mode of swimming, although obviously the PA14 strain did not exhibit as many stops/reorientations, as compared to the

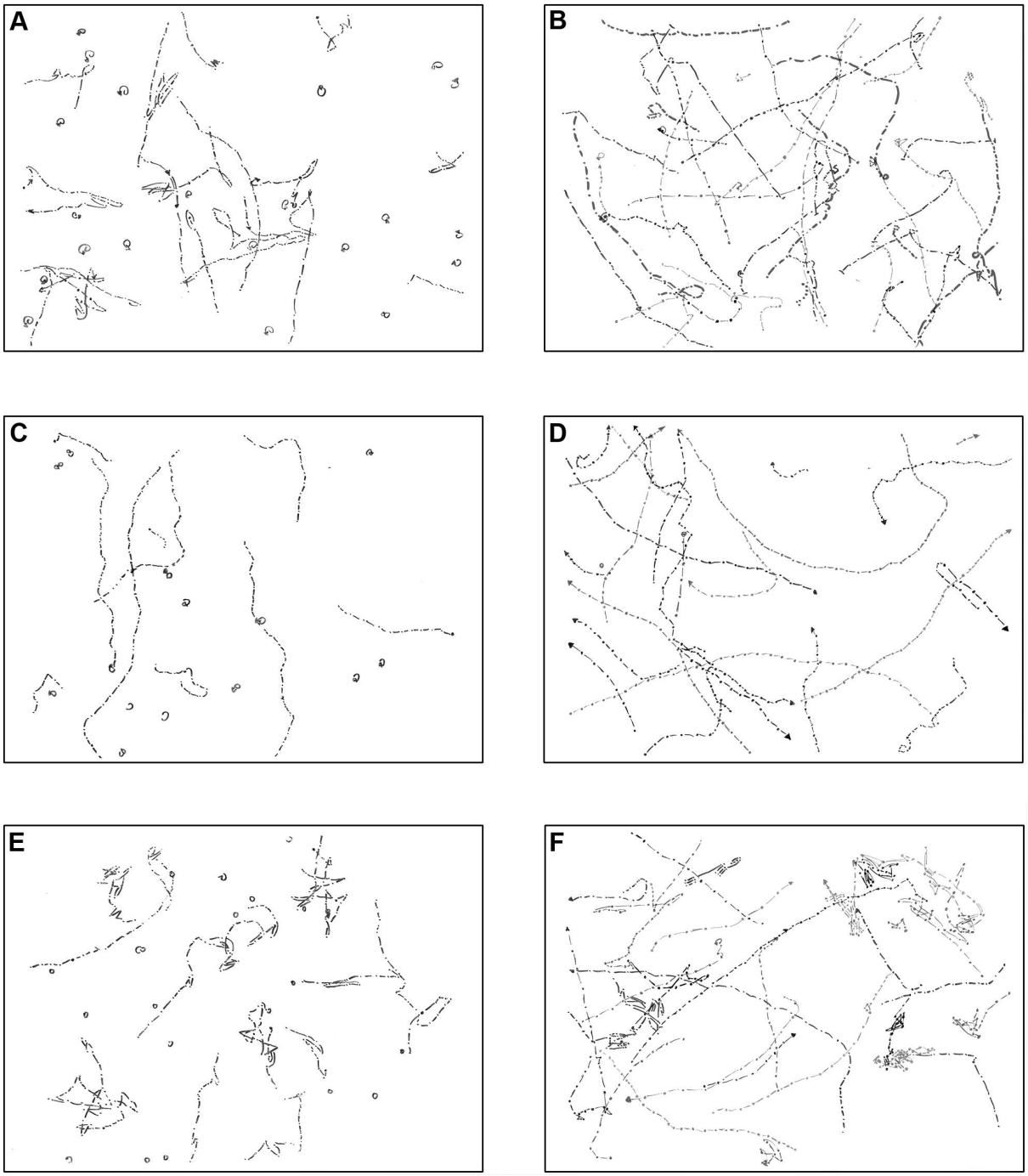

Figure 3.4. Motility defect of the *cheR1* mutant as observed by light microscopy.
(A, B) The wild-type (A, PA01 wt control and B, PA14 wt) exhibits a straight forward - short backup/reversal - straight forward mode of swimming. (C, D) The *cheR1* mutant (C, PA01 and D, PA14) changes its direction less frequently than the wild-type and tends to swim straight. (E, F) The *cheR1* mutant complemented with pUCP20:*cheR1 in trans* (E, PA01 and F, PA14) is oscillating rapidly between forward and backward swimming.

PA01 wild-type control under the tested conditions (Figure 3.4A and B). The *cheR1* mutants were also motile, but tended to swim straight and exhibited less frequent stops/reorientations as opposed to the PA01 and PA14 wild-type controls (Figure 3.4C and D). When the *cheR1* mutants were complemented with *cheR1 in trans*, the effect of CheR became more pronounced. The complemented *cheR1* mutants exhibited clearly more reversals as compared with the respective wild-type control and *cheR1* mutant in both strain backgrounds (Figure 3.4E and F).

3.1.4 Compromised biofilm formation of the *cheR1* mutant

The *cheR1* mutant of PA14 was further monitored for attachment and biofilm formation. A microtiter plate based crystal violet (CV) staining assay was used for the determination of attached biomass following a 24 h incubation period of static cultures. As depicted in Figure 3.5, no clear difference in biomass attached to the well-wall could be observed between the PA14 wild-type, the PA14 *cheR1* transposon mutant and the complemented strain.

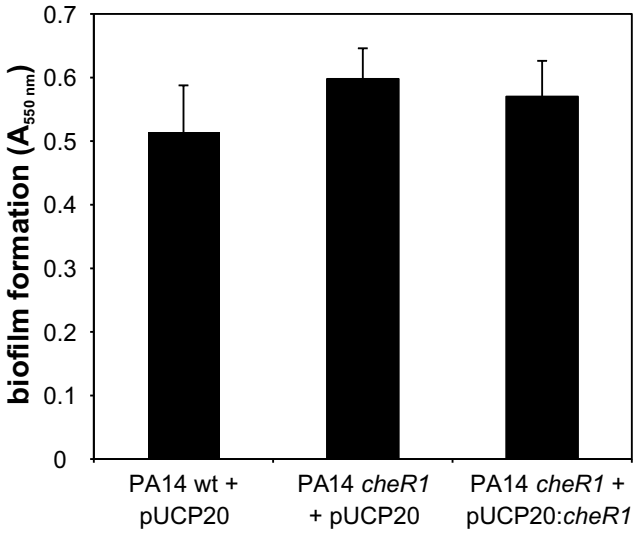

Figure 3.5. Crystal violet (CV) staining assay for the determination of attached biomass. PA14 wild-type carrying the vector control (pUCP20), the PA14 *cheR1* mutant carrying the vector control (pUCP20) and the complemented PA14 *cheR1* mutant (carrying pUCP20:*cheR1*) were grown in LB for 24 h at 37°C under static conditions before staining with CV. Representative data from one experiment out of five are shown. Error bars are standard deviations of eight replicates.

Next, the formation of biofilms on the bottom of a 96-well plate was examined. Confocal laser scanning microscopy (CLSM) of biofilms stained with the BacLight Live/Dead stain revealed a severe biofilm defect of the PA14 *cheR1* mutant after 72 h of static growth in LB. A plasmid-borne copy of the deleted wild-type *cheR1* gene complemented the mutant

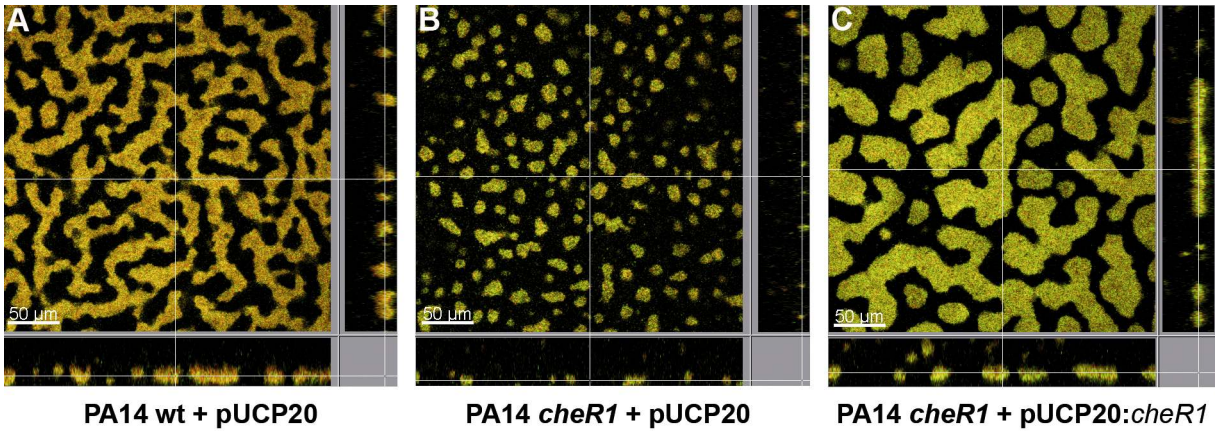

Figure 3.6. Confocal laser scanning micrographs of *P. aeruginosa* biofilms grown in LB at the bottom of a 96-well plate.
Biofilms were stained with the BacLight Live/Dead stain. Biofilm development at 72 h is shown for (A) PA14 wild-type carrying the vector control (pUCP20), (B) the PA14 *cheR1* transposon mutant carrying the vector control (pUCP20) and (C) the complemented PA14 *cheR1* mutant (carrying pUCP20:*cheR1*). The central image shows a XY section through the biofilm and the flanking pictures show vertical sections. Scale bars, 50 µm.

phenotype (Figure 3.6). To characterize the differences in biofilm formation in more detail, PA14 wild-type and *cheR1* mutant cells were tagged with plasmid-borne GFP (which did not alter their phenotypes on swim-agar plates and in the crystal violet biofilm assay, data not shown) and biofilm formation was monitored over time.

After 1 h, only a few cells were found at the bottom of a 96-well plate, in both the wild-type and the *cheR1* mutant, the majority of which was non-motile. Within the next hours, the number of swimming bacteria increased. Thereby, bacteria of the wild-type strain accumulated at the bottom of the well but remained highly motile until the space was

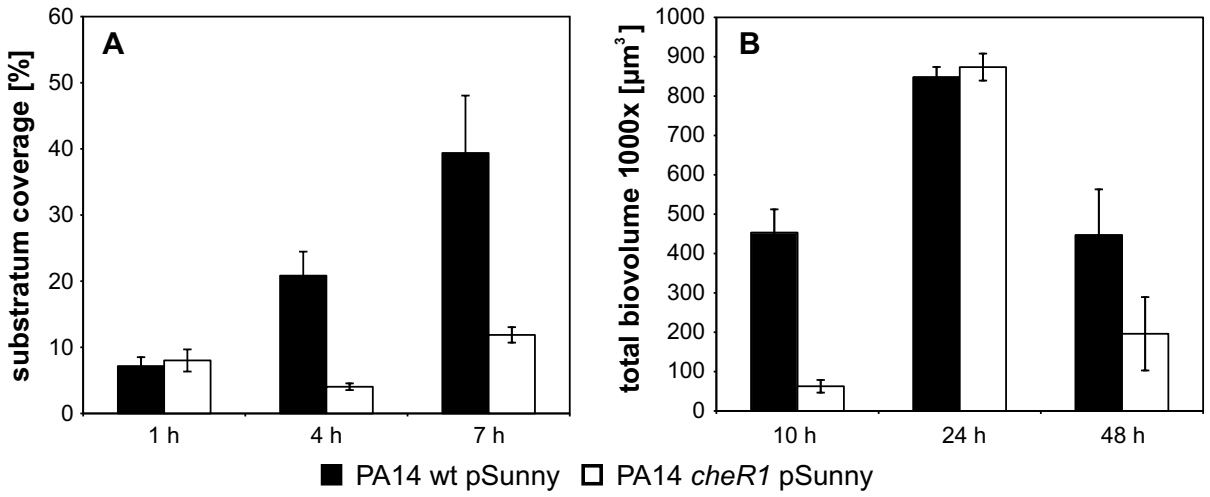

Figure 3.7. Differences in the development of GFP-expressing PA14 wild-type and *cheR1* mutant biofilms.
(A) Quantification of the substratum coverage at the well-bottom of a 96-well plate after 1 h, 4 h and 7 h. (B) Quantification of the biovolume after 10 h, 24 h and 48 h. Representative data from one experiment out of at least two are shown. Error bars are standard deviations of at least four replicates.

completely occupied by bacteria. In contrast, far less bacteria of the *cheR1* mutant strain were found in the proximity of the bottom, and surface sampling of motile bacteria proceeded only slowly. The differences in early substratum coverage by the wild-type and the *cheR1* mutant are quantified in Figure 3.7A and representative pictures for both strains at different time points are depicted in Figure 3.8.

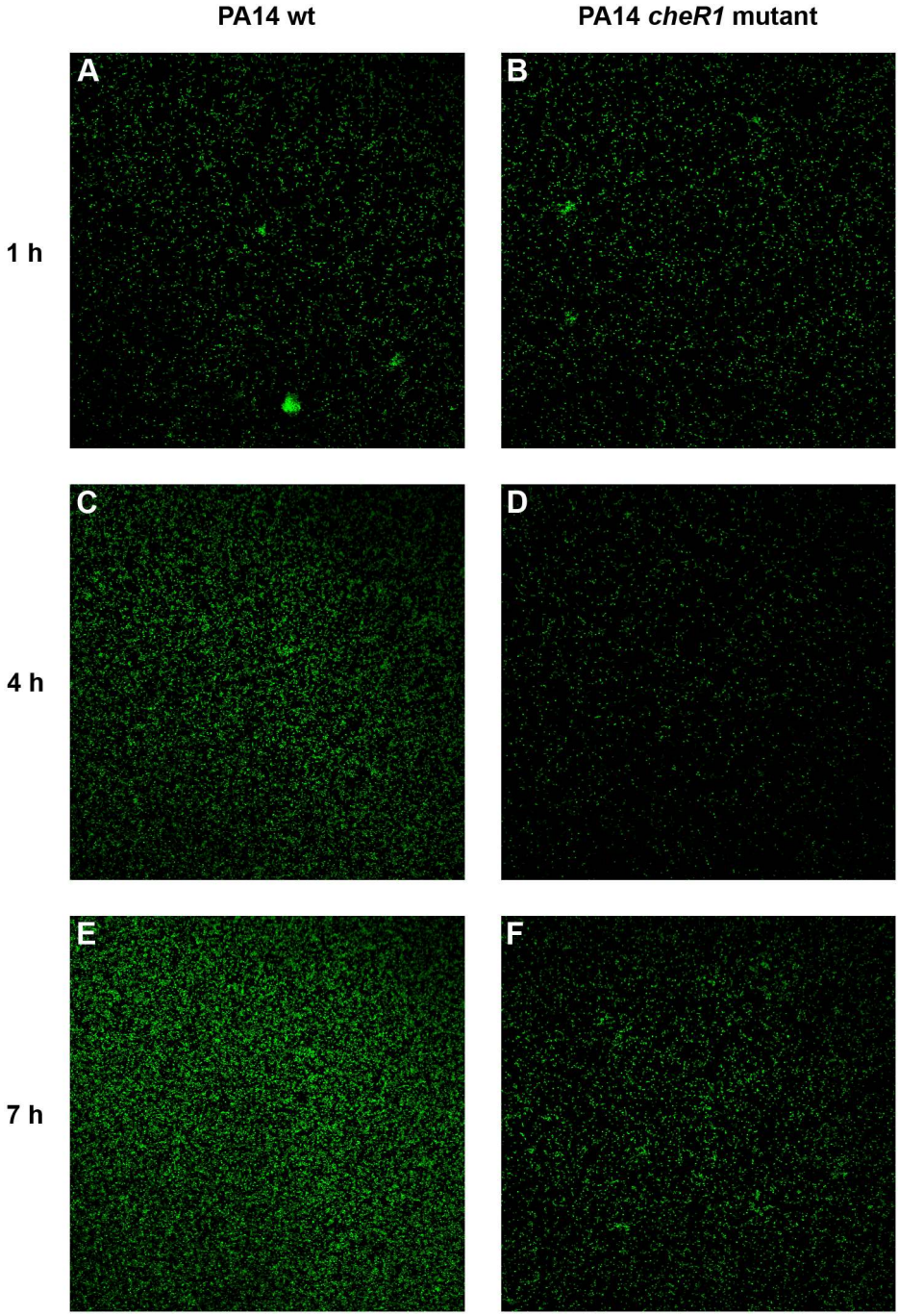

Figure 3.8. Substratum coverage by GFP-tagged bacteria as monitored by CLSM.
The coverage of the well-bottom of a 96-well plate was monitored after (A, B) 1 h, (C, D) 4 h and (E, F) 7 h. The cell clusters observed in (A) and (B) are likely to originate from cell clumps of overnight grown pre-cultures used for inoculation. (A, C, E) PA14 wild-type and (B, D, F) PA14 *cheR1* transposon mutant.

The formation of mature biofilms was then monitored by three dimensional confocal laser scanning microscopy (CLSM). After 10 h, biofilm formation of the *cheR1* mutant was severely delayed as compared with the wild-type (Figure 3.7B and Figure 3.9A and B). Nevertheless, after 24 h, the structure and biovolume of *cheR1* biofilms were found to be very similar to that of wild-type biofilms (Figure 3.7B and Figure 3.9C and D). In the following hours, the wild-type and the *cheR1* mutant biofilm underwent structural rearrangement.

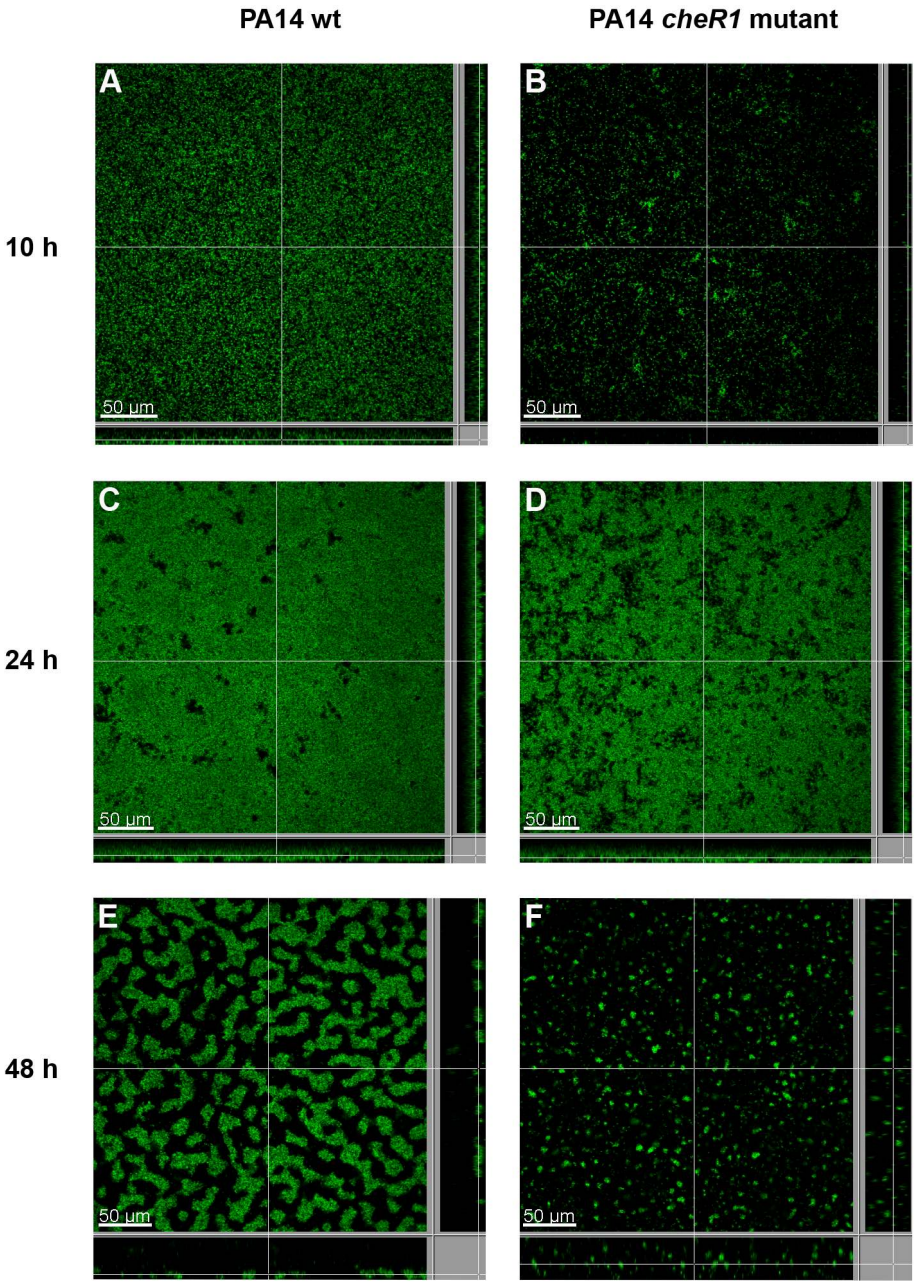

Figure 3.9. Confocal laser scanning micrographs of *P. aeruginosa* biofilms grown in LB.
Biofilm development in a well of a 96-well plate at (A, B) 10 h, (C, D) 24 h and (E, F) 48 h is shown for (A, C, E) PA14 wild-type carrying the GFP-expression vector pSunny and (B, D, F) the PA14 *cheR1* transposon mutant carrying the GFP-expression vector pSunny. The central image shows a XY section through the biofilm and the flanking pictures show vertical sections. Scale bars, 50 µm.

Whereas the wild-type formed cohesive and densely packed biofilm structures, the mutant biofilm was characterized by a more loosely, and in parts disconnected, architecture and an overall lower biomass (Figure 3.7B and Figure 3.9E and F). In summary, cells lacking the chemotaxis methyltransferase CheR1 were delayed in biofilm formation on the bottom of a 96-well plate and their mature biofilms displayed a different architecture compared with the structures of wild-type biofilms.

3.2 Identification and characterization of c-di-GMP binding proteins

3.2.1 Objective

High levels of the second messenger c-di-GMP are known to suppress motility and to promote the establishment of biofilms, but little is known about how c-di-GMP mediate its regulatory effects. The identification of c-di-GMP binding proteins by extensive bioinformatic studies seems to have come to an end and the search for new output targets has been largely hampered by the limited disposability of pure c-di-GMP.

The chemist Michael Morr, working at the Helmholtz Center for Infection Research, was able to perform the complicated and laborious chemical synthesis of c-di-GMP, and in co-operation with Frank Schwede (Biolog Life Science Institute in Bremen), this c-di-GMP was immobilized on sepharose beads. The aim of this thesis was to use the c-di-GMP coupled sepharose as an affinity matrix for the isolation of c-di-GMP binding proteins of *P. aeruginosa*, which subsequently should be identified by mass spectrometry (in co-operation with the group of Lothar Jänsch, Helmholtz Center for Infection Research). Furthermore, phenotypic assays should be employed to elucidate molecular functions of verified c-di-GMP binding proteins.

3.2.2 Coupling of c-di-GMP to sepharose beads

For the utilization of immobilized c-di-GMP as a bait for its cellular effector molecules, chemically synthesized c-di-GMP was coupled to epoxy-activated sepharose under alkaline conditions (communicated by Frank Schwede, Biolog, Bremen). Although very high amounts of c-di-GMP were required and the coupling reaction proceeded only slowly, c-di-GMP was covalently linked to the sepharose beads at sufficient quantities and at an overall efficiency of 75%. Under these conditions, degradation of c-di-GMP was below 15% (data not shown). HPLC analysis during the coupling reaction indicated a final ligand density of 0.45 µmol per 100 mg resin (dry basis).

HPLC, NMR and MS analysis were further used to identify functional groups of the c-di-GMP molecule involved in the chemical binding to the sepharose matrix. As a model compound accessible in larger quantities, the closely related nucleotide cGMP was reacted with epoxybutane under similar coupling conditions resulting in one main product (more than 35%) and at least six byproducts. For the main product, a monosubstitution at position N1 of the guanine-ring was demonstrated by NMR (data not shown). The byproducts seemed to be

partly multisubstituted at position N7 (guanine-ring) and position 2'OH (ribose-ring) as depicted in Figure 3.10. As c-di-GMP contains two guanosine moieties, it cannot be excluded that the compound is, at least partially, coupled to the sepharose beads via both guanosine units.

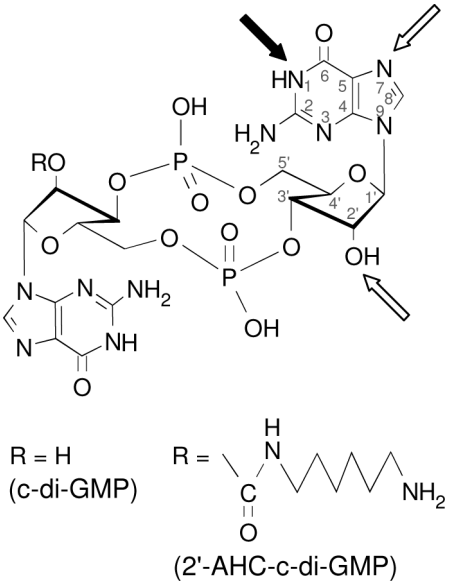

Figure 3.10. Chemical structure of c-di-GMP.
The black arrow indicates the main coupling position of c-di-GMP to the sepharose matrix, framed arrows indicate possible coupling positions of byproducts. Multisubstitutions within the same or with the second guanosine moiety cannot be excluded. In 2'-AHC-c-di-GMP, the 2'OH group of one ribose-ring is substituted with a 6-aminohexylcarbamoyl group.

3.2.3 The *P. aeruginosa* PA01 c-di-GMP interactome

The c-di-GMP coupled sepharose served as an enrichment tool to isolate c-di-GMP binding proteins from the *P. aeruginosa* strain PA01 by affinity chromatography. Epoxy-activated sepharose transformed with ethanolamine was used as a negative control, in order to identify proteins that bind to the sepharose matrix nonspecifically.

Three independent experiments were performed, termed A, B and C. The c-di-GMP affinity and control beads were incubated with freshly prepared soluble PA01 cell lysates obtained from stationary phase cultures. After extensive washing steps, bound proteins were eluted by heat treatment (10 min, 95°C) in experiment A, while in experiment B and C enriched proteins were eluted with a 0.5 M c-di-GMP solution from the c-di-GMP resin and with a 1% SDS solution from the control resin. In experiment C, 1% Triton was included in the lysis-, wash- and elution-buffer. Eluted proteins were analyzed following SDS-PAGE by automated peptide sequencing (LC-MS/MS), and the inspection of the derived result lists was supported

Table 3.1. Pulled down proteins of three distinct experiments performed with PA01 lysates using the c-di-GMP affinity resin and the control resin.

	Experiment A[a]	Experiment B[b]	Experiment C[c]	Number of distinct proteins
Proteins enriched by the c-di-GMP sepharose	13	5	9	18
Proteins enriched by the control sepharose	30	44	61	66
Proteins enriched by the c-di-GMP sepharose, but not by the respective control sepharose	10	5	3	10
Proteins enriched by the c-di-GMP sepharose, but not by any control sepharose	10	5	3	10

[a] performed with soluble cell lysate, elution of bound proteins by heat treatment
[b] performed with soluble cell lysate, elution of bound proteins with 0.5 M c-di-GMP (c-di-GMP resin) or 1% SDS (control resin)
[c] performed with soluble cell lysate, 1% Triton in all buffers, elution of bound proteins with 0.5 M c-di-GMP (c-di-GMP resin) or 1% SDS (control resin)

by the Scaffold software program. Thereby, proteins were only included in the final result list if they had been identified with a very high probability (confidence interval $\geq 95\%$, see chapter 2.8.4).

Table 3.1 displays the total number of proteins identified in each PA01 pull down experiment. Overall, more proteins were isolated on the control sepharose as compared with the respective c-di-GMP sepharose, suggesting that c-di-GMP coupling reduces nonspecific binding of proteins to the resin. Comparison of the results of all three control pull downs revealed a large overlap in the control bead-proteome: 43 out of 66 proteins were found to bind to the control resin in at least two of the three performed experiments (Figure 3.11). To validate specificity of protein binding, results of each of the three c-di-GMP pull down experiments were first compared to the results of the respective control pull down, before using the combined results of all control pull downs (experiment A-C) as a reference. This evaluation led to the identification of ten distinct putative c-di-GMP targets of PA01, listed in Table 3.2.

Among those candidates, there is one protein for which c-di-GMP binding has been recently demonstrated [82]: PA3353 which harbors a conserved PilZ domain. The specific identification of this known c-di-GMP effector molecule in all three performed pull down experiments is strong evidence for the applicability of our approach. Furthermore, two proteins possessing domains involved in c-di-GMP metabolism were identified in at least two of the three pull downs conducted: PA2567 and PA4396. Of particular interest is PA4396, a

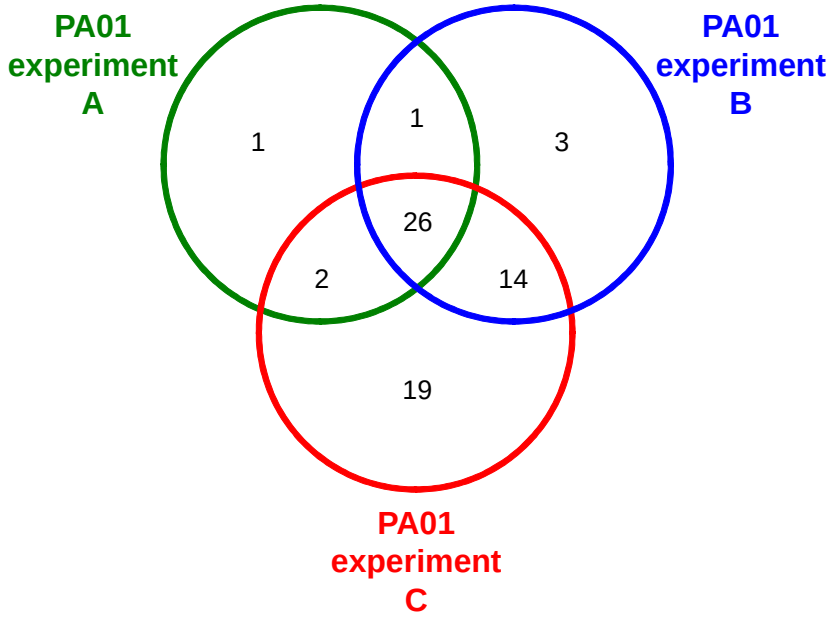

Figure 3.11. Comparison of proteins that were pulled down in *P. aeruginosa* PA01 lysates using the control resin in three different experiments.
In all experiments, the control resin was incubated with soluble lysate of PA01. In experiment C, 1% Triton was included in the lysis-, wash- and elution-buffer. Proteins were eluted from the control resin by heat treatment (experiment A) or with a 1% SDS solution (experiments B and C).

Table 3.2. Putative PA01 c-di-GMP binding proteins.

PA number[a]	(Alternate) gene name	Product name	Comment
PA0174	*cheD*	conserved hypothetical protein	
PA1092	*fliC*	flagellin type B	
PA2567		hypothetical protein	degenerate GGDEF domain without I-site motif, EAL domain [62]
PA3309	*uspK*	conserved hypothetical protein	
PA3348	*cheR1*	probable chemotaxis protein methyltransferase	
PA3353		hypothetical protein	PilZ domain[a]
PA3529	*tsaA*	probable peroxidase	
PA3740		hypothetical protein	
PA3831	*pepA*	leucine aminopeptidase	
PA4396		probable two-component response regulator	degenerate GGDEF domain [62] with I-site motif

[a]Those proteins are listed that were identified with a probability of ≥ 95% in at least one of three c-di-GMP pull downs, but not in any of the controls (with a probability of ≥ 50%). The proteins are listed according to ascending PA numbers.

probable two-component response regulator containing a degenerate GGDEF domain with the additional c-di-GMP binding site (I-site). Thus, this protein might not act as a diguanylate cyclase (DGC), but as a true c-di-GMP effector molecule. The hypothetical protein PA2567 harbors a degenerate GGDEF domain without I-site motif, which is fused to a conserved EAL domain possessing phosphodiesterase (PDE) activity ([143] and own observations). This protein might have been "trapped" on the c-di-GMP sepharose during its attempt to degrade the immobilized c-di-GMP, though the presence of a distinct and unknown c-di-GMP binding site cannot be excluded.

Three other proteins were specifically enriched by the three pull down experiments more than once: the hypothetical protein PA3740, and the two chemotaxis proteins CheR1 (PA3348) and PA0174 (CheD) [144].

3.2.4 The *P. aeruginosa* PA14 c-di-GMP interactome

In the following, the c-di-GMP sepharose was also used for the isolation of c-di-GMP binding proteins from *P. aeruginosa* PA14. Three independent experiments were performed (termed 1, 2 and 3) using soluble lysate in experiment 1, and BugBuster lysate obtained by chemical lysis of cells in experiment 2. Experiment 3 is the combination of two pull downs that were performed in parallel: after cell lysis and the following centrifugation step, the supernatant (soluble lysate) was used for one pull down, and membranes isolated from the insoluble pellet were used for a second pull down. In all cases, freshly prepared cell lysates derived from stationary phase cultures were incubated with the c-di-GMP affinity resin and control beads, and after extensive washing steps, enriched proteins were eluted by the addition of free c-di-GMP (0.1 M).

While a Q-TOF mass spectrometer was used for the analysis of PA01 eluates, all PA14 eluates were analyzed with a highly sensitive Orbitrap XL mass spectrometer, which led to the detection of a significantly higher number of proteins (Table 3.3). As in the PA01 pull downs, more proteins were isolated on the control beads as compared with the respective c-di-GMP affinity resin, and analysis of the control bead proteome once again revealed an extensive overlap of proteins derived from the individual control pull downs (Figure 3.12).

Table 3.3. Pulled down proteins of three distinct experiments performed with PA14 lysates using the c-di-GMP affinity resin and the control resin.

	Experiment 1[a]	Experiment 2[b]	Experiment 3[c]	Number of distinct proteins
Proteins enriched by the c-di-GMP sepharose	23	166	152	236
Proteins enriched by the control sepharose	171	268	377	457
Proteins enriched by the c-di-GMP sepharose, but not by the respective control sepharose	8	78	48	122
Proteins enriched by the c-di-GMP sepharose, but not by any control sepharose	2	59	36	87

[a] performed with soluble cell lysate
[b] performed with BugBuster cell lysate
[c] combination of two pull downs (soluble cell lysate and membrane fraction)

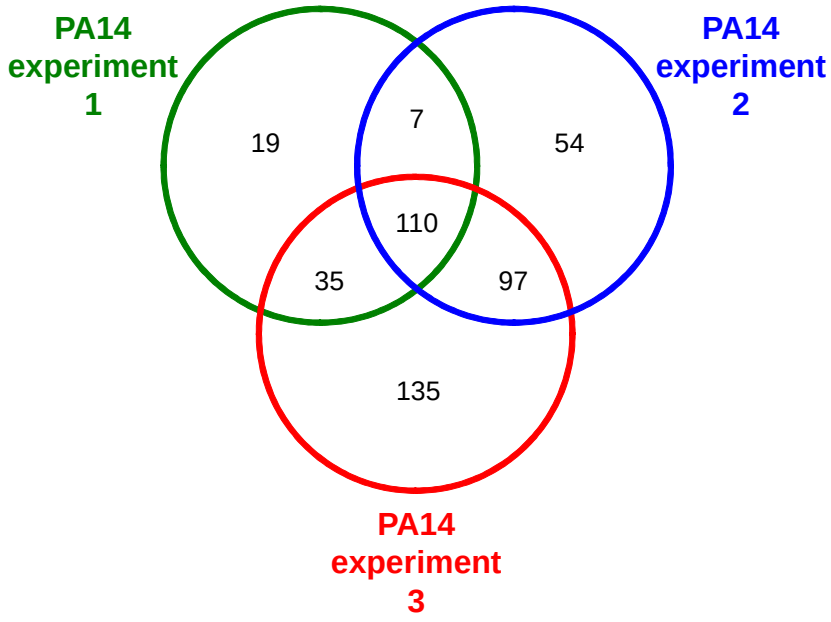

Figure 3.12. Comparison of proteins that were pulled down in *P. aeruginosa* PA14 lysates using the control resin in three different experiments.
In experiment 1, the control resin was incubated with soluble cell lysate and in experiment 2 with BugBuster cell lysate. Experiment 3 is the combination of two pull downs in which the control beads were incubated with soluble lysate and a membrane fraction, respectively.

The various proteins enriched by the c-di-GMP and control resin were categorized according to their function as proposed by the *Pseudomonas* Genome Database (www.pseudomonas.com) [139]. In Figure 3.13, those functional categories are depicted to which at least 5% of the c-di-GMP or control proteins could be assigned to. Approximately 81% of all proteins isolated by the control sepharose could be grouped into six main

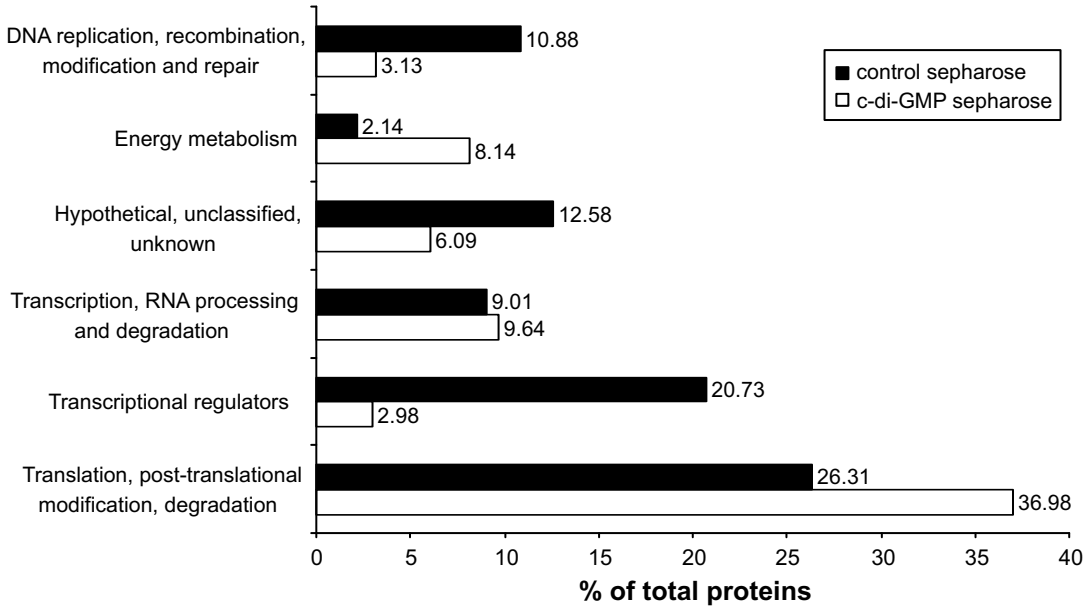

Figure 3.13. Classification of the pulled down proteins in PA14 according to PseudoCAP function.
Proteins isolated by the c-di-GMP sepharose are depicted by white bars, proteins isolated by the control sepharose are depicted by black bars. Only groups including at least 5% of the c-di-GMP or control interactome are shown.

categories, whereas the c-di-GMP sepharose pull down showed a broader distribution and only 67% of the identified proteins belong to the depicted categories. Remarkably, a large number of the enriched proteins were involved in translation, post-translational modification and degradation, and the categorization of proteins isolated by the c-di-GMP sepharose revealed a higher relative number of proteins in this category as compared with the control. Furthermore, the relative proportion of proteins involved in energy metabolism was found to be increased in the c-di-GMP sepharose pull down. This group includes proteins binding ATP and NADH, small molecules with nucleotide-like structures.

3.2.5 PA14 proteins specifically enriched by the c-di-GMP sepharose

In order to reduce the number of false positives on our protein lists, results of all control pull downs (experiment 1-3) were included as a reference to validate the specificity of results in each of the three c-di-GMP pull down experiments. As depicted in Table 3.3, overall 87 distinct putative c-di-GMP binding proteins were identified in *P. aeruginosa* PA14. In order to further minimize the rate of false positives, more stringent parameters were applied in the control samples (i.e. a confidence interval of $\geq$ 50% was accepted for protein identification). When these parameters were applied, 23 of the 87 proteins also appeared in the control bead-

proteome list and were therefore excluded from the list of putative c-di-GMP binding proteins. Remarkably, most of the 23 proteins were identified in the BugBuster experiment in which cells have been lysed chemically. The remaining 64 c-di-GMP binding candidate proteins are listed in Table 3.4.

Table 3.4. Putative PA14 c-di-GMP binding proteins.

PA14 number[a]	PA number	(Alternate) gene name	Product name	Comment
PA14_49030	*		hypothetical protein	anion-transporting ATPase[b]
PA14_00090	PA0008	*glyS*	glycyl-tRNA synthetase beta chain	
PA14_00130	PA0012		hypothetical protein	PilZ domain[b]
PA14_02190	PA0174	*cheD*	putative chemotaxis protein	
PA14_03940	PA0302	*spuF, potG*	polyamine transport protein PotG	ABC-type spermidine/putrescine transport systems, ATPase components[c]
PA14_06750	PA0519	*nirS*	nitrite reductase precursor	
PA14_54640	PA0745		probable enoyl-CoA hydratase/isomerase	
PA14_52180	PA0934	*relA*	GTP pyrophosphokinase	
PA14_51730	PA0971	*tolA*	TolA protein	
PA14_51390	PA0999	*pqsD, fabH1*	3-oxoacyl-[acyl-carrier-protein] synthase III	
PA14_49470	PA1155	*nrdB*	ribonucleoside reductase, small chain	
PA14_49200	PA1178	*oprH*	PhoP/Q and low Mg2+ inducible outer membrane protein	
PA14_45590	PA1458	*cheA*	putative two-component sensor	
PA14_45580	PA1459	*cheB*	putative chemotaxis methylesterase	
PA14_45560	PA1460	*motC, motA2*	chemotaxis protein MotC	
PA14_43950	PA1588	*sucC*	succinyl-CoA synthetase beta subunit	ATP-grasp domain[b]
PA14_41670	PA1770	*ppsA*	phosphoenolpyruvate synthase	
PA14_41470	PA1787	*acnB*	aconitate hydratase 2	
PA14_38440	PA2015	*gnyD, ivd*	Citronelloyl-CoA dehydrogenase, GnyD	
PA14_37690	PA2072		putative sensory box protein	GGDEF domain with I-site motif, EAL domain[b]
PA14_30070	PA2633		putative secretion system protein	
PA14_27930	PA2799		conserved hypothetical protein	PilZ domain[b]
PA14_25840	PA2953		putative electron transfer flavoprotein-ubiquinone oxidoreductase	FAD binding domain[b]
PA14_25520	PA2980		conserved hypothetical protein	
PA14_25420	PA2989		conserved hypothetical protein	PilZ domain[b]
PA14_24445	PA3068	*gdhB*	NAD-dependent glutamate dehydrogenase	
PA14_23010	PA3187	*gltK, ugpC*	putative ATP-binding component of ABC transporter	MalK, ABC-type sugar transport systems, ATPase components[c]
PA14_22020	PA3244	*minD*	cell division inhibitor MinD	MinD, septum formation inhibitor-activating ATPase[c]
PA14_22010	PA3245	*minE*	cell division topological specificity factor	
PA14_20780	PA3346		putative sensor histidine kinase/response regulator	
PA14_20760	PA3348	*cheR1*	putative chemotaxis protein methyltransferase	
PA14_20700	PA3353		putative glycosyltransferase	PilZ domain[b]
PA14_16500	PA3702	*wspR*	probable two-component response regulator	GGDEF domain[b] with I-site motif
PA14_16020	PA3740		conserved hypothetical protein	
PA14_12330	PA3981		PhoH family protein	

Table 3.4. (Continued)

PA14 number[a]	PA number	(Alternate) gene name	Product name	Comment
PA14_12100	PA3999	*dacC*	D-ala-D-ala-carboxypeptidase	
PA14_10820	PA4108		putative HDIG domain protein	HD-GYP domain [95]
PA14_09520	PA4207	*mexI*	probable RND efflux transporter	
PA14_39890	PA4215	*phzF2*	probable phenazine biosynthesis protein	
PA14_09300	PA4223	*pchH*	putative ATP-binding component of ABC transporter	putative ATP-binding
PA14_09230	PA4229	*pchC*	pyochelin biosynthetic protein PchC	
PA14_09050	PA4243	*secY*	secretion protein SecY	
PA14_56000	PA4309	*pctA*	chemotactic transducer PctA	
PA14_56830	PA4370	*icmP*	insulin-cleaving metalloproteinase outer membrane	
PA14_57275	PA4407	*ftsZ*	cell division protein FtsZ	cell division GTPase[c]
PA14_57340	PA4412	*murG*	UDP-N-acetylglucosamine:LPS N-acetylglucosamine transferase	
PA14_57370	PA4414	*murD*	UDP-N-acetylmuramoylalanine-D-glutamate ligase	
PA14_57570	PA4431		putative cytochrome c reductase, iron-sulfur subunit	
PA14_57850	PA4454		conserved hypothetical protein	
PA14_58150	PA4481	*mreB*	rod shape-determining protein MreB	actin-like ATPase involved in cell morphogenesis[c]
PA14_58630	PA4519	*speC*	putative ornithine decarboxylase	
PA14_60970	PA4608		conserved hypothetical protein	PilZ domain
PA14_62860	PA4751	*ftsH, hflB*	cell division protein FtsH	HflB, ATP-dependent Zn proteases[c]
PA14_63250	PA4785	*yfcY*	putative acyl-CoA thiolase	
PA14_64390	PA4868	*ureC*	urease alpha subunit	
PA14_65520	PA4958		conserved hypothetical protein	adjacent to the fimX gene
PA14_66620	PA5040	*pilQ*	type 4 fimbrial biogenesis outer membrane protein PilQ precursor	
PA14_66750	PA5051	*argS*	arginyl-tRNA synthetase	
PA14_66910	PA5064		conserved hypothetical protein	
PA14_68820	PA5210	*gspE*	putative general secretory pathway related protein	PulE, Type II secretory pathway, ATPase PulE/Tfp pilus assembly pathway, ATPase PilB[c]
PA14_69220	PA5241	*ppx, gppA*	exopolyphosphatase	
PA14_72380	PA5483	*algB*	two-component response regulator AlgB	AtoC, Response regulator containing CheY-like receiver, AAA-type ATPase, and DNA-binding domains[c]
PA14_72460	PA5490	*cc4, cycA*	cytochrome c4 precursor	
PA14_73290	PA5558	*atpF*	ATP synthase B chain	

[a]Those proteins are listed that were identified with a probability of ≥ 95% in at least one of three c-di-GMP pull downs, but not in any of the controls (with a probability of ≥ 50%). The proteins are listed according to ascending PA numbers.
[b] as predicted by PFAM
[c] as predicted by COG
[*] not present in PA01

Previously described c-di-GMP binding proteins in *P. aeruginosa* include 7 PilZ domain proteins (there are 8 PilZ domains in *P. aeruginosa*, however, one did not seem to bind c-di-GMP *in vitro* [82]), the membrane associated PelD protein [98], the transcriptional regulator FleQ [88] and the catalytically inert GGDEF-EAL hybrid protein FimX [99]. The

c-di-GMP binding candidate protein list was searched for these known c-di-GMP targets and was found to contain five PilZ domain proteins that were identified either in all experiments (PA3353, PA4608), twice (PA2799, PA2989) or in one experiment (PA0012). Additionally, two proteins containing the c-di-GMP binding motif of the I-site are listed in Table 3.4. One is the response regulator WspR, a characterized DGC known to be prone to allosteric feedback inhibition [39, 145], the second protein is the GGDEF-EAL hybrid protein PA2072. Further analysis of the obtained c-di-GMP interacting proteins revealed 13 proteins containing putative nucleotide binding sites such as GTP- and ATPases, ATP-binding components of ABC transporters or proteins binding the dinucleotide NAD or FAD. Among the remaining identified proteins, 5 are conserved hypotheticals, for example, PA3740 which was also identified in the PA01 pull downs, and 6 are involved in flagellum mediated chemotaxis. Two of these 6 proteins were found in all PA14 c-di-GMP pull down experiments: the chemotaxis methyltransferase CheR1 and CheD (PA0174) both of which have also been identified as putative c-di-GMP binding proteins in pull down experiments using PA01 lysates.

3.2.6 Surface plasmon resonance binding studies with c-di-GMP

To approve c-di-GMP binding to purified proteins *in vitro*, surface plasmon resonance (SPR) was applied with the aim to explore the interaction between an analyte in the mobile phase and a ligand immobilized on a sensor surface. All SPR binding studies were performed in co-operation with the group of F. W. Herberg (Daniela Bertinetti, Stefan Möller; University of Kassel) and Bastian Zimmermann (Biaffin company, Kassel).

Initially, a very sensitive method (Biacore S51 system) was used to detect direct binding of c-di-GMP (690.4 Da) to immobilized proteins (30-45 kDa). In these experiments binding signals were obtained, but the limited stability of the proteins and regeneration of the protein sensor surface restricted the reproducibility of these measurements (data not shown). Recently, a functionalized c-di-GMP derivative became available with a 6-aminohexyl-carbamoyl group attached to the 2' alcohol group of one ribose-ring (2'-AHC-c-di-GMP, Figure 3.10; Biolog, Bremen). This c-di-GMP analog was successfully coupled via its linker-amino group to a sensor chip, and binding of the purified proteins was analyzed at 20°C using a Biacore 3000 instrument.

In order to verify the surface functionality of the sensor chip, interaction analysis was started with PA3353, a PilZ domain protein for which c-di-GMP binding has been demonstrated previously [82]. This protein was identified in pull down experiments of both, PA14 and PA01 lysates. Figure 3.14A shows the association and dissociation of PA3353-His_6 to the

high density 2'-AHC-c-di-GMP sensor surface with increasing binding signals upon rising protein concentrations (2-500 nM). In a solution competition assay, a constant concentration of PA3353-His_6 (15 nM and 5 nM, respectively) together with increasing amounts of free c-di-GMP (50 pM-10 µM) was added to the sensor chip. By plotting the SPR signal (for each c-di-GMP concentration) obtained at the end of the association phase against the concentration of free c-di-GMP, the apparent EC_{50} (half maximal effective concentration) value was determined to be 262 ± 66 nM for PA3353-His_6 (Figure 3.14B).

Next, the putative response regulator PA4396 was examined, which harbors a degenerate GGDEF domain (the conserved sequence motif is changed to DEQHF) with an intact I-site motif. PA4396 was expressed and purified with an N-terminal Strep-tag and tested for DGC

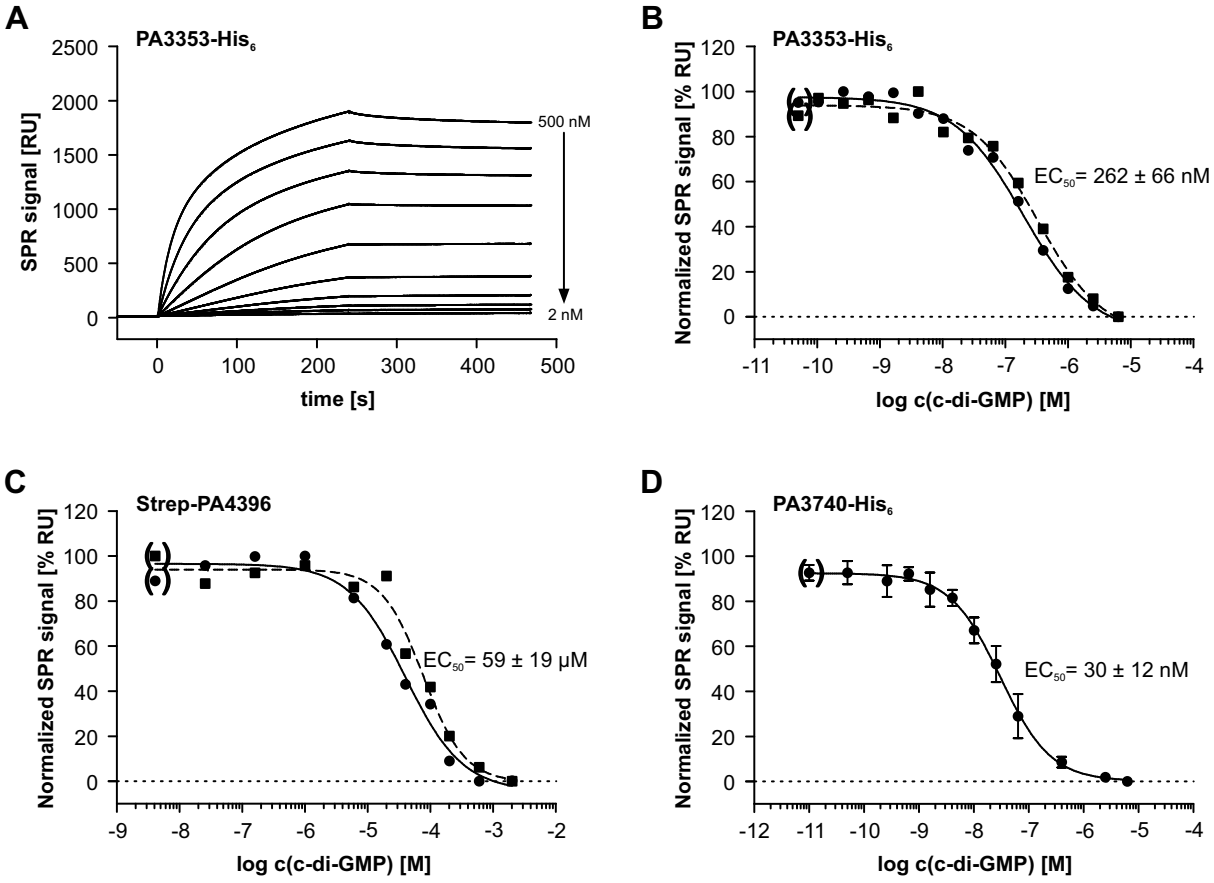

Figure 3.14. C-di-GMP binding analysis by SPR with purified proteins and a 2'-AHC-c-di-GMP sensor chip.

(A) PA3353-His_6 binds to 2'-AHC-c-di-GMP in a concentration dependent manner (protein concentration range 2-500 nM). (B) Solution competition assays of PA3353-His_6 using protein concentrations of 15 nM (dashed line) and 5 nM (continuous line) revealed an EC_{50} value of 262 ± 66 nM. Normalized data are shown. First data points are in brackets, indicating SPR signals of protein incubated without c-di-GMP. (C) For Strep-PA4396 an EC_{50} value of 59 ± 19 µM was determined using 100 nM protein in the competition experiments (n=2, continuous and dashed line, respectively). Normalized data are shown. First data points are in brackets, indicating SPR signals of protein incubated without c-di-GMP. (D) Solution competition assays of PA3740-His_6 revealed an EC_{50} value of 30 ± 12 nM (n=3, using 500 nM, 100 nM and 50 nM of protein). Normalized data are shown. First data points are in brackets, indicating SPR signals of protein incubated without c-di-GMP.

activity. As expected, Strep-PA4396 was not able to synthesize c-di-GMP from [α-^{32}P]GTP (Figure 3.15). The protein was then tested for its ability to interact with the 2'-AHC-c-di-GMP sensor surface. SPR analysis revealed a specific interaction between Strep-PA4396 (100 nM) and immobilized 2'-AHC-c-di-GMP as this binding could be completely competed with free c-di-GMP in solution. The EC_{50} value was determined to be 59 ± 19 µM (Figure 3.14C) in the SPR solution competition assay. This verifies the degenerate GGDEF domain protein PA4396 as a new c-di-GMP binding protein, however, the cellular function of this interaction is still unknown.

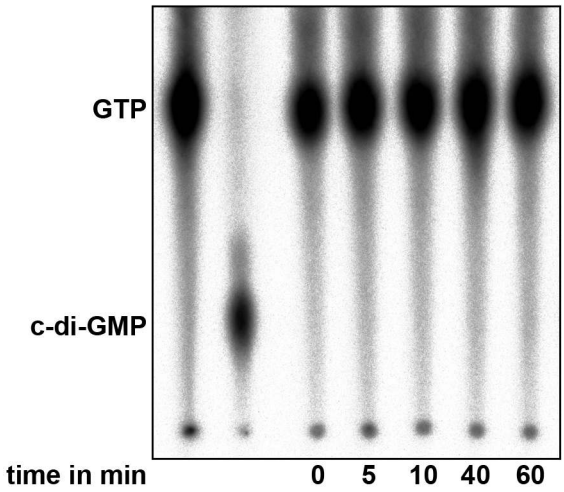

Figure 3.15. Radioactive diguanylate cyclase activity assay.
Purified Strep-PA4396 was assayed for DGC activity by incubation with [^{32}P]GTP at 30°C. Analysis of the reaction mixture by TLC after several time points demonstrated that Strep-PA4396 was not able to synthesize radiolabeled c-di-GMP. As controls, [^{32}P]GTP and [^{32}P]c-di-GMP (enzymatically synthesized by the constitutively active DGC PleD*) were spotted on the TLC plate.

The affinity chromatography performed on PA14 and PA01 also revealed a group of chemotaxis proteins as putative c-di-GMP effectors. Since flagellar driven motility is known as a trait also controlled by c-di-GMP, we analyzed CheR1, which was repeatedly isolated in the pull down experiments (identified in 5 out of the 6 affinity chromatographies performed in this study). CheR1 is a chemotaxis methyltransferase (see chapter 3.1.2) and does not harbor any known c-di-GMP binding motif. In first SPR experiments, the CheR1-His_6 protein was immobilized on a sensor surface (Biacore S51 machine, see above) and the small ligand was injected over the sensor chip. Besides c-di-GMP, *S*-adenosylmethionine (SAM) was also injected, as chemotaxis methyltransferases are known to use this methyl donor as a substrate. In case of the c-di-GMP interaction, no binding signal could be detected, but the interaction between CheR1-His_6 and SAM could be verified (Figure 3.1). Thereafter, 2'-AHC-c-di-GMP

was coupled to the sensor surface (Biacore 3000, see above) and injection of CheR1-His_6 resulted in a SPR signal, however, coinjection of CheR1-His_6 with free c-di-GMP did not result in significant signal reduction. Even when various different parameters, co-factors and detergents (protein concentration up to 1 µM, buffer composition, pH value, SAM, cGMP, cAMP, $MgCl_2$, CM dextran, DTT) were applied, the SPR signals were identical. Furthermore, binding to the c-di-GMP sensor surface could not be competed with a wide range of c-di-GMP concentrations (100 nM – 10 µM), indicating nonspecific binding of CheR1-His_6 to the sensor surface (Figure 3.16A). To further address this question, binding experiments were done in presence of 100 nM c-di-GMP, cAMP and cGMP (Figure 3.16B). Injection of

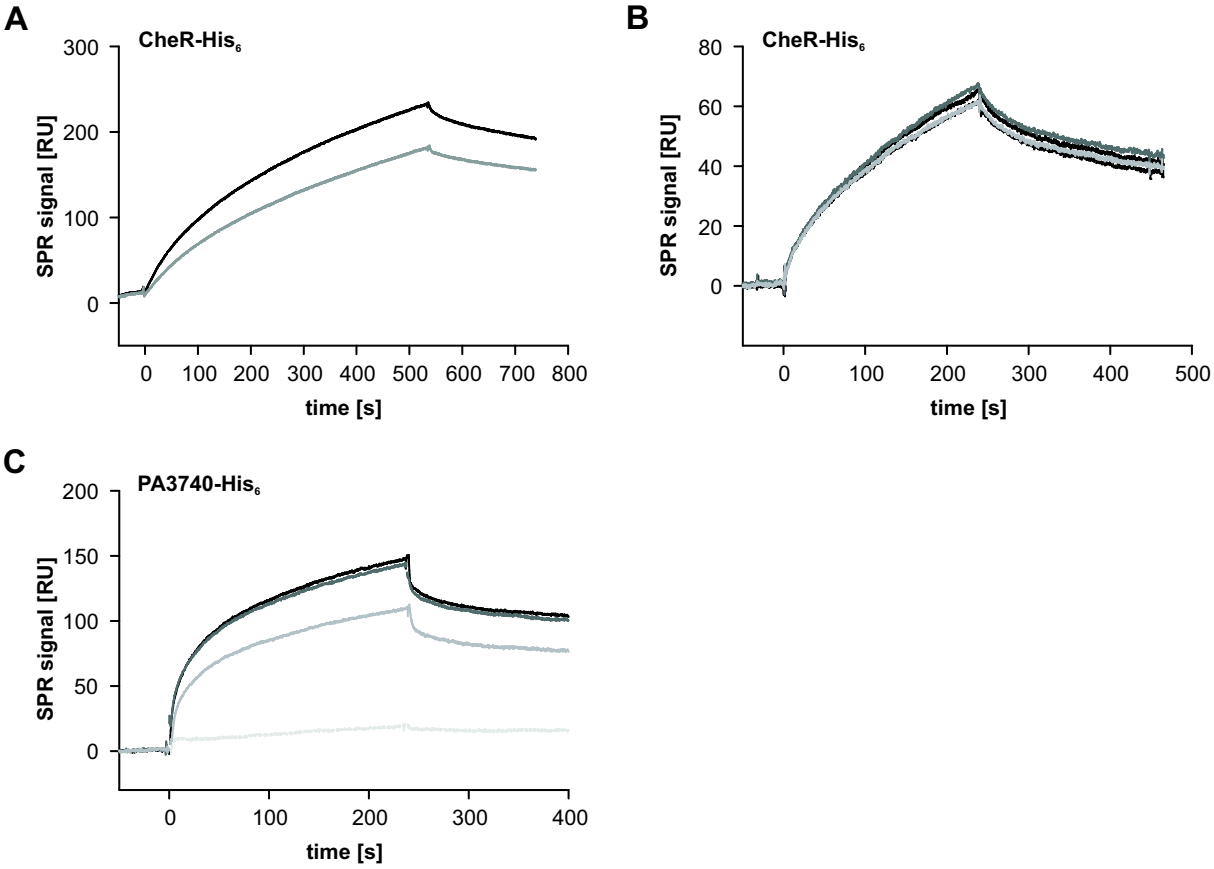

Figure 3.16. C-di-GMP binding analysis by SPR with purified proteins and a 2'-AHC-c-di-GMP sensor chip.

(A) Binding analysis of purified CheR1-His_6 demonstrates that CheR1 (1 µM, black line) binds to the sensor surface, but that binding cannot be competed with free c-di-GMP (e.g. 10 µM, gray line). (B) To analyze whether binding to the sensor chip is unspecific, binding experiments using 1 µM CheR1-His_6 (black line) were done in presence of 100 nM c-di-GMP (light gray), cAMP (dark gray) or cGMP (gray line). Binding was not competed by any of the cyclic nucleotides indicating an unspecific mode of binding. (C) Binding analysis of purified PA3740-His_6 demonstrates that PA3740 (800 nM, black line) binds specifically to the sensor surface. This binding can be competed with c-di-GMP (light gray, 1 µM), but not with cAMP (dark gray, 1 µM). cGMP (gray, 1 µM) causes only a slight shift.

CheR1-His_6 to the sensor surface resulted in a low SPR signal in comparison to the employed protein concentration (1 μM). More importantly, binding of CheR1 could neither be competed with c-di-GMP, nor with cAMP and cGMP. Thus, although repeatedly isolated by affinity chromatography, we were not able to validate CheR1 as a c-di-GMP binding protein.

In our search for novel c-di-GMP effectors, the conserved hypothetical protein PA3740 was identified in pull down experiments with both, PA14 and PA01 lysates. Due to an apparent toxicity to *E. coli* BL21 cells, PA3740-His_6 was expressed by the use of an *in vitro* translation system and purified by Ni-NTA affinity chromatography (see Materials and Methods, chapter 2.5). In SPR binding studies, PA3740-His_6 was able to bind to the 2'-AHC-c-di-GMP sensor surface, however with low stoichiometry. This binding could be competed with free c-di-GMP, but not with cAMP and the injection of protein pre-incubated with cGMP resulted in only a slightly decreased binding signal (Figure 3.16C). In a solution competition assay format, an EC_{50} value of 30 ± 12 nM was determined for the interaction between c-di-GMP and PA3740-His_6 (Figure 3.14D). Overall, the SPR binding studies demonstrated that PA3740 specifically and reproducibly binds 2'-AHC-c-di-GMP with a nanomolar affinity, which highlights PA3740 as a novel c-di-GMP effector. The next challenge will be to reveal the c-di-GMP binding motif of this hypothetical protein.

3.2.7 Phenotypic characterization of mutants affected in the expression of c-di-GMP binding proteins

To examine the molecular function of verified c-di-GMP binding proteins in *P. aeruginosa*, the impact of PA3353, PA4396 and PA3740 on bacterial motility and biofilm formation was analyzed. Therefore, respective transposon mutants in the PA01 strain background (correct insertion of transposon was confirmed by PCR) were tested for their ability to swim, swarm and twitch on agar plates, or to form biofilms at the liquid-air interface in microtiter plate grown cultures. The PA3353 transposon mutant was obtained from the Washington Genome Center PA01 mutant library [101] and compared to another transposon mutant that is unaffected in its motility and biofilm formation behavior (therefore termed wild-type control; see chapter 2.1). The transposon mutants of PA4396 and PA3740 were received from the PA01mini-Tn5 *lux* transposon mutant library ([105], kindly provided by R. E. Hancock, University of British Columbia, Canada) and compared to their isogenic parent strain (PA01 H103 wt).

PA3353

So far, nothing is known about the cellular role of PA3353. The PA3353 gene is part of a predicted operon (www.pseudomonas.com) that contains a gene encoding an anti-sigma factor (FlgM) and a gene encoding the hypothetical protein PA3352. The anti-sigma factor FlgM inhibits the activity of FliA [146], an alternative sigma factor which controls the biosynthesis of flagellin [147]. PA3353 itself encodes a hypothetical protein, consisting of an N-terminal YcgR domain and a C-terminal PilZ domain. The YcgR protein from *E. coli* is a PilZ domain protein that has been shown to interact with the flagellar motor in a c-di-GMP dependent manner thereby acting as a molecular brake [79, 148].

Thus, swimming assays of a PA01 mutant with a transposon insertion within PA3353 were performed. Compared to the wild-type control, the PA3353 transposon mutant displayed an increased ability to swim on 0.3% soft-agar plates (Figure 3.17A). Plasmid-borne complementation of the PA3353 transposon mutant resulted in a reduction of the swimming zone as compared with the PA3353 transposon mutant. Moreover, the swimming zone of this PA3353 overexpressing strain was even smaller than that of the wild-type control, indicating a significantly impaired ability to swim (Figure 3.17A). Growth curves in liquid cultures suggested that these phenotypic differences were not caused by different growth rates (data not shown). To assess, whether PA3353 also impacts surface-associated motility, swarming and twitching assays were performed. While the PA3353 transposon mutant displayed a swarming pattern similar to that of the wild-type control, the PA3353 overexpressing strain had severe difficulties to swarm (Figure 3.17B). The ability to twitch on solid surfaces was found to be unaffected, in both the transposon mutant and in the PA3353 overexpressing strain (Figure 3.17C).

Next, biofilm formation was assayed by crystal violet (CV) staining of adherent cells. In comparison with the wild-type control, more cells attached to the wall of wells incubated with the PA3353 transposon mutant strain, while the attachment ability of cells overexpressing PA3353 was decreased (Figure 3.17D). As motility can have a profound impact on biofilm formation, the biofilm phenotypes may be caused by the altered motility behaviors of the PA3353 transposon mutant and PA3353 overexpressing strain.

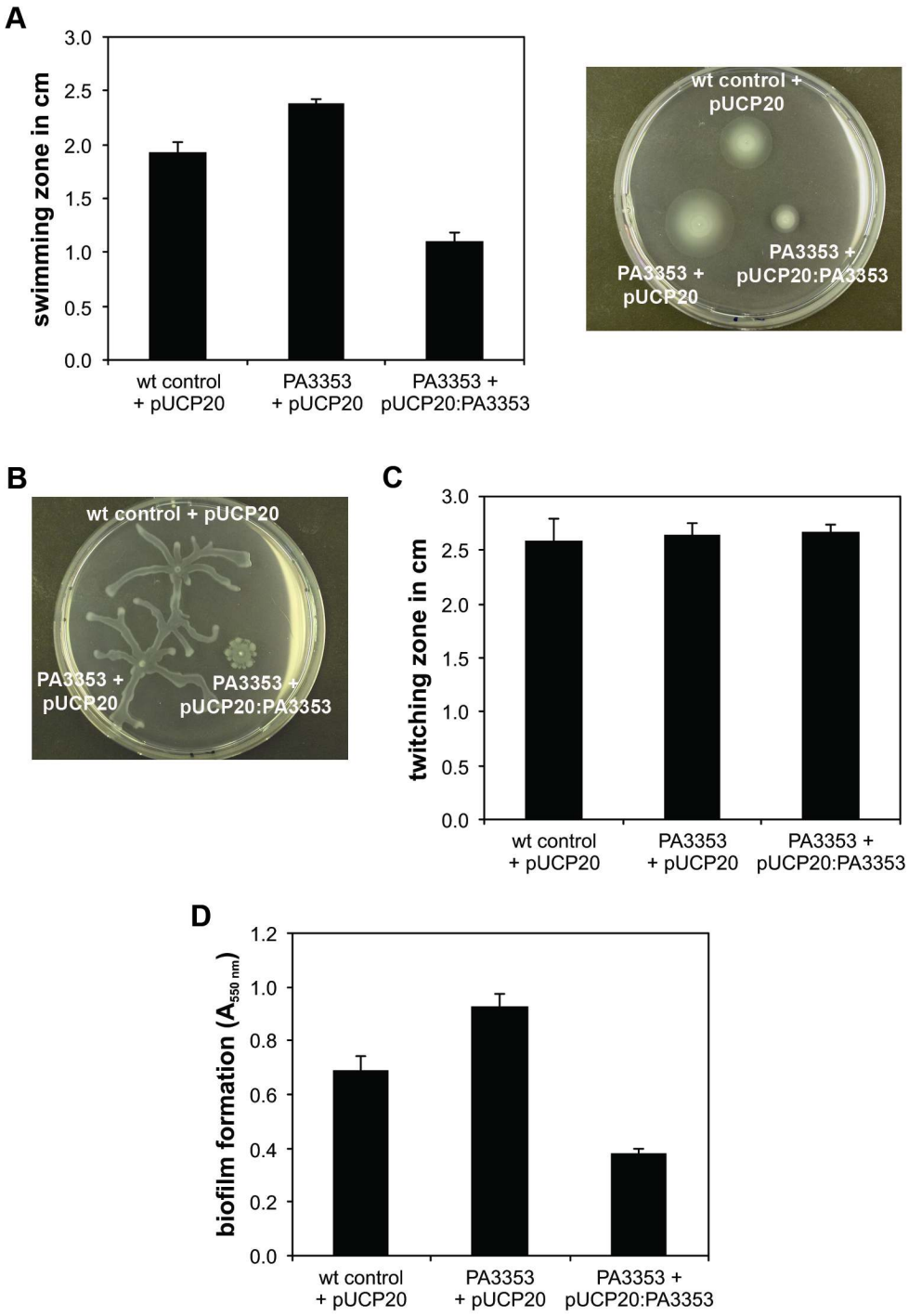

Figure 3.17. Motility and biofilm formation phenotype of the PA01 PA3353 transposon mutant and the PA3353 overexpressing PA01 strain.

(A) Swimming assays were performed on minimal medium soft agar plates supplemented with 0.3% agar. Swimming zones were measured after 18 h of incubation at 37°C. (B) Swarming assays were performed on minimal medium plates supplemented with 0.5% agar. The plates were incubated at 30°C for 18 h. (C) Twitching motility was analyzed at the plastic-agar interface of 1.5% LB agar plates and twitching zones were measured after incubation for 41 h at 37°C. (D) Biofilm formation was monitored in 96-well microtiter plates by crystal violet staining of attached biomass after 24 h of static growth in LB at 37°C.

Each experiment was performed at least twice. Error bars are standard deviations of three replicates (in A, C) and eight replicates (in D), respectively.

In *E. coli*, it has been demonstrated that knockout of the PilZ domain protein YcgR restores the impaired swimming motility of a mutant lacking the c-di-GMP phosphodiesterase YhjH. Genetic inactivation of YhjH is expected to lead to elevated c-di-GMP levels and thus to activation of YcgR, which in turn reduces flagellar motor function [79, 81]. In *P. aeruginosa*, the GGDEF-EAL hybrid protein PA5017 strongly affects swimming and swarming motility ([149] and own observations). The GGDEF motif of this protein is imperfect (ASNEF), but the EAL domain contains all conserved amino acids that are required for PDE activity [62].

To test whether PA3353 can restore the impaired swimming and swarming motility of a PA5017 transposon mutant, a PA5017_PA3353 double mutant was constructed and compared to the wild-type control, to the PA5017 transposon mutant and to a constructed PA3353 knockout mutant of the wild-type control. Both PA5017 strains, the PA5017 transposon mutant and the PA5017_PA3353 double mutant, differed slightly in their planktonic growth rate compared with the PA01 wild-type control (Figure 3.18). After 4 h, the two strains stopped growing for a short period before growing again so rapidly that after 7 h they reached the same optical density as the wild-type control. Swimming assays performed on 0.3% soft-agar plates confirmed the increased swimming ability of a PA3353 mutant (here, in the wild-type control background). Additionally, they demonstrated that inactivation of PA3353 in the PA5017 mutant background also slightly enhances swimming motility, however the impaired swimming ability of the PA5017 mutant could not be fully restored (Figure 3.19A). Furthermore, the PA5017_PA3353 double mutant was still reduced in its swarming motility, as is the case for the PA5017 transposon mutant (Figure 3.19B). Twitching motility was unaffected in all strains tested (wt control, PA5017 transposon mutant, wt control_PA3353

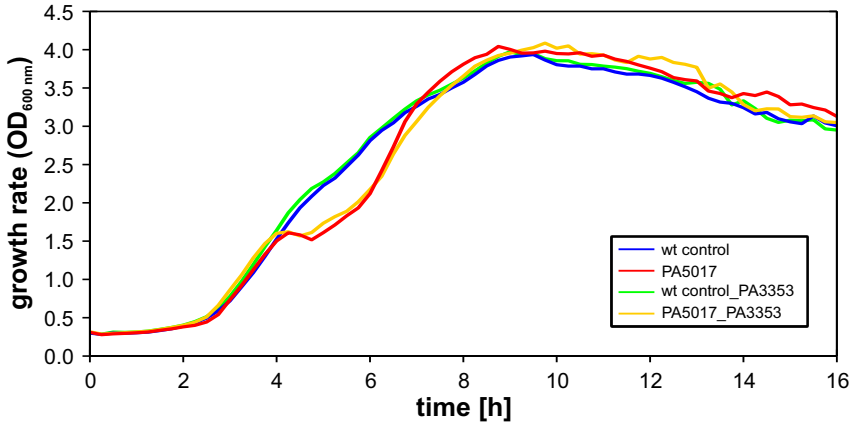

Figure 3.18. Growth rate of the PA01 wt control, PA5017 transposon mutant, wt control_PA3353 double mutant and PA5017_PA3353 double mutant.
Bacterial growth was monitored at 37°C for 16 h. Both strains impaired in the expression of the GGDEF-EAL hybrid protein PA5017 (PA5017 and PA5017_PA3353) show a temporary delay in their growth rate.

mutant, PA5017_PA3353 double mutant, data not shown). Both the PA5017 transposon mutant and the PA3353 mutant in the wt control background displayed a slight increase in biofilm formation as compared with the wt control (Figure 3.19C). This effect was even more pronounced in the PA5017_PA3353 double mutant. Overall, the data derived from the motility and biofilm formation assays indicate that PA5017 and PA3353 are acting independently from each other.

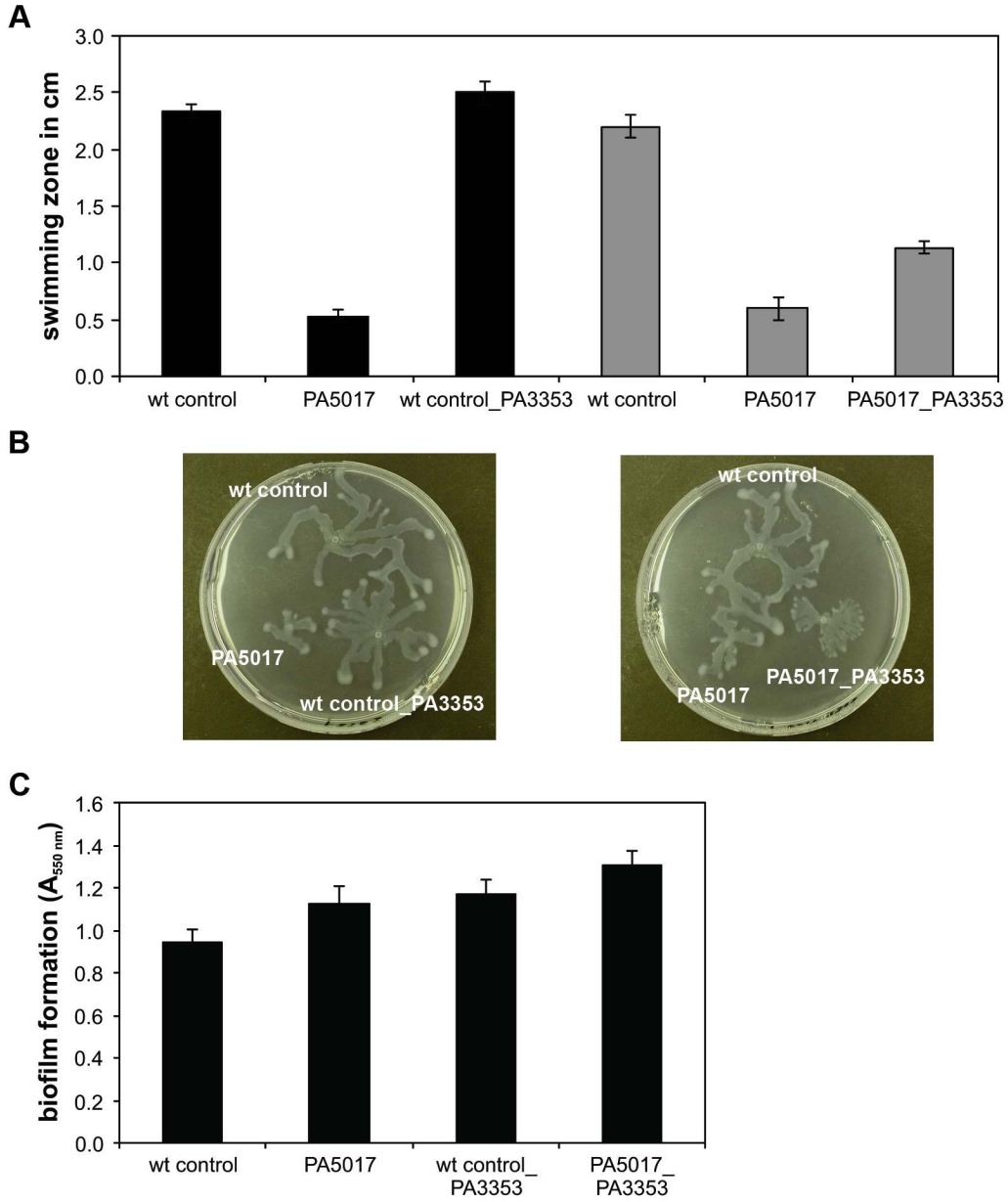

Figure 3.19. Motility and biofilm formation phenotype of a PA01 PA5017 transposon mutant and a PA5017_PA3353 double mutant.

(A) Soft-agar swimming motility assay. The PA5017 transposon mutant was compared to the wt control and a wt control_PA3353 double mutant on one plate (black bars) and to the wt control and a PA5017_PA3353 double mutant on a second plate (gray bars). Error bars are standard deviations of three replicates. The experiment was repeated twice. (B) Swarming motility assay. Representative pictures from one out of two experiments (three replicates each) are shown. (C) Crystal violet staining of attached biomass. Error bars are standard deviations of eight replicates.

PA4396

Next, a mutant with a transposon insertion within the PA4396 gene was characterized. PA4396 encodes a probable two-component response regulator which has an N-terminal receiver domain and a C-terminal degenerate (and inactive) GGDEF domain that harbors the secondary c-di-GMP binding site (I-site). With this domain organization, PA4396 is homologous to the PopA protein of *Caulobacter crescentus*, which has been shown to act as a c-di-GMP effector despite its inactive GGDEF domain [84]. The PA4396 gene is located in a predicted operon that also contains *panE*, encoding a ketopentoate reductase, PA4398, encoding a putative sensor kinase, and PA4399, which encodes a conserved hypothetical protein (www.pseudomonas.com).

A PA01 H103 PA4396 transposon mutant displayed swimming, swarming and twitching motility patterns identical to those of the respective wild-type (Figure 3.20A, B and C). However, plasmid borne overexpression of PA4396 in the PA01 H103 wild-type resulted in an altered motility behavior. Compared with the wild-type, the PA4396 overexpressing strain showed an enhanced swimming ability, displayed a different swarming pattern and was clearly reduced in its ability to twitch (Figure 3.20A-C). This altered phenotype was not due to a difference in the growth rate relative to the wild-type (data not shown).

In a CV biofilm assay, the PA4396 transposon mutant and the PA4396 overexpressing strain were able to attach to the walls of a 96-well plate comparable to the wild-type (Figure 3.20D). Overall, these data indicate that PA4396 impacts on bacterial motility.

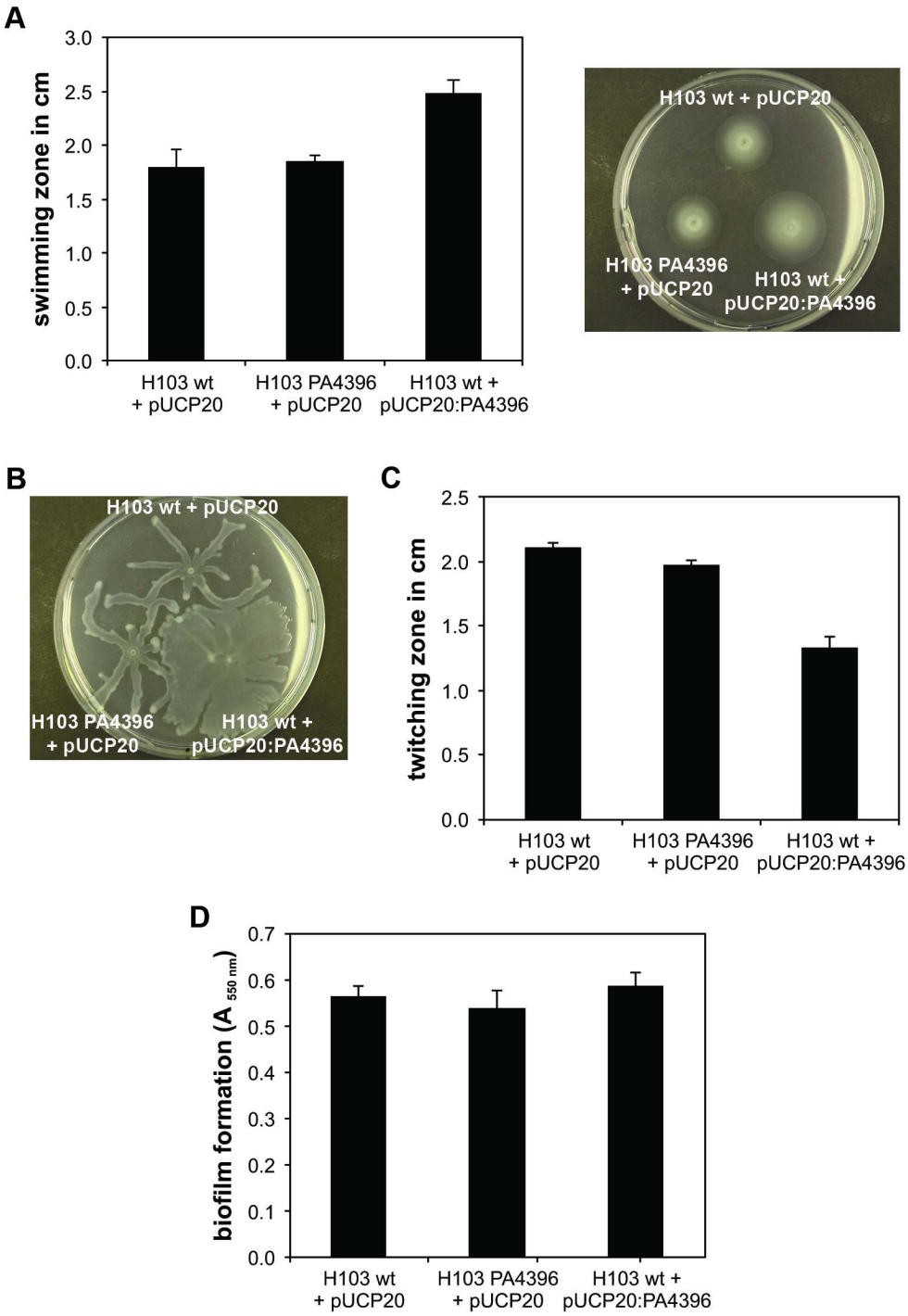

Figure 3.20. Motility and biofilm formation phenotype of the PA4396 transposon mutant and the PA4396 overexpressing strain.

(A) Swimming assays were performed on minimal medium soft agar plates supplemented with 0.3% agar. Swimming zones were measured after 18 h of incubation at 37°C. (B) Swarming assays were performed on minimal medium plates supplemented with 0.5% agar. The plates were incubated at 30°C for 18 h. (C) Twitching motility was analyzed at the plastic-agar interface of 1.5% LB agar plates and twitching zones were measured after incubation for 30 h at 37°C. (D) Biofilm formation was monitored in 96-well microtiter plates by crystal violet staining of attached biomass after 24 h of static growth in LB at 37°C.

Each experiment was performed twice. Error bars are standard deviations of three replicates (in A, C) and eight replicates (in D), respectively.

PA3740

So far, nothing is known about the hypothetical protein PA3740. Phenotypic assays using a PA01 H103 PA3740 transposon mutant and the PA01 H103 wild-type revealed no differences in motility behavior and the ability to form biofilms. Furthermore, overexpression of PA3740 in the wild-type did not alter the swimming/swarming/twitching motility or biofilm formation phenotype (data not shown).

However, an observable phenotype might be readily missed if intracellular c-di-GMP levels are too low and PA3740 is in an inactive state. Therefore, a PA3740 knockout mutant was constructed in the PA5017 mutant background, a strain that lacks the PDE PA5017 and should have an increased c-di-GMP level (judged from the impaired swimming and swarming motility of the PA5017 transposon mutant). However, the PA5017_PA3740 double mutant displayed the same phenotype as the PA5017 transposon mutant (Figure 3.21A-C). It shows a temporary delay in its growth rate, and the knockout of PA3740 could not restore the reduced swimming motility or the enhanced biofilm formation of the PA5017 transposon mutant (compared with the wild-type control). The performance of additional phenotypic assays will be required to elucidate the cellular function of the hypothetical, c-di-GMP binding protein PA3740.

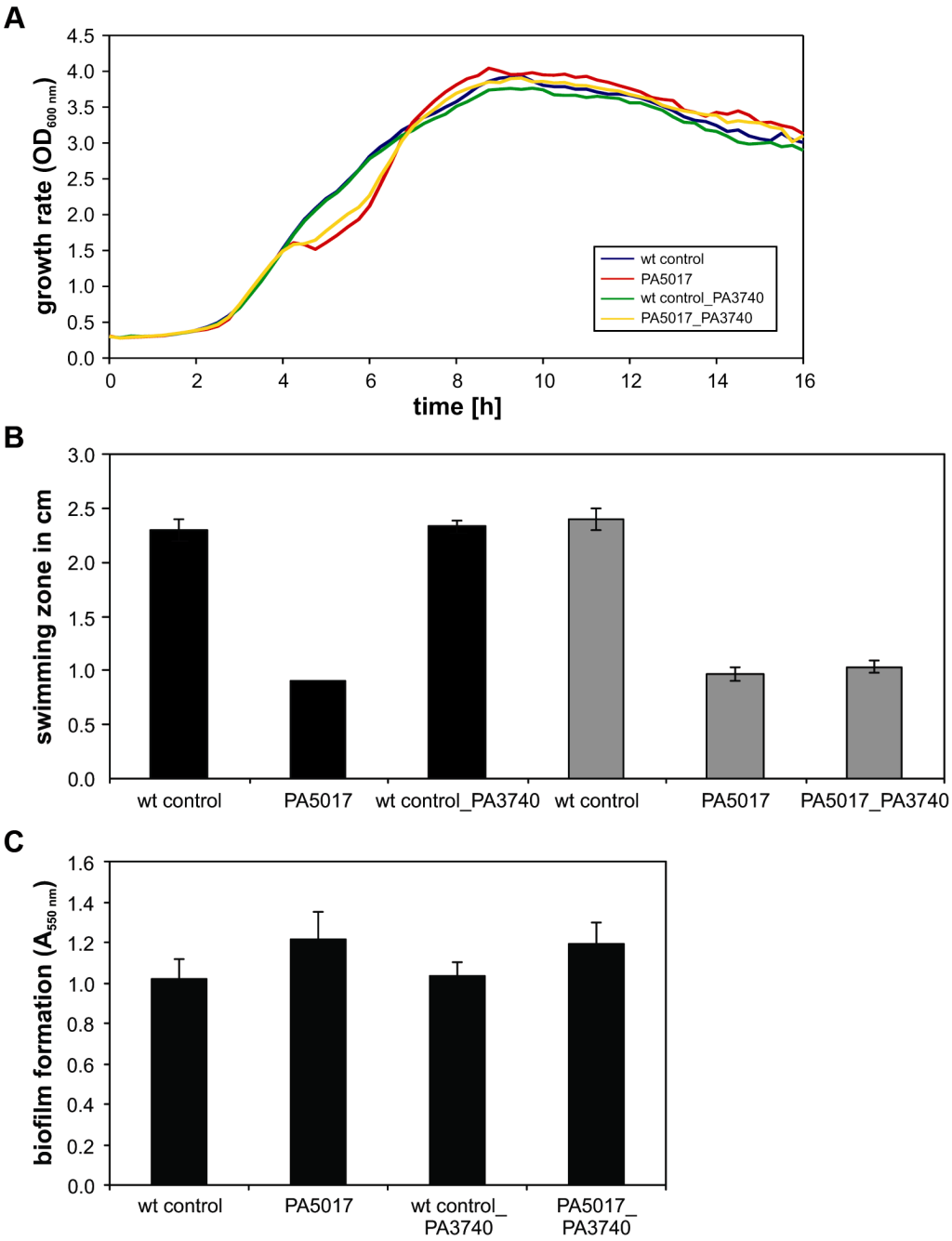

Figure 3.21. Distinct phenotypes of a PA01 wt control_PA3740 double mutant and a PA5017_PA3740 double mutant.

(A) Time course analysis of bacterial growth of the wt_control, wt_control_PA3740 double mutant, PA5017 transposon mutant and PA5017_PA3740 double mutant. (B) Soft agar swimming motility assay. The wt control and PA5017 transposon mutant were compared to the wt control_PA3740 double mutant on one plate (black bars) and to the PA5017_PA3740 double mutant on a second plate (gray bars). Error bars are standard deviations of three replicates. The experiment was repeated once. (C) Crystal violet staining of attached biomass. Error bars are standard deviations of eight replicates.

3.3 Identification of the RpoS regulon by chromatin immunoprecipitation

3.3.1 Objective

To achieve specificity within the complex c-di-GMP signaling system, it is necessary to tightly control the multiple c-di-GMP metabolizing and binding proteins at the transcriptional, post-transcriptional and/or post-translational level. One powerful tool for elucidating transcriptional regulatory mechanisms on a global scale is chromatin immunoprecipitation combined with microarray analysis (ChIP-chip), which enables the identification of DNA regions that are bound by a specific transcription factor under specific growth conditions. In *P. aeruginosa*, expression of genes is tightly controlled by a large collection of transcriptional regulators and alternative sigma-factors which redirect transcription initiation in response to environmental or physiological changes [150]. The stationary phase sigma-factor RpoS has been implicated in the general stress response, but also in the secretion of virulence factors and the formation of biofilms [150-154]. In this context, aim of this thesis was to apply the ChIP-chip technique in order to uncover the RpoS regulon and to reveal a potential link to the c-di-GMP signaling network.

3.3.2 The RpoS regulon as identified by the ChIP-chip technique

To determine RpoS promoter targets on a genome-wide scale, *P. aeruginosa* cultures were grown to the onset of stationary phase (OD_{600} of 2.0) at which DNA-bound RpoS was cross-linked to its DNA targets by formaldehyde fixation. After cell lysis, the RpoS-DNA complexes were isolated by immunoprecipitation using a polyclonal anti-RpoS serum (kindly provided by V. Venturi, International Center for Genetic Engineering and Biotechnology, Trieste, Italy). The cross-link was reversed and isolated promoter targets were further purified and amplified as described in the Materials and Methods section (see chapter 2.9.2). The samples were analyzed with a *P. aeruginosa* genome microarray that has been recently developed in our group (Dötsch *et al.*, [104]). This custom made microarray consists of 25-mer oligonucleotides and targets the whole *P. aeruginosa* PA01 genome at an average of one probe every 29 base pairs. All data analyses were supported by Andreas Dötsch, Helmholtz Center for Infection Research. Thereby, signals from two RpoS ChIP-chip experiments were compared to those of two controls in which an irrelevant polyclonal serum was employed instead of the anti-RpoS serum. The TAS software (Affymetrix) was used to calculate the log_2-fold enrichment values, revealing 474 promoter regions that were enriched

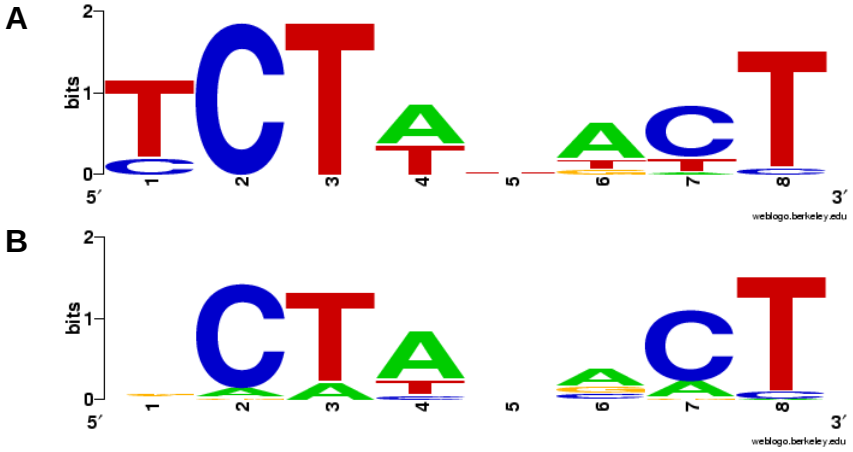

Figure 3.22. Determination of the RpoS consensus sequence.
(A) Based on the calculation by using the 16 target genes selected by Schuster *et al.* [136]. (B) Based on the calculation by using the 32 target genes selected by Schuster *et al.* [136], the previous RpoS consensus box and the ChIP-chip experiment.

by more than 0.5, out of which 128 promoter regions were even enriched by at least 1.0 log_2-fold (for the complete list of enriched promoter regions see Appendix, Table 5.2). In 298 cases, the enriched region could be assigned to two adjacent genes with opposite orientation (signed as “shared promoter” in Table 5.2).

In a previous study, Schuster *et al.* [136] demonstrated that 772 genes are regulated by RpoS in the stationary phase of growth by analyzing the transcriptome of a PA01 *rpoS* mutant in comparison with the transcriptome of the respective wild-type. They also suggested the consensus sequence for the RpoS binding site to be CTATACT (deduced from 16 RpoS regulated genes). Upon comparison of our ChIP-chip data with the transcriptome data of Schuster *et al.*, 128 genes were identified as RpoS regulated genes in both studies. Of those 128 genes, 32 had the CTATACT consensus sequence within the upstream non-coding region (up to 300 bp). Based on these 32 most confident hits, a new consensus sequence was calculated which is depicted in Figure 3.22B and Figure 3.23 shows the distribution of genes that were identified in our ChIP-chip experiments (A), that contain the revised RpoS consensus box in their non-coding upstream region (B) and/or that were differentially expressed in an *rpoS* mutant as compared with the wild-type [136] (C). The 59 genes which were positive in all three criteria are listed in the Appendix (Table 5.3).

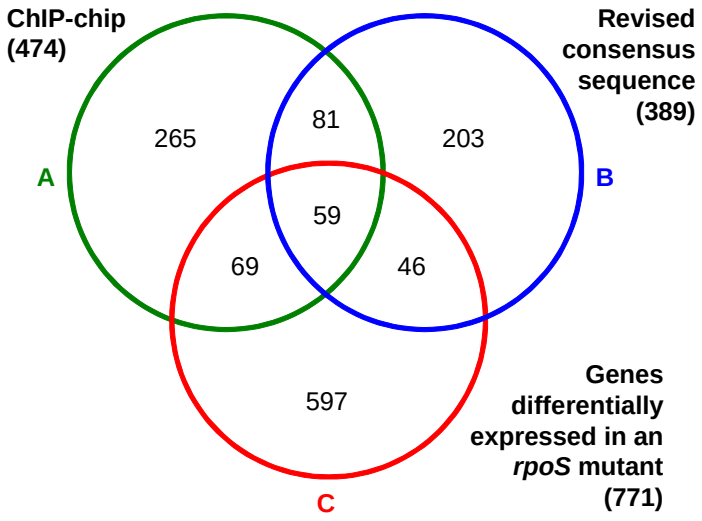

Figure 3.23. Comparison of three different approaches to identify RpoS-regulated genes. (A) Genes that were enriched at least 0.5 log_2-fold by ChIP-chip using an RpoS antibody. (B) Genes harboring one or more (re-calculated) consensus sequences (weight score ≥ 6.0) within the upstream non-coding region (up to 300 bp). (C) Genes differentially regulated in an *rpoS* mutant as compared to the wild-type [136].

3.3.3 Influence of RpoS on chemotaxis, biofilm formation and c-di-GMP signaling

To understand the RpoS regulon in more detail, the list of ChIP-chip identified RpoS targets was scanned for genes involved in chemotaxis, biofilm formation and c-di-GMP signaling.

RpoS has been previously shown to regulate several chemotaxis genes, especially those of cluster II (PA0173-PA0180) and the *mcp* genes PA1930, PA2573, PA2920 and PA4915 [136, 155]. In agreement with those earlier studies, the promoter region of *cheY2* (and thus the whole PA0173-PA0179 operon) was identified as an RpoS-binding target in our ChIP-chip experiments. This region also contains an RpoS consensus sequence located 115 bp upstream of the translational start site. Furthermore, the promoter regions of the *mcp* genes PA1930 (*mcpS*), PA2573, PA4307 (*pctC*) and PA4915 were enriched by chromatin immuno-precipitation by at least 0.5 log_2-fold (Table 3.5).

RpoS has been also reported to affect biofilm formation and production of the exopolysaccharides alginate [136, 151] and Psl [136, 152]. Inspection of the ChIP-chip result list indicates *algP* (encoding an alginate regulatory protein [156, 157]) and *pslA* (part of an operon encoding the Psl biosynthetic machinery [158-160]) as direct RpoS regulated genes (Table 3.5). Furthermore, RpoS was found to bind the promoter region of *sadB*, a gene previously described to be essential for the transition from reversible to irreversible attachment during biofilm formation [161]. In addition, RpoS seems to influence biofilm

Table 3.5. Selected genes that are regulated by RpoS as identified by ChIP-chip.

				ChIP-chip		Revised consensus box 300 bp upstream			Transcrip-tome
PA number[a]	Gene name	Description	Shared promoter[b]	Max. enrichment	Distance to ATG	Weight score	Sequence	Distance to ATG	Fold change[c]
chemotaxis									
PA0179	*cheY2*	probable two-component response regulator		1.19	200	6.71	attgTCTTTACTggaa	115	15.0
PA1930	*mcpS*	probable chemotaxis transducer	x	0.93	61	6.99	ccgaTCTACACTggcg	86	16.3
PA2573		probable chemotaxis transducer		1.08	-7	5.85	gttgACTATCCTtagc	41	12.1
PA4307	*pctC*	chemotactic transducer PctC		0.74	162	3.74	tggaTCATGGCTttcc	82	
PA4915		probable chemotaxis transducer		0.60	51	6.71	accaTCTTTACTctca	35	6.6
biofilm									
PA0905	*rsmA*	RsmA, regulator of secondary metabolites		0.58	161	6.26	ctggTCAATACTgggt	100	2.1
PA0928	*gacS*	sensor/response regulator hybrid	x	0.78	85	7.46	acccGCTAAACTgcgc	71	
PA2231	*pslA*	PslA		0.62	412	5.17	gaatGCTAAGATagct	163	6.5
PA2586	*gacA*	response regulator GacA		0.63	225	4.26	tggcGGTATACTtagc	169	
PA3621.1	*rsmZ*	Regulatory RNA RsmZ		0.56	-5	6.56	agctGCTAGAATcgcg	48	
PA3974	*ladS*	lost adherence sensor, LadS	x	0.62	188	4.29	gtgtGCTAAAGTtcgg	98	
PA4856	*retS*	regulator of exopolysaccharide and type III secretion, RetS		0.66	77	6.74	cttgGCTATAATccgg	38	
PA5253	*algP*	alginate regulatory protein AlgP	x	0.82	58	4.78	gcggGCAATCCTggcg	100	
PA5346	*sadB*	SadB		1.21	50	2.52	tccaGCTCGCATggtc	17	
c-di-GMP									
PA0861	*rbdA*	hypothetical protein		1.32	264	7.13	agccACTAGACTccta	169	2.6
PA1727	*mucR*	MucR	x	1.23	182	5.17	tcgtGCAATAATatca	59	
PA2072		conserved hypothetical protein		0.74	57	6.33	ggatGCTTAACTataa	60	4.2
PA2572		probable two-component response regulator	x	1.39	-1	6.10	tcggACTATGCTtgcc	52	13.2
PA3311		conserved hypothetical protein	x	0.93	6	3.67	acaaGCTCAGCT	8	13.3
PA4108		hypothetical protein	x	0.99	-11	3.87	cccaTCTCGGCTaccg	55	
PA4781		probable two-component response regulator		1.60	58	4.79	agcgTCTTCAATacgg	59	6.2
PA4929		hypothetical protein	x	0.76	22	1.37	tatcTCTAGGAAtggg	50	4.7
PA1097	*fleQ*	transcriptional regulator FleQ		0.89	197	5.82	tttgACTTAACTagtg	104	
PA2799		hypothetical protein	x	1.04	8	5.45	acggTATAAACTttga	70	1.8
PA2960	*pilZ*	type 4 fimbrial biogenesis protein PilZ		0.83	42	-	-	-	
PA3353		hypothetical protein		0.95	19	-	-	-	
PA3740		hypothetical protein		0.59	122	2.2	tgcaTCTAGCCAtcat	31	
PA4608		hypothetical protein	x	0.59	123	5.3	catgGCTTGGCTatag	46	2.9

[a] genes with an RpoS consensus box (>6.0) are underlined, genes differentially expressed in an *rpoS* mutant are in **bold**

[b] enriched promoter region could belong to two adjacent genes on opposite strands

[c] as described by Schuster *et al.* [136]

formation indirectly via the GacS/GacA two-component signal transduction pathway (Table 3.5). This system regulates the expression of a variety of phenotypes, including extracellular virulence factors, quorum sensing molecules and biofilm formation [162, 163]. Upon phosphorylation by the sensor kinase GacS, the GacA response regulator activates transcription of only two genes – *rsmY* and *rsmZ* [164], both specifying small regulatory RNAs which antagonize the activity of the regulatory protein RsmA [165, 166]. RsmA primarily acts as a translation initiation inhibitor by binding at or near the ribosome-binding region of target mRNAs [167, 168], and has been shown to negatively affect the expression of hundreds of genes – including those of the *pel* and *psl* operon [168, 169]. Our genome-wide analysis of RpoS-DNA interactions revealed the promoter regions of *gacS, gacA, rsmZ* and *rsmA* as direct targets of RpoS (Table 3.5). Moreover, two promoters of genes encoding other sensor kinases known to intersect with the GacS/GacA pathway and to influence RsmZ levels, were enriched by at least log_2-fold in the ChIP-chip experiments, namely *retS* (regulator of exopolysaccharide and type III secretion, [170]) and *ladS* (lost adherence sensor, [171]).

A recent transcriptome study in *E. coli* has shown that RpoS significantly impacts the expression of genes associated with the c-di-GMP signaling network [100]. To find out whether RpoS plays a similar role in *P. aeruginosa*, we searched our ChIP-chip result list for genes encoding proteins that metabolize or bind c-di-GMP. Of the 41 GGDEF/EAL/HD-GYP domain encoding genes, we identified 8 as direct targets of RpoS (Table 3.5): one gene encodes a GGDEF domain protein (PA4929), four genes encode GGDEF-EAL hybrid proteins (PA0861, PA1727, PA2072 and PA3311), and three genes encode the HD-GYP proteins of *P. aeruginosa* (PA2572, PA4108, PA4781). With the exception of PA1727 and PA4108, all genes have been reported to be transcriptionally regulated by RpoS [136] and three of those (PA0861, PA2072 and PA2572) additionally contain an RpoS consensus box in their promoter region. Overall these data indicate a strong influence of RpoS on the c-di-GMP metabolism. Furthermore, the expression of four PilZ domain proteins (PA2799, PilZ/PA2960, PA3353, PA4608) seems to be RpoS regulated as suggested by our ChIP-chip results. Only PA2799 and PA4608 were shown to have reduced expression in an *rpoS* mutant [136], and none of the four respective gene promoter regions harbors an RpoS consensus box. RpoS also bound to the promoter regions of the c-di-GMP binding transcriptional regulator FleQ and of the hypothetical, c-di-GMP binding protein PA3740. Both genes have not been described to be RpoS regulated genes by previous transcriptional studies.

3.3.4 Establishment of gel shift assays to validate RpoS-DNA interactions

To confirm the ChIP-chip results, binding of purified His_6-RpoS to DNA was analyzed *in vitro* by electrophoretic mobility shift assays (EMSA or gel shift assays). This method relies on a decreased mobility of protein-bound DNA in a native polyacrylamide gel, as compared with the unbound DNA fragment. For the establishment of EMSAs with the sigma factor RpoS, the promoter region of *cheY2* was chosen as target DNA for three reasons: (i) this region was enriched by more than 1.0 log_2-fold in the ChIP-chip experiment, (ii) this region contains a conserved RpoS binding box and (iii) the expression of *cheY2* strongly depends on the presence of RpoS as revealed by transcriptome analysis [136] (see also Table 3.5). As a nonspecific DNA-probe, either the *rsaL*/*lasI* intergenic region (*igr*) or a part of the *gltA* coding region was chosen (both regions were not enriched in the ChIP-chip experiments).

Initially, purified, his-tagged RpoS was incubated with a fluorescence-labeled, double-stranded 210 bp DNA fragment, spanning the region of –190 to +20 bp relative to the translational start of *cheY2*. However, the level of RpoS binding was very low under a variety of reaction conditions tested (amount of His_6-RpoS, addition of core RNA polymerase, incubation time; data not shown). Previous studies with *E. coli* RpoS have demonstrated that this sigma factor only weakly binds to double-stranded DNA, but tightly binds to "molten" (i.e. partially single-stranded) DNA [172]. Thus, purified His_6-RpoS was incubated with a fluorescence-labeled 30 bp fragment of the *cheY2* promoter region that included the RpoS consensus box (-126 to -96 bp upstream of the translational start). While no shift was observed with the double-stranded DNA probe and the single-stranded template (forward) probe, RpoS clearly shifted the single-stranded non-template (reverse) DNA probe (Figure 3.24A). This shift was demonstrated to be specific because (i) RpoS did not alter the mobility of the nonspecific *igr* DNA fragment, (ii) the RpoS-*cheY2* complex could be partially supershifted with an RpoS antibody and (iii) the RpoS-*cheY2* shift could be reversed by adding single-stranded, non-labeled *cheY2* fragments, but not by adding single-stranded, non-labeled *igr* fragments (Figure 3.24A and B). Interestingly, the addition of non-labeled *cheY2* reverse strand reduced RpoS binding to the labeled reverse strand only partially, while the addition of the *cheY2* forward strand completely abolished the RpoS binding. The total circumvention of RpoS binding could be caused by double strand formation of the non-labeled forward and the labeled reverse DNA strand.

We then used the gel shift assay to verify *rsmA* as direct target of RpoS. An influence of RpoS on the expression of RsmA was already suggested by the transcriptome study of Schuster *et al.* [136] and the promoter region of the respective gene was significantly enriched

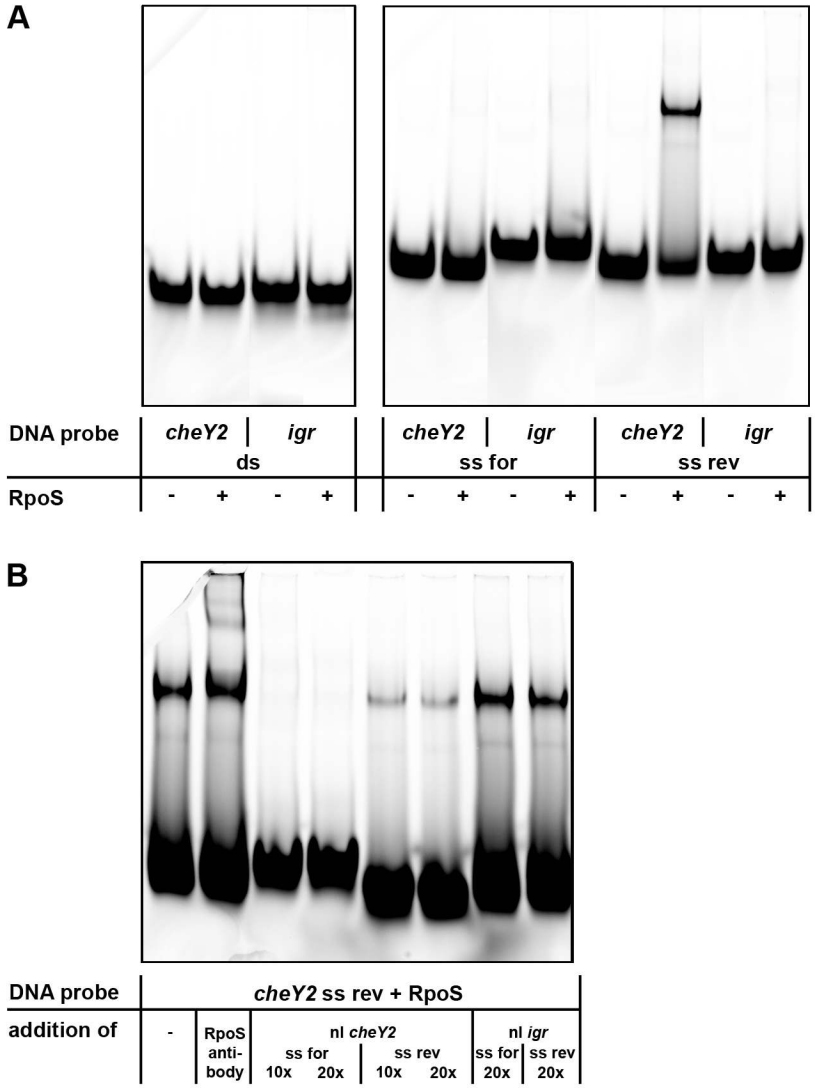

Figure 3.24. Establishment of electrophoretic mobility shift assays (EMSAs) for the stationary phase sigma factor RpoS.
All EMSAs were performed using short DNA probes (30-33 bp) and purified His_6-RpoS. *cheY2* was used as specific RpoS target, while *igr* served as a negative control. (A) RpoS binds to the single-stranded reverse (ss rev) *cheY2* DNA probe, but not to the single-stranded forward (ss for) or the double-stranded (ds) *cheY2* DNA probe. (B) RpoS binds specifically to ss rev *cheY2*, as the complex can be partially supershifted with an RpoS antibody and as binding of RpoS to ss rev *cheY2* can be competed with single-stranded, non-labeled specific DNA probe (nl *cheY2*, 10-20x molar excess) but not with the non-specific control DNA probe (nl *igr*, 20x molar excess).

in our ChIP-chip experiments. For EMSA reactions, a 30 bp DNA fragment was constructed that contains the RpoS binding motif located 100 bp upstream of the translational start site of *rsmA*. Figure 3.25A demonstrates that purified His_6-RpoS is able to bind to the single-stranded template (forward) *rsmA* DNA. The occurrence of two shifted bands may be explained by a partially degraded RpoS protein.

Next, we analyzed RpoS binding to the promoter region of PA0861 (*rbdA*), a gene that encodes a GGDEF-EAL hybrid protein and which is differentially expressed in an *rpoS*

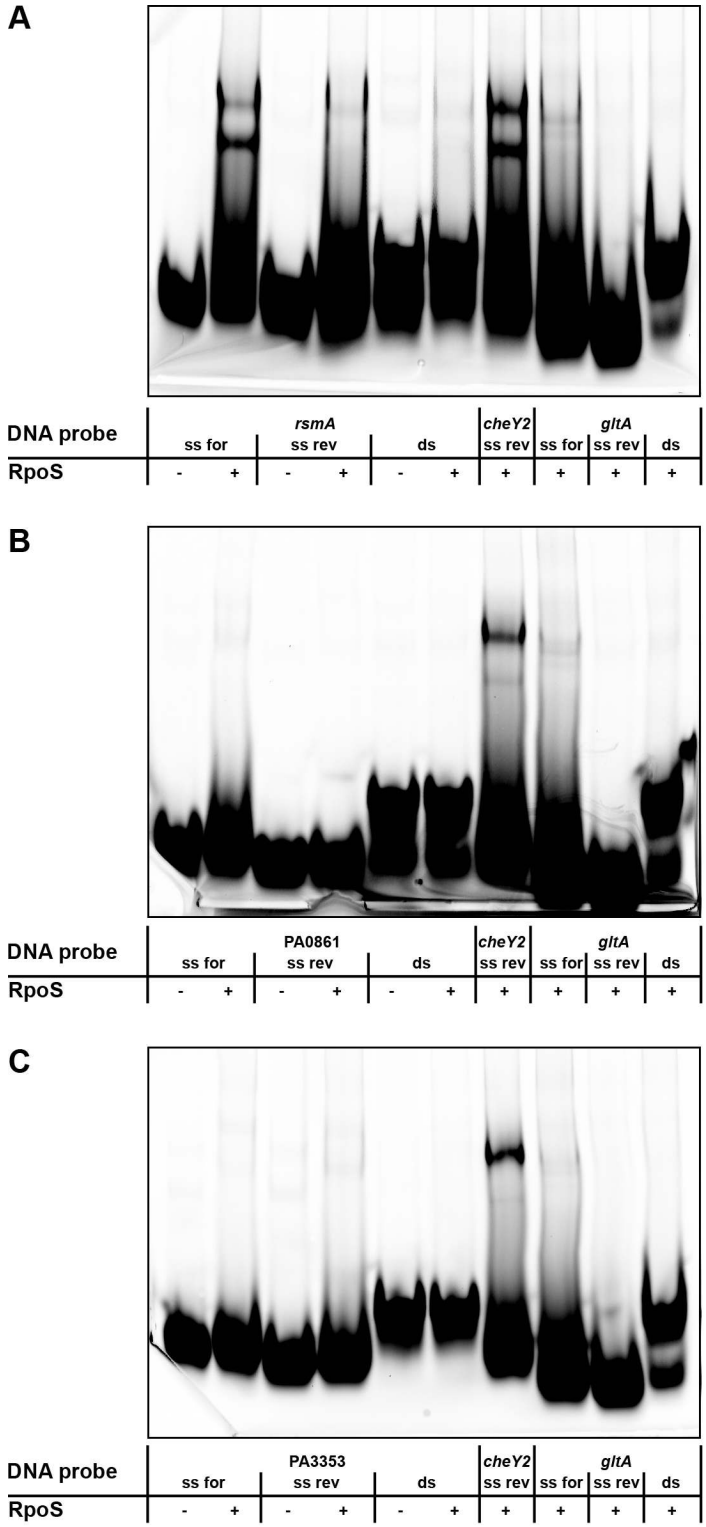

Figure 3.25. EMSA results for three distinct RpoS targets.
All EMSAs were performed using short DNA probes (30-33 bp) and purified His_6-RpoS. *cheY2* served as a positive control and *gltA* as a negative control. (A) Rpos binds to the *rsmA* single-stranded forward DNA probe. The occurrence of two shifted bands might be caused by partially degraded His_6-RpoS. (B) RpoS binding to PA0861 could not be confirmed under the used EMSA conditions. (C) RpoS does not bind to any of the PA3353 DNA fragments (single-stranded or double-stranded). ss for – single-stranded forward, ss rev – single-stranded reverse, ds – double-stranded.

mutant [136]. The promoter region of this gene was strongly enriched by chromatin immunoprecipitation and harbors an RpoS consensus sequence (-169 bp relative to the translational start site). Surprisingly, we were not able to confirm RpoS binding to this region *in vitro* (Figure 3.25B). Perhaps, the DNA fragment used for the gel shift experiments (spanning the region -180 to -150 bp) does not represent the correct RpoS binding site. Alternatively, additional factors may be required for binding of RpoS to this DNA region.

Our ChIP-chip results also suggested PA3353 to be part of the RpoS regulon. The PA3353 gene encodes a PilZ domain protein, which binds c-di-GMP with nanomolar affinity (see chapter 3.2.6). No RpoS binding motif can be found in the PA3353 promoter region. Based on the highest signal in the ChIP-chip experiments, the 33 bp-fragment directly located in front of the translational start site of PA3353 was chosen for EMSA reactions. However, no interaction of RpoS could be detected with either the double-stranded DNA fragment, or the single-stranded template or non-template strand (Figure 3.25C). Again, the wrong DNA fragment could have been chosen for the gel shift assays or RpoS only binds to the promoter regions in co-operation with other regulators which are not present under *in vitro* conditions. On the other hand, it cannot be excluded that ChIP enrichment of the PA3353 promoter region is an artifact and PA3353 thus represents a false-positive.

4 Discussion

Many bacteria are able to adopt two fundamentally different lifestyles. While the planktonic mode of growth enables dissemination and exploration of novel niches, growing within multicellular, matrix-encased biofilms offers protection and survival in unfavorable environments [3]. The formation of biofilms is not only a widespread phenomenon in nature, but also in clinical settings in which they impede successful treatment of chronic infections. Biofilm bacteria are much less susceptible to antibiotics than their planktonic counterparts and the difficulty to eradicate them is a prime concern of modern medicine [9]. There is an exploding interest in knowledge about cellular factors and molecular mechanisms controlling biofilm formation with the aim to identify putative therapeutic targets that will help to fight biofilm-related infections.

An exceedingly suitable model organism for studying the genetic and mechanistic principles of biofilm formation is the opportunistic human pathogen *Pseudomonas aeruginosa*. It is equipped with a large and complex genome which was recently sequenced facilitating the genetic analysis of this versatile organism [11]. Moreover, *P. aeruginosa* displays various types of motility that can be biased by complex chemosensory systems but also readily forms biofilm communities on a wide variety of natural and artificial surfaces. Thereby, a large collection of transcriptional regulators and alternative sigma factors permits this organism to tightly control its lifestyle and to adapt to diverse ecological niches. In this context, the aim of this thesis was to elucidate how *P. aeruginosa* integrates and translates extra- and intracellular signals to regulate the transition between motile and sessile lifestyles in order to give an appropriate response to a changing environment.

4.1 The *P. aeruginosa* chemotaxis methyltransferase CheR1 impacts on bacterial surface sampling

Motility is not only a characteristic trait of planktonic bacteria, but also an integral part of biofilm formation. In *P. aeruginosa*, several studies demonstrated an involvement of flagella- and pili-mediated motility on attachment and subsequent biofilm formation [51, 54, 58, 153, 173-175]. However, the contribution of chemotaxis to the establishment of biofilms has been less intensively studied.

There are several reports concluding that – depending on the model organism and experimental settings – chemotaxis is either required or dispensable for bacterial biofilm formation. The chemotactic signal transduction pathway of *E. coli* and *S.* Typhimurium is most likely the best characterized signal system at all, but studies of other organisms revealed much more diversity and complexity in chemotactic signaling than had been previously anticipated. Most motile environmental bacteria have multiple homologs of the *E. coli che* genes and many more *mcp* genes than the five found in the enteric bacteria [19]. *P. aeruginosa* is chemotactic to most of the organic compounds that it can grow on and encodes 26 *mcp* genes and four chemotaxis-like signal transduction systems [41]. One chemotaxis system (Pil-Chp, PA0408-PA0417) has been implicated in pili-mediated twitching motility [37, 38] and another one (Wsp, PA3702-PA3708) is involved in the regulated expression of Pel and Psl exopolysaccharides [39]. The two remaining chemotaxis systems (Che1, PA1456-PA1464 and PA3348-PA3349; Che2, PA0173-PA0179) are both involved in flagella-mediated chemotaxis [32-35]: while the Che1 system is absolutely required for this chemotactic response, the precise role of the Che2 system is still unclear. This complex chemotactic signaling equipment renders *P. aeruginosa* probably a good model microorganism for investigating the roles of chemotaxis in bacterial adaptation to diverse environmental niches, including the establishment of structured bacterial communities.

4.1.1 Characterization of the chemotaxis methyltransferase CheR1

In this thesis we provide evidence that CheR1 (PA3348) is a *P. aeruginosa* chemotaxis methyltransferase which transfers a methyl group from the methyl donor SAM to a methyl-accepting chemotaxis protein. As determined by surface plasmon resonance studies, CheR1 binds SAM at a K_D of approximately 60 μM, which is in the same order of magnitude as has been demonstrated for *Salmonella* CheR [176]. Receptor methylation by CheR is required for adaptation to persistent stimuli and binding of attractants causes increased methylation levels [18]. It has previously been shown that the MCPs PctA, PctB and/or PctC are responsible for the detection of several amino acids in *P. aeruginosa* [142]. In accordance with these results, we could demonstrate in this thesis that *in vitro* methylation of the MCP PctA by CheR1 could be enhanced by the addition of serine but not of glutamine, the latter of which was shown to be specifically detected by PctB [142].

In *E. coli,* highly abundant transmembrane receptors harbor a conserved NWETF motif at the extreme C-terminal end of the MCP which recruits CheR to the receptor cluster and is required for efficient methylation and demethylation [137, 138]. Here we demonstrate that the

MCP PctA was methylated by CheR1 despite the lack of a conserved C-terminal pentapeptide sequence. Similarly, a pentapeptide-independent methyltransferase has been characterized in the thermophilic bacterium *Thermotoga maritima* [177]. Co-crystallization of CheR from *S.* Typhimurium with the conserved NWETF pentapeptide demonstrated that the CheR β-subdomain is the region that interacts with the pentapeptide sequence [178]. β-subdomains can be divided into two groups: those with longer β-loops, found in CheR proteins from organisms containing MCPs with the pentapeptide recognition motif, and those with shorter β-loops, found in organisms that lack MCPs with the pentapeptide recognition motif [177-179]. Interestingly, in *P. aeruginosa*, CheR2 (PA0175) has a long β-loop and CheR1 has a short β-loop [177]. Moreover, only two out of 26 chemoreceptors have the conserved C-terminal pentapeptide motif and both genes encoding those chemoreceptors are located in the close proximity of the *che2* system. Overall, this might indicate that CheR2 uses a pentapeptide-dependent methylation mechanism, whereas CheR1 uses a pentapeptide-independent methylation mechanism and that this is one way of preventing crosstalk between different chemotaxis systems in *P. aeruginosa*.

4.1.2 CheR1 impacts on bacterial surface sampling

A recent publication on the influence of motility and chemotaxis in *Agrobacter tumefaciens* revealed an impact of chemotaxis on both, attachment and biofilm formation [53]. In this thesis, the *P. aeruginosa cheR1* mutant did not exhibit a phenotype in the CV assay. Nevertheless, soft-agar plate assays and confocal microscope analysis of static biofilms clearly demonstrate that CheR1 activity is not only essential for flagella-mediated chemotaxis but that it is also involved in the formation of structured biofilms. Interestingly, CheR1 activity seems to be important at two developmental steps within the process of biofilm formation. In the initial phase of biofilm formation, chemotaxis seems to promote bacterial movement in close proximity to the surface, which enables surface sampling prior to irreversible attachment. Later, flagella-mediated chemotaxis seems to be required for the formation and consolidation of a more structured community.

As far as we are aware, the only study examining biofilm formation of a *P. aeruginosa che1* chemotaxis mutant (*cheY*) was performed by Barken *et al.* [58]. They demonstrated that not type IV pili-driven but flagellum-driven motility is involved in the formation of cap structures in biofilms grown in a flow chamber irrigated with glucose minimal medium. Besides *cheY* and *fliM* mutants (the latter lack the polar flagellum), also a *P. aeruginosa rhlA* mutant

deficient in biosurfactant production displayed reduced cap formation [180]. Since swarming motility requires both the presence of biosurfactants and flagellar activity, Barken *et al.* [58] suggested that flagellum-driven surface-associated motility (by means of swarming) rather than directed motility (swimming in response to the sensing of certain metabolites) is required for cap formation. In this thesis, we used different experimental settings (static growth conditions, nutrient-rich medium), nevertheless, we also demonstrated a role of flagellum-mediated motility in the formation of structured biofilms. However, since our *cheR1* mutant displayed normal swarming motility on 0.5% agar plates, we rather hypothesize that chemotaxis driven swimming motility is necessary for formation of mature biofilm structures. A role for a substrate gradient that directs the motile bacteria has been suggested before [181].

In conclusion, one reasonable model for the role of motility and chemotaxis in biofilm formation in *P. aeruginosa* is that the efficiency and frequency of surface sampling may be influenced through chemotactic processes. This is important for initial sampling of bacteria to the surface and as the biofilm matures, chemotactic cues may stimulate dispersion. The released motile bacteria in the planktonic phase have the potential to colonize new sites and promote lateral expansion of the biofilm or to reattach in a coordinated chemotaxis-driven way, thus fine-tuning the architecture of biofilm structures.

4.2 A chemical proteomics approach identifies c-di-GMP binding proteins of *P. aeruginosa*

The chemotaxis system is one system which is able to translate environmental signals into an adaptive answer of the bacterial cell. Another system is the c-di-GMP signaling network in which an extra- or intracellular (first) signal is translated into a c-di-GMP (second) signal via the activity of diguanylate cyclases and phosphodiesterases. High levels of the second messenger c-di-GMP are known to promote the switch from motility to sessility and much effort has been undertaken to understand the particular role of c-di-GMP in the establishment and maintenance of bacterial biofilms. Thus far, research has mainly focused on cellular processes responsible for the synthesis and degradation of c-di-GMP, whereas we are only at the beginning to understand the role of c-di-GMP effectors and downstream signaling pathways.

In this thesis, we aimed at the identification of c-di-GMP binding proteins by using an enrichment tool that particularly targets the c-di-GMP effector sub-proteome. Chemically synthesized c-di-GMP was immobilized on a solid support and used for the isolation of c-di-GMP binding proteins out of complex protein mixtures in *P. aeruginosa*. Our chemical proteomics approach [182] also involved high-resolution mass spectrometry which assures unambiguous identifications of the affinity purified c-di-GMP binding proteins.

No c-di-GMP affinity resin has been described so far, although other cyclic nucleotide affinity beads have been previously used for the isolation of their respective interactomes [183, 184]. The main obstruction for the development of c-di-GMP affinity beads was the lack of ample amounts of this cyclic di-nucleotide needed for the synthesis of c-di-GMP resins.

4.2.1 Preparation of a c-di-GMP affinity resin

Groundwork for this thesis was the chemical synthesis of sufficient amounts of c-di-GMP and the performance and optimization of a coupling reaction with epoxy-activated sepharose (Michael Morr, Helmholtz Center for Infection Research and Frank Schwede, Biolog company, Bremen). C-di-GMP was successfully immobilized on the sepharose beads with an overall efficiency of 75%. Especially when small ligands are immobilized, a critical step is to retain binding activity of the molecule. In c-di-GMP, the N7 and O6 of the guanyl-ring act as main hydrogen bond acceptors and, in addition, H-bonds to the phosphate groups of the c-di-GMP backbone have been shown to mediate interactions between c-di-GMP and amino

acids of the target protein [68, 99, 145, 185-187]. Analysis of the functional groups involved in the chemical binding to the sepharose beads revealed that c-di-GMP was linked to this matrix mainly via its guanyl-N1 group (Figure 3.10). Although this group generally also can be involved in protein binding, the variety of other interactions between c-di-GMP and its target and the presence of various byproducts in the coupling reaction seemed to be sufficient to mediate binding of the immobilized c-di-GMP to PA14 and PA01 effector proteins.

4.2.2 The c-di-GMP and control bead sub-proteome

In addition to specific interaction partners, a large number of proteins are expected to co-purify during affinity chromatography because of their abundance and a nonspecific binding mode to the sepharose matrix. To identify common contaminating proteins, an epoxy-activated sepharose transformed with ethanolamine was used as a negative control. Analysis of this control revealed a "bead-proteome" [188] that proved to be larger than the c-di-GMP sub-proteome. This bead-proteome served as a reference to validate the results of the c-di-GMP pull down and to reduce the rate of false-positives. However, especially the large size of the reference bead-proteome bears the risk of the elimination of true-positives. For example, the transcriptional regulator and approved c-di-GMP effector FleQ [88] was found in the c-di-GMP pull down but also in the controls and thus was excluded from the list of c-di-GMP binding proteins.

Our final lists of protein candidates that directly or indirectly interact with c-di-GMP included PilZ domain proteins and proteins with I-site motifs, but also proteins without any known c-di-GMP binding motif (Table 3.2 and Table 3.4). These lists are not only largely impacted by the definition of the inclusion and exclusion criteria based on protein identification scores and the reference proteome, but the listed c-di-GMP interacting proteins are also those of a certain time point (here: stationary phase of bacterial growth) and a certain subcellular localization (here: mainly cytoplasmic fraction). Thus, differences in culture conditions and cell extract preparations, the use of altered parameters defining the identification of proteins and an alternative bead-proteome, are expected to originate in the identification of additional c-di-GMP effector candidates.

4.2.3 SPR is a useful tool to validate c-di-GMP/protein interactions

Another part of this thesis was the generation of a robust and sensitive c-di-GMP binding assay in order to verify c-di-GMP binding *in vitro*. In co-operation with the group of F. W.

Herberg (University of Kassel), a SPR based assay using a 2'-AHC-c-di-GMP sensor chip to detect c-di-GMP/protein interactions was established. 2'-AHC-c-di-GMP is a novel, functionalized c-di-GMP analog with a linker group attached to 2'OH of one ribose-unit (Figure 3.10) and can be easily immobilized via the terminal amino group of the linker using primary amine coupling. Advantages of the SPR technique are the low sample consumption, the high sensitivity and that binding reaction can be followed in real time. In a solution competition assay, it furthermore enables the determination of EC_{50} (half-maximal effective concentration) values for unmodified ligands reflecting the potency of a ligand to interact with the target. This value can then be used to estimate whether the affinity is in the range of biologically effective c-di-GMP concentrations (<50 nM to a few μM) [59].

In pull down experiments using either PA01 or PA14 lysates, the PilZ domain protein PA3353 was repeatedly identified. SPR solution competition experiments for PA3353 revealed an EC_{50} value of approximately 260 nM, which is in agreement with the sub-micromolar K_D values observed for other PilZ domains [59] and thus demonstrates the applicability of our method.

We also examined the putative response regulator PA4396, which is included in our list of putative c-di-GMP binding proteins and harbors a degenerate GGDEF domain with the c-di-GMP binding I-site motif. Purified Strep-PA4396 was able to bind to the 2'-AHC-c-di-GMP sensor surface, however, in SPR competition experiments, the EC_{50} value was determined to be approximately 60 μM, which is slightly higher than any known affinity of a c-di-GMP binding site [59]. The *in vitro* binding assays might be impeded by the use of improperly folded proteins, the absence of important co-factors or interaction partners and the lack of post-translational modifications. Further investigations should reveal whether, for example, phosphorylation of the receiver domain of PA4396 might enhance the affinity of this response regulator to its ligand.

A third protein from the list of putative c-di-GMP effectors, the chemotaxis methyltransferase CheR1, was tested in SPR for c-di-GMP binding. CheR1 has no common c-di-GMP binding motif, but the repeated identification in pull downs in both the PA01 and PA14 strains, and the correlation to flagellum mediated motility renders CheR1 an interesting c-di-GMP binding candidate. However, SPR binding studies revealed a nonspecific binding mode of CheR1-His_6 to c-di-GMP as the binding event could not be efficiently competed with up to 10 μM free c-di-GMP. Further investigations should reveal whether the absence of important co-factors or interaction partners *in vitro* might be responsible for the lack of specific binding or whether CheR1 itself is not binding c-di-GMP but stably interacts with a c-di-GMP effector protein.

Besides PA3353 and PA4396, we identified PA3740, a conserved hypothetical protein, as a novel type of c-di-GMP effector protein. Upon injection of PA3740-His_6, a specific and reproducible binding to the 2'-AHC-c-di-GMP sensor chip was observed, despite the lack of any domain previously described to specifically interact with c-di-GMP. With an EC_{50} value of approximately 30 nM, PA3740 shows a high affinity to c-di-GMP similar to those of PilZ domain effectors. The next challenge will be to identify the exact binding site of c-di-GMP to this protein. One way to achieve this is by determining the tertiary structure of PA3740 in presence and absence of c-di-GMP via X-ray crystallography or NMR studies. However, those experiments require a large amount of highly pure PA3740 protein, which can currently not be provided as heterologous overexpression of PA3740 in *E. coli* is impeded by an apparent toxicity of PA3740 to its host cells.

4.2.4 The c-di-GMP binding proteins PA3353 and PA4396 influence motility behavior of *P. aeruginosa*

To reveal the cellular function of verified c-di-GMP binding proteins, cells lacking or overexpressing the respective protein were analyzed for their motility behavior and ability to form biofilms. Those phenotypic assays suggested that the PilZ domain protein PA3353 interferes with flagella-mediated motility. Mutants affected in the expression of PA3353 displayed an enhanced swimming motility, but normal ability to swarm and twitch. Overexpression of PA3353 impaired swimming as well as swarming motility, while twitching motility remained unaffected. The PA3353 gene is directly located downstream of one of the three chromosomal regions that are associated with flagellar regulons (Region III, PA3348-PA3352) [189] supporting the link of PA3353 to flagellar motility. With the YcgR-PilZ-domain organization, PA3353 might be the *P. aeruginosa* counterpart of the PilZ domain protein YcgR in *E. coli*, which has been demonstrated to slow down the flagellar motor upon c-di-GMP binding [79, 148]. Further studies are required to clarify the role PA3353 plays in swimming and/or swarming motility.

Our phenotypic analyses indicated an involvement in bacterial motility also for the putative response regulator PA4396. Whereas a PA4396 transposon mutant displayed wild-type motility behavior, overexpression of this protein in the wild-type enhanced swimming and swarming motility, while twitching motility was reduced. The ability to form biofilms in CV assays was unaffected in both strains, the PA4396 mutant and PA4396 overexpressing strain. A recent study performed by Kulasekara *et al.* [62] furthermore demonstrated that cells

overexpressing PA4396 were impaired in their ability to kill Chinese hamster ovary (CHO) cells. This might have been caused by a dysfunction of adherence factors, such as pili or flagella [190-192], leading to reduced attachment of bacteria to host cells. Alternatively, overexpression of PA4396 might have impacted the functionality of the type three secretion system which is activated upon adherence to mammalian cells and which delivers toxins from the bacteria into host cells [193]. More work is necessary to understand how PA4396 influences motility behavior and cytotoxicity towards CHO cells.

4.2.5 The cellular function of PA3740 is still unknown

Despite much effort, our motility and biofilm formation assays did not reveal a particular phenotype of a mutant affected in the expression of the hypothetical protein PA3740 nor of a strain overexpressing PA3740. This protein might be involved in processes which we did not examined yet (such as the production of virulence factors), or we might have missed the right conditions under which PA3740 becomes activated. Recently, we developed a polyclonal anti-PA3740 serum which will be a useful tool for further studies aiming at the identification of the cellular role of PA3740. First western blot analyses using purified PA3740 protein indicated the functionality of this antiserum (data not shown). This offers the opportunity to perform PA3740 pull down assays in order to isolate potential interaction partners of PA3740. Another possibility would be to use the serum in conjunction with immunofluorescence to identify the localization site of PA3740 in the bacterial cell.

Taken together, we have validated a c-di-GMP affinity resin as a valuable novel tool for the isolation of c-di-GMP binding proteins and demonstrated the applicability of the 2'-AHC-c-di-GMP sensor chip for SPR binding studies. In general, affinity chromatography proved to be sufficient for the isolation of c-di-GMP binding proteins harboring known but also new c-di-GMP binding motifs in the model organism *P. aeruginosa*. The next challenge will be to unravel the cellular function of those c-di-GMP binding proteins and to access which role they play in the downstream communication of the c-di-GMP signal. The use of chemical proteomics for the discovery of novel c-di-GMP binding motifs also in other bacterial species might be the basis for new studies and will significantly contribute to our understanding of the c-di-GMP signaling network.

4.3 The regulon of the *P. aeruginosa* stationary phase sigma factor RpoS as revealed by ChIP-chip analysis

Environmental signals can not only be integrated and processed via the chemotaxis and c-di-GMP signaling systems, but also via the activation of global regulators which control the transcription of specific subsets of genes. A major challenge is to identify those particular regulons on a global scale, and to understand how they are intertwined with other regulatory networks. *P. aeruginosa* possesses an extraordinary number of two-component regulatory systems, transcriptional regulators and alternative sigma factors allowing successful adaptation to diverse ecological niches. The alternative sigma factor RpoS is activated upon entry into the stationary phase of growth and has been shown to affect production of virulence factors and to mediate stress response [151, 194, 195]. Moreover, RpoS seems to be involved in the control of biofilm growth as cells lacking RpoS develop significantly thicker biofilms in a flow chamber than respective wild-type cells [153]. Thereby it would be interesting to know whether RpoS controls transcription of genes directly linked to biofilm formation or of genes encoding components of other regulatory systems, such as the c-di-GMP signaling network, which in turn impact biofilm formation.

In the past years, transcript profiling was used in a wide range of bacteria to identify global regulons of alternative sigma factors (for example [196-201]). However, a transcriptomic approach does not reveal the primary binding targets of the transcription factor under study and is unable to reveal regulatory cascades in which one regulator controls expression of many others. Recently, chromatin immunoprecipitation in combination with hybridization to microarrays (ChIP-chip) has emerged as a powerful and complementary tool, since it measures protein-DNA interaction *in vivo* on a genomic scale. Initially developed for eukaryotic cells, ChIP-chip was now also successfully applied in bacteria (reviewed in [202, 203]) and has been used in some cases to analyze the chromosome-wide binding profile of RNA polymerase with different sigma factors [132, 204-206].

4.3.1 Evaluation of the RpoS regulon

In this thesis, we aimed at the identification of the *P. aeruginosa* RpoS regulon by performing ChIP experiments in combination with a high-resolution *P. aeruginosa* genome microarray [104]. Our ChIP-chip approach proved to be a very robust and reproducible method that led to the identification of more than 400 RpoS promoter targets. Categorization of those RpoS

targets revealed a large subset of enriched promoter sites (128) upstream of genes that have been shown to be subject of differential transcription in an *rpoS* mutant (Schuster *et al.* [136]) and approximately half of those (59) harbored an RpoS consensus sequence (Figure 3.23). Since transcript profiling measures the consequences of protein binding rather than the binding event itself, the transcriptional profile also reflects secondary effects on gene expression. This may account for the large number of genes that were differentially regulated in an *rpoS* mutant but that did not show RpoS binding *in vivo* (643).

On the other hand, for a large fraction of ChIP-chip identified RpoS targets (345 of which 81 harbor an RpoS binding motif) no detectable effect on transcription of the neighboring genes was observed by Schuster *et al.* [136] in an *rpoS* mutant. This phenomenon of "unexpected" protein-DNA interaction has been also observed by other groups comparing ChIP-chip experiments with transcriptional profiling data and several explanations have been proposed [202, 207]. For example, the transcriptome profile might have been determined under non-activating conditions in which a bound transcription factor does not influence the transcript level of specific genes. Alternatively, the influence of the transcription factor on gene expression might be only weak and is easily overridden by a second regulatory protein. Furthermore, a DNA-bound transcription factor may have a different task than regulating gene transcription or it has bound to a target site with no functional relevance.

We also observed that a subset of genes identified to be RpoS regulated by our ChIP-chip approach as well as by the transcriptome study of Schuster *et al.* [136] does not harbor the conserved RpoS binding motif in their upstream region (69 out of 128). A likely explanation for this phenomenon – that has also been described before – could be that co-operative interactions with other transcriptional factors enable the binding to those non-consensus regions or that differences in local DNA topology influence the sequence preference of transcription factors [202].

4.3.2 Influence of RpoS on chemotaxis and biofilm formation

The RpoS regulon as revealed by our ChIP-chip approach contained several chemotaxis related genes confirming the role of RpoS in the expression of the Che2 system and some methyl-accepting chemotaxis proteins (Table 3.5) [136, 155].

Furthermore, some of the identified RpoS targets are evidently linked to biofilm formation, such as *pslA*, a gene required for the synthesis of exopolysaccharides [158-160] (Table 3.5). A recent study by Irie *et al.* [152] demonstrated that *pslA* is transcriptionally activated by RpoS and translationally repressed by binding of the regulatory protein RsmA to the large 5'

untranslated region of the *pslA* transcript. Interestingly, RsmA itself seems to be regulated by RpoS as indicated by several, independent observations. Although continuously expressed, intracellular levels of RsmA peak in the stationary phase [167, 168] and a mutant affected in the expression of RpoS displays reduced *rsmA* transcript levels in the stationary phase but not in the logarithmic phase of growth [136]. Moreover, the non-coding region located upstream of *rsmA* harbors a conserved RpoS binding motif and was demonstrated to be bound by RpoS in our ChIP experiments (Table 3.5). This binding could be verified *in vitro* by electrophoretic mobility shift assays. We also identified other RpoS targets in the ChIP-chip assays that interfere with RsmA and thus exopolysaccharide production (Table 3.5), namely *rsmZ*, *gacA*, *gacS*, *retS* and *ladS*. The activity of RsmA is antagonized by the small regulatory RNA RsmZ,

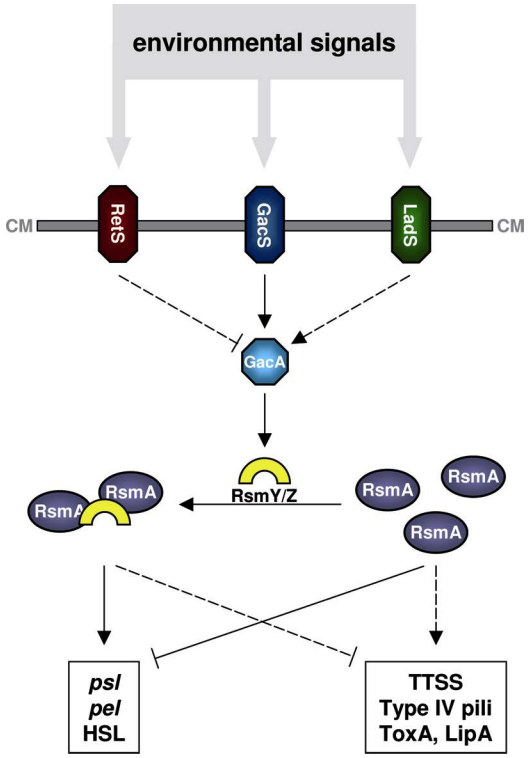

Figure 4.1. A model of the complex Gac/Rsm regulatory network in *P. aeruginosa*.
Upon phosphorylation by the sensor kinase GacS, GacA activates expression of the small regulatory RNAs RsmY and RsmZ, which are antagonizing the activity of the translational repressor RsmA. Free RsmA promotes the production of virulence factors (e.g. type three secretion system – TTSS, type IV pili, Toxine A, Lipase A), while it represses translation of transcripts required for biofilm formation (psl, pel) and for production of homoserine lactone (HSL) quorum sensing signals. The positive influence of RsmA on virulence factor production is believed to occur via indirect mechanisms, e.g. by controlling expression of regulatory factors. Sequestration of RsmA by RsmY/Z leads to a shift from acute virulence to chronic, biofilm-related virulence. There are two other sensor kinases influencing the expression levels of RsmY/Z and thus, RsmA activity: RetS inhibits activation of GacA leading to high levels of free RsmA, while LadS promotes GacA activity and thus inhibition of RsmA by RsmY/Z binding. The environmental signals leading to activation of the RetS/GacS/LadS sensor kinases are still unknown. This figure is based on previously published models [168, 208]. Dashed lines – indirect regulation, continuous lines – direct regulation.

which is transcriptionally regulated by the GacS/GacA two component signaling system and the entangled sensor kinases LadS and RetS [164-166, 170, 171]. While RetS is an antagonist of the GacS sensor kinase and negatively influences GacA dependent *rsmZ* expression, LadS promotes transcription of *rsmZ* [170, 171, 209]. Thus, RpoS seems to contribute to the expression of nearly all components (with the exception of RsmY that also antagonizes RsmA activity [165]) of a complex regulatory network that can integrate yet unidentified signals via the sensor kinases LadS, GacS and RetS to regulate either biofilm formation and the production of quorum sensing signals or the synthesis and secretion of various virulence factors [208] (Figure 4.1).

4.3.3 RpoS strongly influences the c-di-GMP signaling network

Our ChIP-chip data also revealed a strong link between RpoS and the c-di-GMP signaling network. Of the 41 genes encoding GGDEF/EAL/HD-GYP domain proteins in the strain PA01, we identified eight as direct RpoS targets (Table 3.5 and Table 4.1). Three of those harbor the conserved RpoS binding motif in their promoter region and they have also been demonstrated to be expressed at lower levels in an *rpoS* mutant as compared to the parent wild-type strain [136]. Another three do not have an RpoS consensus sequence in their non-coding upstream region but still were differentially expressed in an *rpoS* mutant [136] and thus are obviously directly regulated by RpoS.

RpoS targets that were identified by ChIP-chip, transcriptional profiling and the presence of an RpoS box

The three c-di-GMP associated genes identified by all three criteria (ChIP-chip, transcriptome, RpoS box) are PA0861, PA2072 and PA2572. So far, RpoS/target-DNA interactions under *in vitro* conditions (electrophoretic mobility shift assays) were only tested for PA0861. In those gel shift assays, we could not prove binding of RpoS to a 30 bp fragment of the PA0861 promoter region, which was most likely due to inappropriate reaction conditions.

PA0861 was recently characterized by An *et al.* and is a GGDEF-EAL hybrid protein involved in the *r*egulation of *b*iofilm *d*ispersal therefore also termed RbdA [210]. RbdA seems to promote swarming and swimming motility as well as rhamnolipid production, thus factors required for biofilm dispersal, while it negatively influences exopolysaccharide production. Although RbdA contains both a highly conserved GGDEF and EAL domain, it

Table 4.1. The RpoS controlled c-di-GMP regulon.

	ChIP-chip log_2-fold enrichment	**RpoS-Box** weight score	**Transcriptome** fold change [136][a]
GGDEF			
PA0169			-2.3
PA0290			
PA0338			
PA0847			5.4
PA1107		6.61	
PA1120			3.6
PA1851			
PA2771			11.6
PA2870			
PA3177			
PA3343			2.1
PA3702			2.1
PA4332			
PA4396			
PA4843			-2.1
PA4929	0.76		4.7
PA5487			
GGDEF-EAL			
PA0285			
PA0575		6.99	
PA0861	1.32	7.13	2.6
PA1181			2
PA1433			
PA1727	1.23		
PA2072	0.74	6.33	4.2
PA2567			-1.7
PA3258			
PA3311	0.93		13.3
PA4367			
PA4601			
PA4959			
PA5017		6.33	
PA5295			
PA5442			
EAL/HD-GYP			
PA2133			
PA2200			
PA2572	1.39	6.10	13.2
PA2818			
PA3825			4.8
PA3947			
PA4108	0.99		
PA4781	1.60		6.2
PilZ			
PA0012		6.10	
PA2799	1.04		1.8
PA2960	0.83		
PA2989			
PA3353	0.95		
PA3542			
PA4324			
PA4608	0.59		2.9

primarily seems to function as a phosphodiesterase. An and co-workers [210] were unable to detect any diguanylate cyclase activity of purified RbdA protein. Instead, the GGDEF domain appears to stimulate PDE activity of the neighboring EAL domain by binding GTP, a phenomenon that already has been described for a GGDEF-EAL protein in *C. crescentus* [122]. Furthermore, the RbdA PDE activity is also modulated by a PAS domain which is located upstream of the GGDEF and EAL domain and which is probably involved in oxygen sensing [210].

The hypothetical protein PA2072 has not been studied in detail so far. Analysis of the amino acid sequence reveals that the protein has an extracellular sensory domain (CHASE4, [211]) in combination with an intracellular PAS domain, GGDEF domain and EAL domain [62]. The frequent occurrence of GGDEF-EAL hybrid proteins has been termed a “biochemical conundrum” [212], and it was suggested that either one of the two domains is enzymatically inactive or the protein can switch between both catalytic activities (c-di-GMP synthesis and degradation, respectively) in response to the oligomerization state or the sensing of environmental signals. Alternatively, both domains might be active and create a very precise concentration of c-di-GMP [71, 212]. In PA2072, the GGDEF as well as the EAL domain is highly conserved and detailed biochemical studies are required to uncover the preferential enzymatic activity of this protein.

The third c-di-GMP associated gene identified to be RpoS regulated by ChIP-chip, transcriptional profiling and the presence of an RpoS box is PA2572. It was recently characterized by Ryan *et al.* [95] and encodes a putative response regulator with an HD-GYP domain. The PA2572 gene is adjacent to a gene encoding a probable sensor kinase (PA2571). The two genes are divergently transcribed and thus RpoS could regulate the expression of both PA2571 and PA2572. Consistently, both genes are differentially expressed in an *rpoS* mutant [136]. Cells affected in the expression of PA2572 produce higher levels of rhamnolipids and display a biofilm architecture that is different from the wild-type. They are furthermore reduced in their ability to kill larvae of the Greater Wax Moth *Galleria mellonella* [95]. The HD-GYP domain of the PA2572 protein differs from other HD-GYP domains by having variant key residues (YN-GYP) and it seems not to harbor any phosphodiesterase activity. It would be interesting to know whether this “degenerate” HD-GYP domain is still able to bind c-di-GMP and is thus acting as a c-di-GMP effector. However, it was not identified as a c-di-GMP binding protein in our pull down experiments using the c-di-GMP affinity resin.

RpoS targets that were identified by ChIP-chip and transcriptional profiling

There are three further genes that are involved in c-di-GMP metabolism and that were identified as RpoS dependent genes by both our ChIP-chip approach and the transcriptome study of Schuster *et al*. [136]: PA4929, PA3311 and PA4781 (Table 4.1). However, they do not posses the conserved RpoS binding motif in their non-coding upstream region suggesting that RpoS either binds to an altered sequence motif or that other factors mediate DNA-binding of RpoS to the promoter region of PA4929, PA3311 and PA4781, respectively.

PA4929 encodes for a hypothetical protein whose cellular role is still uncharacterized. The presence of a highly conserved GGDEF domain proposes a function as a diguanylate cyclase which might be activated in response to external signals sensed by the associated 7TMR-DISMED2 domain (seven-transmembrane receptor with diverse intracellular signaling modules, [213]).

The PA3311 gene product is a conserved hypothetical protein and another example of a GGDEF-EAL fusion protein. Additionally it harbors an N-terminal MHYT domain which has been suggested to be able to sense oxygen, carbon monoxide or nitrogen monoxide [214]. Both the GGDEF and EAL domain of PA3311 are well conserved although the characteristic sequence motif within the GGDEF domain is changed to AGDEF. So far, the catalytic activity of this protein has not been described, but a mutant with a transposon insertion within the PA3311 coding sequence was shown to have an enhanced ability for pellicle (biofilm) formation [62].

The last gene identified by ChIP-chip and by transcriptional profiling is PA4781, which encodes an HD-GYP domain that is fused to an N-terminal response regulator domain. No gene encoding a sensor kinase is found in the genomic proximity of PA4781. The work of Ryan *et al.* [95] provides evidence that PA4781 acts as a c-di-GMP degrading enzyme which positively influences swarming and twitching motility and which contributes to virulence in the *Galleria* model.

RpoS targets either identified by ChIP-chip or by transcriptional profiling

In the ChIP experiments, RpoS also bound to the promoter regions of PA1727, encoding a GGDEF-EAL protein regulating alginate biosynthesis [215], and PA4108, encoding a HD-GYP domain protein with PDE activity [95] (Table 4.1). However, these genes were expressed at same rates in an *rpoS* mutant and the respective wild-type strain [136] and no RpoS binding motif can be detected in their promoter region. Thus, the influence of RpoS on

these genes should be further tested by gel shift assays or transcriptional reporter fusion studies to verify RpoS dependent transcription of these genes.
On the other hand, some promoter regions of genes for which RpoS regulated transcription was suggested by the transcriptome study of Schuster *et al.* [136] were not bound by RpoS in our ChIP-experiments (Table 4.1). Only one of those ten genes, PA1120 (*tpbB*/*yfiN*), harbors a conserved RpoS binding sequence located in the non-coding upstream region of the PA1121-PA1120-PA1119 operon, supporting the hypothesis of a direct RpoS regulation. For the remaining genes further studies are required to determine whether they are directly affected by RpoS, or whether their expression depend on transcription factors which in turn are regulated by RpoS.

RpoS may establish a c-di-GMP signaling sub-network

In addition to RpoS activated expression of c-di-GMP metabolizing enzymes, the ChIP-chip and transcriptional profiling studies also revealed a role for RpoS in the transcription of genes encoding for c-di-GMP binding proteins, such as the PilZ domain proteins PA2799 and PA4608 (Table 3.5 and Table 4.1). Thus, a whole c-di-GMP signaling sub-network seems to be established by RpoS upon entry into the stationary phase of growth. A strong impact of RpoS on c-di-GMP signaling has also been demonstrated for *E. coli* [100] in which RpoS triggers expression of c-di-GMP metabolizing proteins controlling the production of biofilm-associated curli fimbriae.
By promoting transcription of genes only under certain environmental (growth) conditions, RpoS might help to enable specificity within the complex c-di-GMP signaling network in which a multitude of c-di-GMP synthesizing and degrading enzymes regulate bacterial behavior via multiple c-di-GMP effectors. The challenge will be to identify the nature of the bacterial response that is triggered by RpoS controlled c-di-GMP signaling pathways in *P. aeruginosa*.

In summary, we have successfully applied the ChIP-chip technique to an alternative sigma factor of *P. aeruginosa* providing exciting insights into the global RpoS “sigmolon” [207]. The use of the powerful combination of ChIP-chip and transcriptional profiling studies for the rapid identification of diverse regulons will be an important step on our way to understand the various mechanisms of gene regulation in *P. aeruginosa* and their interdependencies with other complex regulatory networks that determine bacterial behavior.

4.4 The decision how to live: Conclusions

Bacteria often thrive in protected, surface-associated biofilm communities but also occasionally return to the planktonic mode of growth to rapidly multiply and disperse to colonize novel habitats. The successful transition between motile and sessile lifestyles is essential for fitness and survival of microorganisms and requires the sensing and integration of various environmental cues into an adaptive response.

Based on results of this thesis, a model is provided of how *Pseudomonas aeruginosa* – and most likely other bacterial species – can use different mechanisms to determine an appropriate response to changes in its surroundings (Figure 4.2). One way is to directly react in a behavioral manner upon sensing of environmental cues. This mechanism is for instance enabled by the chemotaxis machinery that promotes swimming motility into a favorable direction upon detection of a substrate gradient. Moreover, as demonstrated in this thesis, the

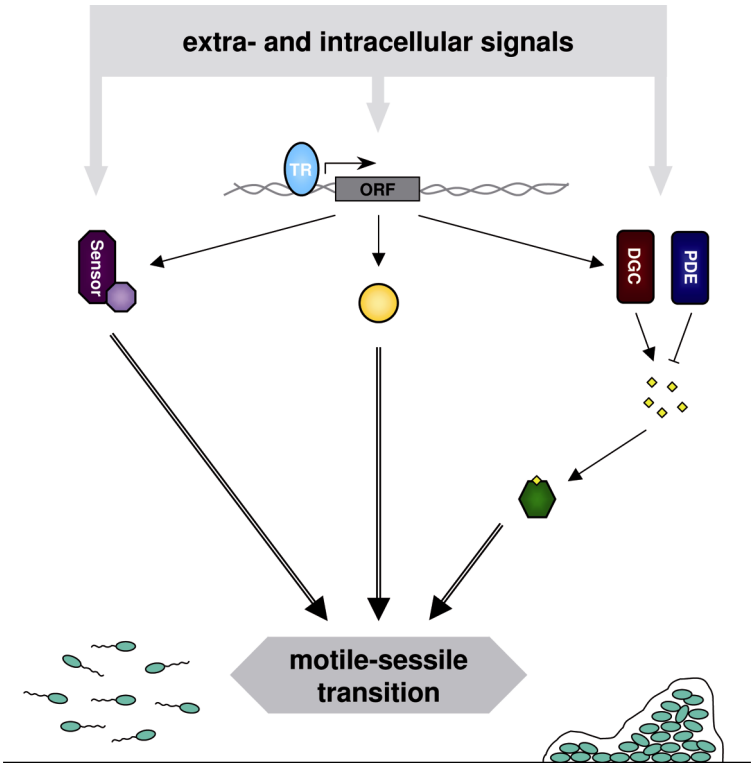

Figure 4.2. Model of how bacteria can use different mechanisms to integrate extra- and intracellular signals into the regulation of motility versus sessility.
Some bacterial signaling systems are able to transmit perceived signals to associated regulators which directly influence motility or biofilm formation. Other signal systems translate sensed signals into the second messenger c-di-GMP which is a key player in the regulation of motility versus sessility by binding to diverse effector molecules. Alternatively, sensing of certain signals first trigger a switch in gene expression by the activation of transcriptional regulators (TR). This may lead to the production of factors directly required for a motile or sessile lifestyle and/or to the expression of other regulatory pathways which control bacterial behavior on the single-cell level.

Che1 chemotaxis system of *P. aeruginosa* also plays an important role in efficient surface sampling and the formation of biofilm structures. It will be interesting to see whether the chemotaxis system also influences biofilm formation in other bacterial species.

A second possibility to integrate environmental signals into regulatory pathways that control the transition between a motile or a sessile lifestyle is via the c-di-GMP signaling system. In this case, external or cellular cues are firstly translated into the second messenger c-di-GMP, which then can bind to diverse effector molecules able to interfere with motility or biofilm formation. Many details of the c-di-GMP network are still uncharacterized, but tools such as presented in this thesis will significantly contribute to the analysis and thus understanding of this complex signaling system.

Changes in the environment can also trigger the activation of transcriptional regulators causing a switch in gene expression. This may lead to the selective production of factors directly required for motility or biofilm formation. Alternatively, other regulatory systems might be expressed enabling the integration of further signals and thus a fine-tuning of the bacterial output response that determines bacterial behavior. For example, in this thesis we demonstrated that the alternative sigma factors RpoS regulates transcription of genes being part of the GacS/GacA and/or the c-di-GMP signaling system. Future studies will reveal how other sigma factors and global regulators contribute to the careful decision whether to settle down or move away.

Overall, bacteria can rely on diverse traits to regulate the transition between motile planktonic and sessile multicellular lifestyles. Knowledge on factors that are essential for the switch between both lifestyles is an important step on our way to counteract problems caused by the persistent, biofilm-associated mode of growth.

5 Appendix

Table 5.1. Genes encoding GGDEF and/or EAL/HD-GYP domains in *P. aeruginosa* PA01.

PA number	Gene name	I-site motif[a]	GGDEF sequence	EAL or HD-GYP sequence	Partner domains[b]	Selected references
PA0169	*siaD*	yes	GGEEF			[62, 216]
PA0290		yes	GGEEF		PAC	[62]
PA0338		yes	GGEEF		PAC	[62]
PA0847		yes	GGDEF		TM, CHASE4, HAMP, PAS, PAC	[62]
PA1107	*roeA*	yes	GGEEF		TM	[62, 217]
PA1120	*tpbB, yfiN*	yes	GGDEF		TM, HAMP	[62, 126, 218, 219]
PA1851		yes	GGEEF		TM	[62]
PA2771		yes	GGEEF		GAF	[62]
PA2870		yes	GGEEF			[62]
PA3177		yes	GGEEF			[62]
PA3343		yes	GGEEF		TM	[62]
PA3702	*wspR*	yes	GGEEF		REC	[40, 62, 145, 220]
PA4332	*sadC*	yes	GGEEF		TM	[62, 217, 221]
PA4396		yes	DEQHF		REC	[62]
PA4843		yes	GGEEF		REC	[62]
PA4929		yes	GGDEF		7TMR-DISMED2	[62]
PA5487		yes	GGEEF			[62]
PA0285		no	GGDEF	ESL	TM, PAS, PAC	[62]
PA0575		yes	GGDEF	EAL	TM, SBP bac 3, PAS, PAC	[62]
PA0861	*rbdA*	yes	GGDEF	ELL	TM, PAS	[62, 210]
PA1181		yes	GGDEF	ELL	MASE1, PAS, PAC	[62]
PA1433		no	RGGEF	KVL	TM, HAMP	[62]
PA1727	*mucR*	yes	GGDEF	EAL	TM, MHYT	[62, 215]
PA2072		yes	GGDEF	EAL	TM, CHASE4, PAS	[62]
PA2567		no	SPTRF	EAL	GAF	[62]
PA3258	*rapA*	no	GGDDF	EAL	CBS	[62, 222]
PA3311		yes	AGDEF	EAL	TM, MHYT	[62]
PA4367	*bifA*	no	GGDQF	EAL	TM	[62, 223]
PA4601	*morA*	no	GGDEF	EAL	TM, PAS, PAC	[62, 126, 224]
PA4959	*fimX*	no	GDSIF	EVL	REC	[62, 99, 225]
PA5017		no	ASNEF	EAL	GAF, PAS, PAC	[62, 149]
PA5295		no	GSDEF	EAL		[62]
PA5442		no	SGDEF	EAL	TM, PAC, PAS	[62]

Table 5.1. (Continued)

PA number	Gene name	I-site motif[a]	GGDEF sequence	EAL or HD-GYP sequence	Partner domains[b]	Selected references
PA2133		-	-	ETL		[62]
PA2200		-	-	EAL		[62]
PA2572		-	-	YN-GYP	REC	[95]
PA2818	*arr*	-	-	EAL	TM	[62, 226]
PA3825		-	-	EVL	TM	[62]
PA3947	*rocR*	-	-	EVL	REC	[62, 143, 227]
PA4108		-	-	HD-GYP		[95]
PA4781		-	-	HD-GYP	REC	[95]

[a] RXXD motif located five amino acids in front of the GGDEF sequence
[b] as listed by Kulasakara *et al.* [62]

Table 5.2. Genes identified by ChIP-chip that were enriched at least 0.5 log_2-fold.

				RpoS ChIP-chip		RpoS consensus sequence (revised, 300 bp upstream)			Transcriptome
PA number[a]	gene name	shared promoter[b]	non-coding gene[c]	log_2-fold enrichment	distance to ATG	weight score[d]	sequence	distance to ATG	fold change[e]
PA0001	*dnaA*			0.54	93	*5.89*	*tccgGCTACAATaggc*	*55*	0
PA0016	*trkA*			0.65	6	*0.00*			0
PA0026	*plcB*			0.87	68	*5.84*	*tcagGCTTCACTcact*	*26*	2.40
PA0051	*phzH*			0.58	4	*5.29*	*ctgtTCTATCATtggc*	*185*	0
PA0052				0.87	-2	6.51	gccgGCTTGACTgagg	40	7.10
PA0053				0.75	505	6.10	cgttACTATGCTcgaa	0	0
PA0081		x		0.62	90	*4.85*	*tgccGCAAGGCTtgtc*	*231*	0
PA0082		x		0.62	276	*4.48*	*tgccACAAGAATtttg*	*128*	0
PA0094		x		0.90	254	*3.58*	*acgtCCATCACTggcg*	*232*	-2.40
PA0095		x		0.90	-2	*5.92*	*cgcgCCTATGCTgctt*	*65*	0
PA0105	*coxB*			0.93	245	7.84	gctgTCTATACTccca	151	18.30
PA0109		x		1.60	26	*0.00*			16.40
PA0110		x		1.60	-12	*0.00*			3.10
PA0122				0.80	139	*3.96*	*ccagCCTATAGTgaag*	*126*	1.7
PA0179				1.19	200	6.71	attgTCTTTACTggaa	115	15.00
PA0195	*pntAA*			0.63	454	*4.57*	*gtgaGCTAGACCtccg*	*72*	2.00
PA0296		x		0.62	287	*4.48*	*ttcgGATTGACTcata*	*60*	0
PA0297	*spuA*	x		0.62	-10	6.24	caacGCTAAGCTcggc	47	0
PA0309		x		0.69	36	*0.00*			0
PA0310		x		0.69	11	*2.57*	*cggcGAAAGCCTcgtc*	*30*	0
PA0311		x		0.63	182	*2.10*	*acagAGTAGCCTgccg*	*235*	0
PA0312		x		0.63	82	6.37	cagtTCTATCCTaagg	187	1.8
PA0314		x		0.63	83	6.24	cccgGCTAAGCTgaac	60	2.40
PA0315		x		0.63	208	*5.92*	*cgggCCTATGCTgttc*	*256*	4.10
PA0330	*rpiA*	x		0.55	158	6.74	ggccGCTATAATtcgt	128	0
PA0331	*ilvA1*	x		0.55	98	*3.57*	*ctggAGTAGACTccgg*	*42*	0
PA0332				0.64	57	6.24	ggctGCTAAGCTtcac	93	2.1
PA0354				1.24	80	6.74	ctgcGCTATAATcgcg	34	0
PA0366		x		1.22	160	*4.68*	*agagTATTTACTctag*	*113*	0
PA0367		x		1.22	128	*5.78*	*acctTCTACGCTgtca*	*59*	0
PA0376	*rpoH*			1.56	77	6.97	gagtGCTACACTgcgc	37	0
PA0380				0.64	12	6.56	tcggGCTAGAATgccg	41	0
PA0394		x		1.07	11	*3.00*	*agcaGGTAGAATgccg*	*189*	0
PA0395	*pilT*	x		1.07	202	*0.00*			0
PA0397		x		0.70	61	*5.67*	*attgCCTATCCTgtag*	*47*	2.40
PA0398		x		0.70	91	*5.99*	*ctccGCTAACCTgcgg*	*53*	0
PA0422				1.13	56	*4.82*	*tgccGCTAGTCTtgag*	*37*	0
PA0432	*sahH*	x		0.64	193	6.74	cgccGCTATAATcgcc	173	0
PA0433		x		0.64	94	*2.67*	*caggCCTAGGCCtgct*	*190*	0
PA0450		x		1.20	296	*4.25*	*caagACATAACTtgtc*	*62*	0
PA0451		x		1.20	82	7.13	ctggACTAGACTgaga	105	2.40
PA0455	*dbpA*	x		0.63	19	7.64	ggctGCTAGACTagcc	40	1.9
PA0456		x		0.63	327	*5.22*	*gttcGCTTTCCTcagt*	*184*	0
PA0458		x		2.15	180	6.63	cttcTCTATGCTtggg	38	0
PA0459		x		2.15	439	*2.05*	*aactGCATTACCgcca*	*145*	18.30

				RpoS ChIP-chip		RpoS consensus sequence (revised, 300 bp upstream)			Transcriptome
PA number[a]	gene name	shared promoter[b]	non-coding gene[c]	log_2-fold enrichment	distance to ATG	weight score[d]	sequence	distance to ATG	fold change[e]
PA0482	*glcB*	x		0.71	312	*1.42*	*ctggTCTAGAGCagag*	*23*	0
PA0483		x		0.71	-7	7.13	cttgCCTATACTcccg	34	5.20
PA0484				1.37	38	*1.35*	*ACTCCCATtcgt*	*31*	10.3
PA0506				0.70	13	6.69	atggGCTTTACTgaga	249	5
PA0547		x		2.03	25	7.13	cggtACTAGACTgcgc	16	0
PA0548	*tktA*	x		2.03	220	*4.82*	*tgtaTCAAAAATtttt*	*201*	0
PA0563				0.76	186	6.97	tacgGCTACACTgtgc	89	0
PA0577	*dnaG*			0.63	41	6.61	aattGCTATGCTgccg	47	0
PA0588				1.64	212	6.00	tcttCCTTTACTccgt	229	4.7
PA0607	*rpe*			0.69	54	*5.89*	*aacgGCTACAATgcgc*	*41*	0
PA0610	*prtN*			0.50	104	*2.84*	*ccgcTCTACAACttca*	*80*	0
PA0652	*vfr*	x		0.70	240	*3.20*	*gagcTCTCCGCTgagc*	*101*	0
PA0653		x		0.70	30	6.24	ctgtGCTAAGCTggcg	37	0
PA0671		x		0.86	154	*3.53*	*acagCAAATACTgtat*	*158*	0
PA0672	*hemO*	x		0.86	150	*4.54*	*gcatCCTTTCCTgtga*	*109*	0
PA0704				0.58	126	*4.75*	*atggGCTATACCtccc*	*96*	24.20
PA0715				0.74	439	*5.26*	*ttttTCTCTACTggga*	*173*	0
PA0730				0.81	319	*4.54*	*ccggCCTTTCCTgccc*	*219*	1.9
PA0732				0.58	5	6.24	cgacGCTAAGCTgaat	63	1.9
PA0743				0.51	71	6.26	agcgTCTAAGCTgttt	57	4
PA0759		x		0.86	138	*5.55*	*gagtTCTATGATgacg*	*42*	0
PA0760		x		0.86	133	6.05	ccgcCCTATAATgccg	34	0
PA0769				0.77	56	6.47	aataACTACACTgaca	23	1.8
PA0775				0.66	17	*5.89*	*ctcgGCTACAATtcgg*	*47*	0
PA0788				1.03	71	7.13	gacaACTAGACTtccc	23	3.10
PA0789				0.61	493	*4.38*	*atccGCTTCCCTaccc*	*70*	0
PA0805		x		0.94	493	*4.72*	*ggaaACTTTCCTgcca*	*177*	0
PA0806		x		0.94	66	*4.48*	*gcctGATTGACTttca*	*207*	0
PA0826.2	*ssrA*		x	0.60	20	n.d.			n.d.
PA0833				1.69	66	6.61	cttgGCTATGCTctaa	68	0
PA0837	*slyD*			0.85	-3	*5.56*	*caggACAAGACTgcca*	*155*	0
PA0838				2.30	178	6.24	aactGCTAAGCTggta	156	3.4
PA0858				0.75	106	7.64	ctgcGCTAGACTacgc	121	0
PA0861				1.32	264	7.13	agccACTAGACTccta	169	2.60
PA0872	*phhA*	x		0.59	41	*5.00*	*tccgTCAAGAATatgt*	*214*	0
PA0873	*phhR*	x		0.59	241	*2.29*	*gtcaCATATTCTtgac*	*80*	0
PA0887.1			x	0.90	22	n.d.			n.d.
PA0888	*aotJ*			0.66	196	6.69	atttGCTTTACTcatt	276	0
PA0905	*rsmA*			0.58	161	6.26	ctggTCAATACTgggt	100	2.1
PA0905.1			x	0.54	-8	n.d.			n.d.
PA0905.2			x	0.56	60	n.d.			n.d.
PA0916		x		1.34	29	6.56	tgccGCTAGAATtgcg	63	2.50
PA0917	*kup*	x		1.34	216	*5.99*	*gGCTAACCTcggt*	*245*	0
PA0928	*gacS*	x		0.78	85	7.46	acccGCTAAACTgcgc	71	0
PA0929		x		0.78	99	*2.70*	*atcgTGAATACTggca*	*41*	0
PA0938				0.69	15	6.40	cagtTCTAAAATaact	116	0
PA0945	*purM*	x		0.63	58	*4.60*	*cgtgGCAAGCCTgata*	*98*	0

				RpoS ChIP-chip		RpoS consensus sequence (revised, 300 bp upstream)			Transcriptome
PA number[a]	gene name	shared promoter[b]	non-coding gene[c]	log_2-fold enrichment	distance to ATG	weight score[d]	sequence	distance to ATG	fold change[e]
PA0946		x		0.63	154	*4.18*	*gcgtGCAACGCTgttt*	*163*	0
PA0962		x		1.01	284	*4.16*	*ggatTATAGCCTgaaa*	*243*	0
PA0963	*aspS*	x		1.01	154	6.74	tcagGCTATAATcccc	202	0
PA0968				0.57	2	*4.49*	*tggtTCTAGAGT*	*8*	0
PA0976.1			x	0.88	6	n.d.			n.d.
PA1003	*mvfR*			0.62	480	*5.84*	*ttgcGCTTCACTgacc*	*164*	0
PA1004	*nadA*			0.69	209	*4.37*	*cgggTATAAAATcgag*	*45*	0
PA1013.1			x	0.78	3	n.d.			n.d.
PA1014				2.42	164	*5.22*	*tgcaGCTTTCCTagga*	*205*	0
PA1040		x		0.70	96	*4.82*	*tcagGCTAGTCTtggc*	*35*	0
PA1041		x		0.70	33	6.71	ggggTCTTTACTccct	49	29.2
PA1054				0.50	240	6.24	tcttGCTAAGCTtcaa	250	1.8
PA1064		x		0.51	10	*0.00*			0
PA1065		x		0.51	8	*0.00*			2.80
PA1074	*braC*	x		0.76	124	6.99	ccgcTCTACACTgtac	115	0
PA1075		x		0.76	173	*4.40*	*agtGCTCCACTcttc*	*295*	0
PA1076				0.87	15	7.64	cctgGCTAGACTgatt	36	0
PA1097	*fleQ*			0.89	197	*5.82*	*tttgACTTAACTagtg*	*104*	0
PA1113				0.90	455	*5.99*	*cggtGCTAACCTgcgg*	*38*	0
PA1117				0.50	40	6.56	ggctGCTAGAATatcc	59	2.4
PA1118				2.20	37	7.64	ggatGCTAGACTga	10	3.00
PA1127		x		0.57	85	*4.49*	*gtgaTCTAGAGTaatc*	*71*	0
PA1128		x		0.57	48	*5.05*	*tggcTCAATGCTgcat*	*42*	0
PA1157				0.53	61	*5.89*	*attgGCTACAATgcgg*	*66*	0
PA1168				0.88	203	*5.50*	*ggttTCTTTGCTgttt*	*61*	0
PA1176	*napF*			0.77	3	*0.00*			39
PA1177	*napE*	x		1.02	8	6.44	agggTCTAGGCTttct	39	50.00
PA1178	*oprH*	x		1.02	212	*3.88*	*aaagCCTAGACCctac*	*188*	0
PA1190				1.09	46	7.13	cgttCCTATACTgcga	111	3.30
PA1199				1.18	86	*3.65*	*ggaaGCATTCCTcacc*	*27*	0
PA1208				0.65	21	*1.55*	*tgggTCCATACTttgc*	*118*	0
PA1284		x		0.66	137	*2.98*	*ctggCCTATAACtcgc*	*68*	0
PA1285		x		0.66	-7	*1.35*	*gagtTATAGGCCagcg*	*69*	0
PA1289				0.94	67	6.47	tttcACTACACTtcaa	103	30.60
PA1290		x		0.53	-2	*5.09*	*gcgtGCTAGCATgaac*	*41*	0
PA1291		x		0.53	112	*3.80*	*gcctTCTTACATaccg*	*101*	0
PA1299				0.71	64	7.13	ggggACTAGACTatcg	37	0
PA1304		x		0.58	140	*0.83*	*cgcgCCTACCCAccga*	*85*	0
PA1305		x		0.58	7	*5.27*	*agcgGCTATCATaagc*	*43*	0
PA1317	*cyoA*			1.15	506	*5.04*	*atccGCTTGCCTtctc*	*154*	0
PA1333				0.62	72	6.95	gggaCCTAGACTcaat	98	0
PA1342		x		0.71	93	6.47	tgccACTACACTgttc	129	1.6
PA1343		x		0.71	357	*5.06*	*cacgTCTTGCCTtcct*	*40*	0
PA1366				0.91	222	*4.40*	*atgGCTTTGATgcta*	*297*	2.70
PA1414				0.86	31	*0.22*	*ccgcAGTAAAGTtgtt*	*24*	0
PA1415				1.26	-7	*5.67*	*acgCCTATCCTtctg*	*41*	2.30
PA1421	*gbuA*	x		0.74	105	*2.62*	*gaccCCTAAAACaacc*	*34*	0

				RpoS ChIP-chip		RpoS consensus sequence (revised, 300 bp upstream)			Transcriptome
PA number[a]	gene name	shared promoter[b]	non-coding gene[c]	log_2-fold enrichment	distance to ATG	weight score[d]	sequence	distance to ATG	fold change[e]
PA1422	*gbuR*	x		0.74	100	7.64	agcgGCTAGACTtcgc	82	2.30
PA1430	*lasR*			1.62	289	*3.66*	*ttcgCATAAAATgtga*	*293*	2.40
PA1440		x		1.07	61	*5.39*	*ctggACTACAATccag*	*41*	0
PA1441		x		1.07	125	*2.12*	*tgctCCATCCCTtgcg*	*51*	0
PA1474		x		0.73	175	7.82	ggccGCTATACTggtg	201	0
PA1475	*ccmA*	x		0.73	109	*3.87*	*cctaTCTCGGCTggca*	*196*	0
PA1525	*alkB2*	x		0.62	157	*2.11*	*tgatCCTTTTATccag*	*174*	0
PA1526		x		0.62	22	*2.03*	*catcCATATACCcccg*	*42*	0
PA1528	*zipA*			0.56	115	*3.91*	*gcagTGTAAACTtgtg*	*153*	0
PA1544	*anr*	x		1.49	194	*3.32*	*gaatTCTTCCATtgga*	*219*	0
PA1545		x		1.49	50	*1.71*	*ggggGCTCAAGTtcgc*	*64*	0
PA1551				1.09	97	*2.49*	*caggCGTATAATcagt*	*84*	0
PA1554				1.10	224	6.26	cgcgTCTAAGCTgctc	240	0
PA1562	*acnA*	x		0.52	206	*3.68*	*tcgaACAACGCTatcc*	*204*	2
PA1563		x		0.52	119	*4.96*	*gccaTATACACTggac*	*82*	0
PA1580	*gltA*	x		1.28	86	*4.67*	*tcccTCTATAGTggtg*	*64*	0
PA1581	*sdhC*	x		1.28	261	7.84	actgTCTATACTcggc	128	0
PA1590	*braB*			2.65	289	*5.27*	*atgcGCTATCATtgcc*	*212*	0
PA1603				0.82	-9	6.56	GCTAGAATgaag	38	0
PA1639				0.86	86	*3.98*	*cggcGCTCGAATtccc*	*88*	0
PA1644				0.55	173	*3.25*	*taggGCAAGTCTagcc*	*112*	0
PA1650				1.20	162	*5.48*	*ggggACTAACCTgggt*	*63*	3.30
PA1674	*folE2*			0.54	22	*4.82*	*acgtCCTACCCTccgc*	*39*	0
PA1677		x		0.98	84	*3.01*	*taccACTTTAGTgcgc*	*84*	0
PA1678		x		0.98	85	6.56	atcgGCTAGAATgtcg	44	0
PA1727		x		1.23	182	*5.17*	*tcgtGCAATAATatca*	*59*	0
PA1728		x		1.23	169	*5.51*	*tgacGCTACCCTgaaa*	*134*	4.30
PA1730				2.32	197	7.66	ctgtTCTAGACTtatc	232	3.00
PA1736				0.67	285	*3.86*	*tGCATGAATcagt*	*299*	0
PA1753				1.17	1	*4.64*	*tgctGCTAATCTgcta*	*47*	0
PA1754	*cysB*			0.72	-9	*3.35*	*caaaCCATTAATatgg*	*67*	1.8
PA1758	*pabB*	x		0.50	164	6.05	gcgaACTAGAATtcct	37	0
PA1759		x		0.50	-1	*3.45*	*taccACAATGATaatg*	*29*	0
PA1777	*oprF*			0.66	-5	*5.43*	*ttctGATAAACTtgcc*	*73*	0
PA1799		x		1.32	134	*4.03*	*ggcgCATATAATgcca*	*41*	0
PA1800	*tig*	x		1.32	96	6.05	ctctACTAGAATgcat	69	0
PA1802	*clpX*			0.63	75	6.24	ctccGCAATACTggcg	98	0
PA1812	*mltD*			0.56	41	6.58	cattTCTAGAATcggc	42	0
PA1838	*cysI*			1.11	447	*5.10*	*ttacCATATACTcaaa*	*126*	0
PA1859		x		0.88	3	6.61	catcGCTATGCTtcgg	35	0
PA1860		x		0.88	81	*3.70*	*caggGCAATCATtgcc*	*72*	5.60
PA1881		x		0.71	154	7.66	ttgaTCTAGACTttcg	119	11.40
PA1882		x		0.71	175	*5.35*	*acgcGCTAGGATcgct*	*121*	0
PA1888		x		0.98	199	*2.45*	*ccggAAAAGAATctcc*	*26*	19.20
PA1889		x		0.98	29	*2.82*	*ccgcGAAAGGCTgggg*	*68*	0
PA1899	*phzA2*			1.08	311	*3.09*	*cctgTCAAATCTggtt*	*196*	0
PA1929		x		0.93	309	*5.53*	*ccgcGCTATGATcgct*	*80*	0

				RpoS ChIP-chip		RpoS consensus sequence (revised, 300 bp upstream)			Transcriptome
PA number[a]	gene name	shared promoter[b]	non-coding gene[c]	log_2-fold enrichment	distance to ATG	weight score[d]	sequence	distance to ATG	fold change[e]
PA1930		x		0.93	61	6.99	ccgaTCTACACTggcg	86	16.30
PA1941				0.62	10	*3.70*	*cgccGCAATCATcgcc*	*264*	-2.00
PA1951				0.58	-1	*4.84*	*ttgaTCTAGTCTgaaa*	*53*	42.20
PA2009	*hmgA*	x		0.66	118	*3.30*	*ttccACTCAAATtacg*	*108*	0
PA2010		x		0.66	41	*3.67*	*tcaaGCTATAACgtcg*	*37*	0
PA2024		x		1.88	4	6.61	atggGCTATGCTtgtc	28	6.70
PA2025	*gor*	x		1.88	139	*4.86*	*cgcGCTTACCTccac*	*141*	0
PA2047		x		0.91	32	*5.06*	*gggtTCTTGCCTgaaa*	*118*	2.00
PA2048		x		0.91	380	*3.95*	*tcccCCTAATCTggct*	*256*	0
PA2072				0.74	57	6.33	ggatGCTTAACTataa	60	4.20
PA2076				0.58	229	7.82	cctgGCTATACTggcg	261	0
PA2196				0.71	40	7.82	cggcGCTATACTcatg	63	0
PA2231	*pslA*			0.62	412	*5.17*	*gaatGCTAAGATagct*	*163*	6.5
PA2246	*bkdR*	x		1.02	271	*4.48*	*aactACAAGAATcgct*	*32*	0
PA2247	*bkdA1*	x		1.02	37	7.13	gaagCCTATACTgaaa	211	0
PA2363				1.02	55	*0.00*			6.2
PA2364		x		0.62	8	*3.84*	*gcaaAATAAAATtttc*	*23*	4.90
PA2365		x		0.62	199	*3.90*	*cgatGCATTGCTcccc*	*37*	14.20
PA2384				0.53	111	*3.85*	*ggatGCTCGGCTtcgg*	*53*	0
PA2425	*pvdG*	x		0.98	405	*5.03*	*tcgcGCAATGCTccgc*	*197*	0
PA2426	*pvdS*	x		0.98	237	*4.94*	*cgacGCATGACTgcaa*	*230*	0
PA2466	*foxA*			0.58	101	*3.62*	*tccgGCTTTACCgatt*	*46*	0
PA2475				0.81	40	7.84	gccaTCTATACTccct	42	3.30
PA2501				0.89	114	7.64	tggaGCTAGACTgaca	45	0
PA2534		x		1.22	-3	*4.65*	*tcatTCTTCGCTctgc*	*80*	0
PA2535		x		1.22	120	*3.69*	*ttttCCTTCCCTcccg*	*25*	0
PA2562		x		0.58	67	6.26	cggtTCTAAGCTatcg	44	1.9
PA2563		x		0.58	288	6.61	atcaGCTATGCTgccg	223	0
PA2571		x		1.39	77	*3.52*	*tcagGCAAGCATagtc*	*36*	5.80
PA2572		x		1.39	-1	6.10	tcggACTATGCTtgcc	52	13.20
PA2573				1.08	-7	*5.85*	*gttgACTATCCTtagc*	*41*	12.10
PA2581.1			x	1.01	158	n.d.			n.d.
PA2583.1			x	0.96	-1	n.d.			n.d.
PA2586	*gacA*			0.63	225	*4.26*	*tggcGGTATACTtagc*	*169*	0
PA2618				1.24	57	*4.74*	*ctggCATAAACTtgct*	*36*	4.10
PA2621		x		0.97	145	*4.67*	*aaagGCAAAGCTtttt*	*18*	0
PA2622	*cspD*	x		0.97	211	*5.82*	*agcgCCTTGACTaact*	*146*	0
PA2623	*icd*	x		1.09	95	*5.51*	*ctggGCTACCCTagaa*	*50*	0
PA2624	*idh*	x		1.09	262	*5.24*	*caacGCTCTACTggcg*	*131*	0
PA2712				0.73	351	*2.09*	*gctcGCACAGCTcgct*	*280*	0
PA2736.1			x	0.73	22	n.d.			n.d.
PA2745		x		1.42	156	*3.88*	*cggcCCTAGACCtatt*	*139*	0
PA2746		x		1.42	34	*5.92*	*ctggACTAGGCTggaa*	*35*	7.60
PA2779		x		1.78	78	*3.91*	*ggaaCCAAGCCTcgcc*	*53*	3.00
PA2780		x		1.78	328	*5.10*	*ttcgCATATACTccgg*	*217*	-3.20
PA2790				1.96	332	6.17	caggGCTAGCCTtatc	264	0
PA2798		x		1.04	237	*4.78*	*actgGCAATCCTggcg*	*207*	2.20

				RpoS ChIP-chip		RpoS consensus sequence (revised, 300 bp upstream)			Transcriptome
PA number[a]	gene name	shared promoter[b]	non-coding gene[c]	log_2-fold enrichment	distance to ATG	weight score[d]	sequence	distance to ATG	fold change[e]
PA2799		x		1.04	8	*5.45*	*acggTATAAACTttga*	*70*	1.8
PA2800		x		0.67	56	*5.81*	*agccTATATACTgcgc*	*66*	0
PA2801		x		0.67	45	*4.94*	*ctttGCATGACTagtc*	*87*	0
PA2813				0.72	-3	*1.48*	*tcctTCTTCGGTccat*	*89*	0
PA2814		x		0.51	55	*2.23*	*gtcaGCTTGGCCggtt*	*75*	0
PA2815		x		0.51	96	6.24	acggGCTAAGCTcgag	44	2.50
PA2816				0.64	68	6.56	attgGCTAGAATcgac	42	2.00
PA2817				0.83	21	*1.90*	*ccgcGAAACCCTttat*	*42*	0
PA2823		x		1.18	44	*0.00*			0
PA2824		x		1.18	37	*2.08*	*ttctCCTCGGATcgga*	*74*	2.30
PA2840		x		0.56	246	*5.90*	*ccggTCAAAACTgacc*	*174*	0
PA2841		x		0.56	63	*4.77*	*gacgTCTATACCgacg*	*41*	3.50
PA2851	*efp*			0.66	25	*4.17*	*tttgTCTTTCATccat*	*23*	0
PA2853	*oprI*			1.12	-3	*4.29*	*tactGCTAAAGTcggg*	*146*	0
PA2854				0.67	66	*5.24*	*actgTCTTTCCTactc*	*42*	0
PA2910		x		0.90	261	6.61	gcctGCTATGCTgccg	184	0
PA2911		x		0.90	374	*3.20*	*ctgcGATTTCCTgcgc*	*46*	0
PA2931		x		0.63	35	*5.43*	*gatgGCTTGAATatct*	*93*	0
PA2932	*morB*	x		0.63	89	*4.16*	*tataAATTTACTtgac*	*93*	0
PA2937				0.72	-1	*2.39*	*caggGAAAACCTcgcc*	*28*	8.40
PA2938		x		1.14	125	*3.82*	*attgTCTACAGTgtgc*	*114*	0
PA2939		x		1.14	374	*4.13*	*cgctCCTAGTCTggca*	*100*	137.40
PA2958.1			x	0.76	8	n.d.			n.d.
PA2960	*pilZ*			0.83	42	*0.00*			0
PA2971		x		0.91	8	6.05	cgtcCCTATAATggcg	17	0
PA2972		x		0.91	100	*1.67*	*tagcCATAAACCgctg*	*61*	0
PA2975	*rluC*			0.58	-3	*4.87*	*tgttTCAAGGCTttgg*	*218*	0
PA3016		x		0.55	195	*3.91*	*cgccTGTAAACTgcgc*	*95*	0
PA3017		x		0.55	11	*2.86*	*aatgAAAACACTatcc*	*32*	0
PA3019		x		1.25	49	*5.56*	*ctcgCCTAAGCTtagc*	*93*	0
PA3020		x		1.25	175	6.24	aacgGCTAAGCTtagg	144	0
PA3032	*snr1*			0.50	169	*3.46*	*ttttCATAGCCTgagt*	*216*	10.7
PA3039		x		0.65	124	*4.05*	*tcatTAAAGACTgcca*	*183*	0
PA3040		x		0.65	170	*5.63*	*gcagTCTTTAATgaaa*	*118*	0
PA3046		x		0.59	58	*0.99*	*gtcgGCTACTGTctgt*	*57*	0
PA3047		x		0.59	251	*5.53*	*atttTCTACCCTccgt*	*31*	0
PA3050	*pyrD*			0.89	63	6.74	gacgGCTATAATcggc	42	0
PA3103	*xcpR*	x		0.79	178	*5.74*	*actaACAATACTgacg*	*75*	0
PA3104	*xcpP*	x		0.79	40	*2.61*	*agtaGGTAGCCTactg*	*25*	0
PA3109				1.00	67	6.38	ctctGCTAAAATgcag	38	0
PA3133				0.51	54	*4.03*	*tatgCATATAATattt*	*38*	0
PA3138	*uvrB*	x		1.27	42	*2.11*	*ggcgTCACAGCTccct*	*24*	0
PA3139		x		1.27	144	6.76	ggtgTCTATAATaacc	91	0
PA3143				0.72	-5	*0.00*			0
PA3162	*rpsA*			0.71	205	*4.54*	*cccgACTTGCCTggcg*	*171*	0
PA3179		x		0.71	86	*4.13*	*ccggCCTAGTCTagcg*	*113*	3.20
PA3180		x		0.71	60	7.64	tcccGCTAGACTaggc	45	0

				RpoS ChIP-chip		RpoS consensus sequence (revised, 300 bp upstream)			Transcriptome
PA number[a]	gene name	shared promoter[b]	non-coding gene[c]	log_2-fold enrichment	distance to ATG	weight score[d]	sequence	distance to ATG	fold change[e]
PA3200		x		0.69	219	*5.86*	*ccatTCTTCACTggaa*	*25*	3.00
PA3201		x		0.69	-5	*3.92*	*ggttGCTATTATgccg*	*37*	0
PA3215		x		0.69	10	*2.28*	*gtttAGTATCCTtggg*	*65*	0
PA3216		x		0.69	131	6.95	ggatACTAAACTggcc	80	3.30
PA3223	*acpD*			0.66	141	*5.53*	*attcTCTACCCTcacc*	*47*	0
PA3236		x		0.51	249	*3.78*	*ggctGCTCTCCTttga*	*289*	0
PA3237		x		0.51	43	*4.40*	*cctgGATAGGCTttcg*	*49*	0
PA3260		x		1.74	79	*3.14*	*gcctGATAAGATggcg*	*30*	0
PA3261		x		1.74	23	7.82	actgGCTATACTgctg	50	2.60
PA3288		x		0.75	35	*3.10*	*tcagGCTAGCCCagtt*	*50*	0
PA3289		x		0.75	43	6.17	ctggGCTAGCCTgagg	35	2.10
PA3300	*fadD2*	x		0.50	227	*4.48*	*gaggACAAGAATaa*	*10*	0
PA3301		x		0.50	18	6.56	cgctGCTAGAATgcgc	44	0
PA3309				0.59	41	*4.17*	*ggctTCTTTCATttca*	*231*	0
PA3310		x		0.93	148	*2.44*	*gcccGATAGAGTtcgg*	*65*	0
PA3311		x		0.93	6	*3.67*	*acaaGCTCAGCT*	*8*	13.30
PA3326		x		0.64	112	6.61	catgGCTATGCTtcac	190	0
PA3327		x		0.64	367	*4.98*	*ccctGCAAGAATtaac*	*192*	-4.30
PA3338		x		0.70	1	*3.92*	*ggcgGCTATTATaggc*	*38*	0
PA3339		x		0.70	66	6.05	cgcgCCTATAATagcc	41	0
PA3340				1.65	258	6.56	ttccGCTAGAATcgcc	256	3.60
PA3347				0.58	94	*4.62*	*tgatTCAAGCCTtccc*	*42*	3.7
PA3353				0.95	19	*0.00*			0
PA3418	*ldh*	x		1.80	69	7.13	cctgCCTATACTgaag	69	18.10
PA3419		x		1.80	175	*2.93*	*tgggGCTCCCCTgctt*	*239*	0
PA3450		x		1.17	199	*1.44*	*gttgGGTATTCTattt*	*99*	0
PA3451		x		1.17	5	6.29	cccgCCTACACTgaaa	44	35.70
PA3452	*mqoA*			1.06	210	*1.83*	*acgcACTCACATcggg*	*96*	3.8
PA3464		x		0.99	205	*2.86*	*cattGGTAGGCTtgcc*	*43*	0
PA3465		x		0.99	10	7.64	ggcgGCTAGACTttcc	47	7.70
PA3477	*rhlR*			0.67	7	*4.85*	*atcgGCAAGGCTgcgc*	*78*	1.8
PA3479	*rhlA*			0.50	260	*3.19*	*agttACTTGTCTgccg*	*103*	0
PA3529		x		0.51	262	*3.35*	*cggaCAAAGACTtagc*	*136*	0
PA3530		x		0.51	-4	*4.37*	*tccaACTCAACTtccc*	*27*	0
PA3531	*bfrB*			0.97	195	*4.08*	*tatgCCTTCAATtcaa*	*152*	0
PA3572				1.17	-12	7.13	caggACTAGACTgaag	43	0
PA3573		x		0.55	339	*4.36*	*agtgCCTTGCCTgcca*	*38*	0
PA3574		x		0.55	24	6.38	cgcgGCTAAAATcggt	59	0
PA3580		x		0.83	265	*3.71*	*cctcTCTTGTCTgttc*	*256*	0
PA3581	*glpF*	x		0.83	-2	*3.65*	*gacaGCATTCCTttgt*	*86*	0
PA3621	*fdxA*			0.81	69	6.56	agctGCTAGAATcgcg	48	0
PA3621.1	*rsmZ*		x	0.56	-5	n.d.			n.d.
PA3629	*adhC*	x		0.51	121	6.99	gtttTCTACACTttcc	66	0
PA3630		x		0.51	9	*5.17*	*tcagGCAATAATcaaa*	*40*	0
PA3687	*ppc*	x		1.93	113	*4.06*	*tcagACTAGACCcgat*	*125*	0
PA3688		x		1.93	92	*5.30*	*accaGCTTGGCTcagg*	*177*	12.90
PA3722				0.58	72	*2.99*	*tggcAATATGATgtta*	*61*	0

				RpoS ChIP-chip		RpoS consensus sequence (revised, 300 bp upstream)			Transcriptome
PA number[a]	gene name	shared promoter[b]	non-coding gene[c]	log_2-fold enrichment	distance to ATG	weight score[d]	sequence	distance to ATG	fold change[e]
PA3740				0.59	122	*2.20*	*tgcaTCTAGCCAtcat*	*31*	0
PA3745	*rpsP*			0.66	60	*2.57*	*gcgtGCATTCATtttg*	*41*	0
PA3786		x		0.75	134	6.63	gccgTCTATGCTggcg	140	0
PA3787		x		0.75	36	*3.93*	*gtttGCAACCCTtgcg*	*78*	3.20
PA3815				1.16	123	*5.09*	*ttctGCTAGCATgtag*	*124*	0
PA3817		x		0.94	43	*3.34*	*ctgaCCTCTGCTgtag*	*55*	0
PA3818		x		0.94	107	6.56	ttctGCTAGAATggcc	43	0
PA3824	*queA*	x		0.98	97	*2.93*	*ctggGCTCCCCTggaa*	*219*	0
PA3824.1		x	x	0.98	3	n.d.			n.d.
PA3833				0.68	9	*0.00*			2.40
PA3834	*valS*			0.50	-7	7.82	ccccGCTATACTcccg	62	0
PA3855				0.56	-1	*5.56*	*atctCCTAAGCTcgcc*	*36*	2
PA3858		x		0.70	106	*5.48*	*atgcGCTTTGCTaagg*	*173*	4
PA3859		x		0.70	189	*3.87*	*gcgcACTTCCCTtagc*	*140*	0
PA3902		x		0.72	63	*5.61*	*gccgGATAGACTgctt*	*40*	0
PA3903	*prfC*	x		0.72	156	6.74	taccGCTATAATcctg	67	0
PA3918	*moaC*			0.71	45	*3.89*	*tatgTATACAATcatc*	*97*	0
PA3919		x		0.99	438	*4.06*	*taacACTAGACCtcgc*	*264*	0
PA3920		x		0.99	64	*4.87*	*gatgTCAAGGCTgaac*	*83*	0
PA3945				1.07	77	6.47	aaagACTACACTccgg	132	5.90
PA3956				0.65	39	*5.92*	*ctggCCTATGCTtgac*	*36*	0
PA3957		x		1.10	53	*1.68*	*tgacGCAAGGGTtcgc*	*37*	3.00
PA3958		x		1.10	7	*1.94*	*gcGGTACCCTcccg*	*59*	0
PA3974	*ladS*	x		0.62	188	*4.29*	*gtgtGCTAAAGTtcgg*	*98*	0
PA3975	*thiD*	x		0.62	21	*2.68*	*tagtGGTAAGCTcacg*	*16*	0
PA4005				0.65	-2	*0.00*			0
PA4027				0.96	20	*0.00*			0
PA4031	*ppa*			1.14	89	6.05	tatgCCTATAATcgcg	47	0
PA4107		x		0.99	333	*2.44*	*gccgCGTTTACTgtgg*	*21*	0
PA4108		x		0.99	-11	*3.87*	*cccaTCTCGGCTaccg*	*55*	0
PA4116				1.20	64	*4.16*	*tcctGCTACTCTtttc*	*44*	0
PA4241	*rpsM*			0.96	91	*5.32*	*ccttTCTTGGCTtcct*	*47*	0
PA4242	*rpmJ*			0.63	15	*0.00*			0
PA4249	*rpsH*			0.58	100	6.58	gatcTCTAGAATaccc	102	0
PA4277	*tufB*			0.57	85	*1.23*	*acccGCTCCAGTcaag*	*185*	0
PA4277.1			x	0.70	7	n.d.			n.d.
PA4277.2			x	0.74	0	n.d.			n.d.
PA4277.3			x	0.73	143	n.d.			n.d.
PA4280.5	16S rRNA	x	x	0.55	374	n.d.			n.d.
PA4281	*sbcD*	x		0.55	297	*5.42*	*ggcgTCAACACTtatt*	*152*	0
PA4294		x		0.61	23	*1.28*	*ggatTAATACCTtttc*	*31*	16.10
PA4295	*fppA*	x		0.61	39	*2.31*	*cgaaAAAAGGCTgaag*	*18*	0
PA4305	*rcpC*	x		1.15	321	*5.45*	*tggtTCTTGAATaacg*	*176*	11.20
PA4306	*flp*	x		1.15	87	7.66	tgaaTCTAGACTcggg	192	76.00
PA4307	*pctC*			0.74	162	*3.74*	*tggaTCATGGCTttcc*	*82*	0
PA4311				1.73	100	6.95	ctttCCTAGACTtgaa	107	3.50
PA4314	*purU1*	x		0.54	105	6.56	tgccGCTAGAATggcg	41	0

				RpoS ChIP-chip		RpoS consensus sequence (revised, 300 bp upstream)			Transcriptome
PA number[a]	gene name	shared promoter[b]	non-coding gene[c]	log_2-fold enrichment	distance to ATG	weight score[d]	sequence	distance to ATG	fold change[e]
PA4315	*mvaT*	x		0.54	153	*4.26*	*gGGTATACTccag*	*258*	0
PA4361		x		0.55	141	*4.47*	*ggttGCTAGAGTcgcg*	*40*	0
PA4362		x		0.55	42	6.01	aaggTCTAACCTgaaa	38	9.2
PA4366	*sodB*			0.59	185	*5.74*	*ggagCCTAGGCTccga*	*161*	0
PA4383		x		0.70	103	6.95	gttcCCTAGACTggca	197	0
PA4384		x		0.70	124	*1.06*	*atgcCATCTCCTgtcg*	*117*	0
PA4421		x		0.52	17	*4.67*	*gattTCTATAGTgtgc*	*82*	0
PA4421.1	*rnpB*	x	x	0.52	280	n.d.			n.d.
PA4433	*rplM*	x		0.51	31	*5.82*	*ctgtCCTTGACTtgtc*	*76*	0
PA4434		x		0.51	213	*4.16*	*tcgtTATAGCCTcagg*	*241*	0
PA4456		x		0.88	84	*5.03*	*GCAATGCTctgt*	*300*	0
PA4457		x		0.88	328	*4.93*	*cccgCCTTTAATccag*	*24*	0
PA4462	*rpoN*			0.77	192	*4.03*	*caggCATATAATttgc*	*96*	0
PA4494		x		0.83	59	7.82	cttgGCTATACTcgcg	30	0
PA4495		x		0.83	216	*5.38*	*tggtCCAAGACTggcg*	*87*	0
PA4496				0.84	196	6.99	aacaTCTACACTgaac	114	0
PA4514		x		1.07	155	*3.27*	*attgCCAATGATattg*	*189*	0
PA4515		x		1.07	61	*3.70*	*attgGCAATCATttcg*	*29*	0
PA4523		x		1.25	264	6.76	tatcTCTATAATgaat	126	1.80
PA4524	*nadC*	x		1.25	20	*4.80*	*aatgGCAAAAATcggg*	*246*	0
PA4546	*pilS*			0.53	210	7.46	cttgGCTAAACTgcag	271	0
PA4568	*rplU*	x		0.87	195	*4.54*	*tggcACTTGCCTcggc*	*164*	0
PA4569	*ispB*	x		0.87	44	*4.54*	*cgggCCTTTCCTtgac*	*68*	0
PA4595		x		1.21	147	*5.10*	*ctgtCATATACTtggc*	*47*	0
PA4596		x		1.21	344	*5.89*	*gtctGCTACAATtgat*	*166*	0
PA4602	*glyA3*			0.82	114	*3.46*	*atggCCTTTCATgtgc*	*76*	0
PA4606				1.90	119	7.66	ccgcTCTAGACTaagg	90	0
PA4607		x		0.59	78	*3.98*	*ctcgCCAAAGCTgcta*	*50*	5.1
PA4608		x		0.59	123	*5.30*	*catgGCTTGGCTatag*	*46*	2.90
PA4613	*katB*	x		0.63	409	*4.18*	*cgctCCTTACCTtggt*	*54*	0
PA4614	*mscL*	x		0.63	116	7.48	ttccTCTAAACTtcgt	161	3.1
PA4631				0.82	65	6.95	tcggCCTAGACTgctg	33	0
PA4634		x		0.57	223	*2.53*	*tcgcAATCGACTaggg*	*184*	0
PA4635		x		0.57	201	*3.69*	*tgtcCCTTCCCTcgcg*	*119*	0
PA4639				0.55	215	*5.03*	*caagGCAATGCTgcgg*	*71*	0
PA4648				0.83	134	*4.94*	*tcaaGCATGACTggcg*	*162*	83.10
PA4656		x		0.73	201	*4.61*	*tgttCCTTGGCTgagt*	*162*	2
PA4657		x		0.73	211	6.24	acgcGCAATACTgtac	80	0
PA4658				0.81	67	*5.37*	*aagtTCTAGGATgtgt*	*74*	0
PA4674				0.57	496	*5.03*	*gctcGCAATGCTtcat*	*191*	0
PA4675				0.70	38	*3.47*	*ccagGCATGCCTcatt*	*97*	0
PA4690.5	16S rRNA		x	0.62	299	n.d.			n.d.
PA4702				0.83	84	7.84	ctctTCTATACTcacg	39	11.20
PA4703				0.91	169	6.97	ggccGCTACACTtctg	183	15.2
PA4726.2		x	x	0.79	93	n.d.			n.d.
PA4727	*pcnB*	x		0.79	267	*3.47*	*atccGCATGCCTtgcc*	*271*	0
PA4758	*carA*			0.83	46	*3.91*	*attcTGTAAACTacag*	*135*	0

				RpoS ChIP-chip		RpoS consensus sequence (revised, 300 bp upstream)			Transcriptome
PA number[a]	gene name	shared promoter[b]	non-coding gene[c]	log_2-fold enrichment	distance to ATG	weight score[d]	sequence	distance to ATG	fold change[e]
PA4758.1			x	0.99	1	n.d.			n.d.
PA4764	*fur*	x		0.72	48	*5.32*	*actaTCTTGGCTgggc*	*78*	0
PA4765	*omlA*	x		0.72	48	*2.80*	*tcggGCTTTTATttgc*	*41*	0
PA4781				1.60	58	*4.79*	*agcgTCTTCAATacgg*	*59*	6.2
PA4826				1.01	226	*2.77*	*gaggTCTATAAAaccc*	*223*	0
PA4837		x		0.60	44	*3.89*	*cattTCTTTTCTggtg*	*21*	0
PA4838		x		0.60	96	*5.79*	*aaatGATATACTataa*	*117*	0
PA4849				0.67	2	6.35	cggtGCTATCCTcgtc	36	0
PA4856	*retS*			0.66	77	6.74	cttgGCTATAATccgg	38	0
PA4874		x		0.78	87	7.64	agtcGCTAGACTtcag	53	7.50
PA4875		x		0.78	308	7.64	cgcgGCTAGACTgacg	275	2.10
PA4915				0.60	51	6.71	accaTCTTTACTctca	35	6.60
PA4922	*azu*	x		0.63	164	*3.31*	*ctgtGCTAAAACagga*	*158*	0
PA4923		x		0.63	110	*5.51*	*agccGCTACCCTgtgc*	*42*	0
PA4928		x		0.76	47	*2.96*	*cctcCCATTCCTagag*	*31*	0
PA4929		x		0.76	22	*1.37*	*tatcTCTAGGAAtggg*	*50*	4.70
PA4935	*rpsF*			0.88	138	6.58	cttcTCTAGAATgtcg	123	0
PA4971	*aspP*	x		1.87	108	*3.34*	*tcgcGCTTGAGTtcgg*	*172*	0
PA4972		x		1.87	133	*5.34*	*actcACTTCACTcggg*	*233*	2.30
PA4973	*thiC*	x		0.52	181	*4.25*	*tggaCCATGACTgccg*	*293*	0
PA4974		x		0.52	273	*3.57*	*tggcTCTTCGATcagt*	*89*	0
PA4997	*msbA*	x		0.64	107	6.97	ctgtGCTACACTccgg	36	0
PA4998		x		0.64	-1	*3.80*	*ggttTCTTACATgctg*	*103*	0
PA5014	*glnE*	x		1.32	16	*4.24*	*taatTCTTGGATgttc*	*202*	0
PA5015	*aceE*	x		1.32	264	6.37	ggTCTATCCTgttt	279	0
PA5033				0.51	-9	*5.92*	*ctgtCCTATGCTgctg*	*57*	0
PA5036	*gltB*			0.90	181	*4.17*	*ttcgTCTTTCATttg*	*163*	0
PA5044	*pilM*	x		1.32	114	*2.16*	*ctggTATCTAATgtga*	*60*	0
PA5045	*ponA*	x		1.32	69	6.33	attcGCTTAACTcttt	39	0
PA5058	*phaC2*	x		0.62	144	*3.67*	*acagGCTATAACtgag*	*77*	13.5
PA5060	*phaF*	x		0.69	14	*0.00*			0
PA5103				1.15	120	*3.92*	*agcgTCTACACCgaaa*	*115*	4.60
PA5110	*fbp*			0.71	87	*1.82*	*cgtcGATCGGCTgcgc*	*131*	0
PA5143	*hisB*	x		0.72	53	6.05	cctgCCTATAATgctg	54	0
PA5144		x		0.72	106	*1.84*	*cacaGCTAACACtgca*	*147*	0
PA5156				1.14	324	*3.97*	*tgccGCTTGCATcgtg*	*294*	0
PA5160.1			x	1.05	-4	n.d.			n.d.
PA5161	*rmlB*			0.64	236	*4.02*	*ttcgAATAGAATgccg*	*157*	0
PA5170	*arcD*			0.82	226	*5.86*	*aatgTCTTCACTctca*	*35*	2.80
PA5195		x		0.65	132	*2.37*	*aggcGATCCACTcgcg*	*191*	0
PA5196		x		0.65	76	6.56	ccctGCTAGAATgccg	102	2.8
PA5208		x		1.22	10	7.13	gtggCCTATACTtttc	37	1.8
PA5209		x		1.22	102	*3.71*	*cgcgCCTTTGATctgg*	*60*	0
PA5210				0.67	28	*1.56*	*GCTTCGCCgcta*	*37*	0
PA5253	*algP*	x		0.82	58	*4.78*	*gcggGCAATCCTggcg*	*100*	0
PA5254		x		0.82	66	*4.06*	*ccatACTAGACCcgca*	*92*	0
PA5282		x		0.61	93	*2.23*	*ttaaGCACAAATccga*	*123*	0

				RpoS ChIP-chip		RpoS consensus sequence (revised, 300 bp upstream)			Transcriptome
PA number[a]	gene name	shared promoter[b]	non-coding gene[c]	log_2-fold enrichment	distance to ATG	weight score[d]	sequence	distance to ATG	fold change[e]
PA5283		x		0.61	68	6.33	ttgtGCTTAACTgttc	41	0
PA5285				1.06	86	*5.48*	*tataACTAACCTgctt*	*34*	0
PA5286				0.63	1	6.56	ccgcGCTAGAATgcgc	47	0
PA5288	*glnK*	x		1.16	368	*2.78*	*gcACTATCCCcggg*	*298*	0
PA5289		x		1.16	70	7.64	tcgtGCTAGACTgccg	37	0
PA5300	*cycB*			0.84	208	*4.85*	*tgccGCAAGGCTttgc*	*147*	0
PA5304	*dadA*			0.55	30	7.13	tcttCCTATACTgcgc	71	0
PA5319	*radC*	x		0.83	25	*5.17*	*atggGCTAAGATagca*	*57*	0
PA5320	*coaC*	x		0.83	113	*4.60*	*taagGCAAGCCT*	*8*	0
PA5343		x		0.63	105	6.29	gacgCCTACACTgccc	39	0
PA5344		x		0.63	31	6.61	agccGCTATGCTtggc	34	0
PA5346	*sadB*			1.21	50	*2.52*	*tccaGCTCGCATggtc*	*17*	0
PA5347				0.56	34	*5.89*	*aacaGCTACAATgcgc*	*43*	0
PA5359		x		0.59	48	*5.06*	*ggTCTTGCCTcggg*	*102*	6.50
PA5360	*phoB*	x		0.59	55	*2.99*	*cgagGCAAGACC*	*8*	0
PA5369.5	16S rRNA		x	0.53	411	n.d.			n.d.
PA5424				0.52	96	6.99	ctttTCTACACTgtcc	59	4
PA5426	*purE*	x		1.21	189	*4.26*	*ttgcGGTATACTgcgc*	*127*	0
PA5427	*adhA*	x		1.21	157	*2.34*	*ggggGCTACCGTccgt*	*192*	0
PA5438		x		0.84	78	*1.05*	*acggCGTTGGCTgggc*	*69*	0
PA5439		x		0.84	6	*1.92*	*ctgtAGTAACCTtgta*	*64*	0
PA5491		x		0.71	3	*4.73*	*gaagTATATAATgccg*	*116*	0
PA5492		x		0.71	179	*5.81*	*gcatTATATACTtccg*	*73*	0
PA5528		x		0.68	49	*4.59*	*gcagACTAGCATccgc*	*294*	0
PA5529		x		0.68	311	*4.82*	*ggatGCTAGTCTgcgg*	*73*	0
PA5536		x		0.67	19	*1.73*	*ttgtTATAGTATaacg*	*36*	0
PA5537		x		0.67	92	*5.51*	*tccgGCTACCCTgggc*	*35*	0
PA5561	*atpI*			0.66	148	7.13	ccccCCTATACTctgc	97	0

[a] Genes with an RpoS consensus box (> 6.0) are underlined, genes differentially expressed in an *rpoS* mutant in **bold**

[b] Enriched promoter region could belong to two adjacent genes on opposite strands

[c] Non-coding gene, for which consensus sequence and transcriptome were not determined (n.d.)

[d] Low scoring (< 6.0) consensus sequences are in *italics*

[e] as described by Schuster *et al.* [136]

Table 5.3. Genes identified by ChIP-chip, that also possess an upstream RpoS sequence motif and exhibited a difference of gene expression in an *rpoS* mutant [136].

		ChIP-chip		Revised consensus box 300 bp upstream			Transcriptome
PA number	gene name	log_2-fold enrichment	distance to ATG	weight score	sequence	distance to ATG	fold change[a]
PA0052		0.87	-2	6.51	gccgGCTTGACTgagg	40	7.1
PA0105	*coxB*	0.93	245	7.84	gctgTCTATACTccca	151	18.3
PA0179		1.19	200	6.71	attgTCTTTACTggaa	115	15.0
PA0312		0.63	82	6.37	cagtTCTATCCTaagg	187	1.8
PA0314		0.63	83	6.24	cccgGCTAAGCTgaac	60	2.4
PA0332		0.64	57	6.24	ggctGCTAAGCTtcac	93	2.1
PA0451		1.20	82	7.13	ctggACTAGACTgaga	105	2.4
PA0455	*dbpA*	0.63	19	7.64	ggctGCTAGACTagcc	40	1.9
PA0483		0.71	-7	7.13	cttgCCTATACTcccg	34	5.2
PA0506		0.70	13	6.69	atggGCTTTACTgaga	249	5.0
PA0588		1.64	212	6.00	tcttCCTTTACTccgt	229	4.7
PA0732		0.58	5	6.24	cgacGCTAAGCTgaat	63	1.9
PA0743		0.51	71	6.26	agcgTCTAAGCTgttt	57	4.0
PA0769		0.77	56	6.47	aataACTACACTgaca	23	1.8
PA0788		1.03	71	7.13	gacaACTAGACTtccc	23	3.1
PA0838		2.30	178	6.24	aactGCTAAGCTggta	156	3.4
PA0861		1.32	264	7.13	agccACTAGACTccta	169	2.6
PA0905	*rsmA*	0.58	161	6.26	ctggTCAATACTgggt	100	2.1
PA0916		1.34	29	6.56	tgccGCTAGAATtgcg	63	2.5
PA1041		0.70	33	6.71	ggggTCTTTACTccct	49	29.2
PA1054		0.50	240	6.24	tcttGCTAAGCTtcaa	250	1.8
PA1117		0.50	40	6.56	ggctGCTAGAATatcc	59	2.4
PA1118		2.20	37	7.64	ggatGCTAGACTga	10	3.0
PA1177	*napE*	1.02	8	6.44	agggTCTAGGCTttct	39	50.0
PA1190		1.09	46	7.13	cgttCCTATACTgcga	111	3.3
PA1289		0.94	67	6.47	tttcACTACACTtcaa	103	30.6
PA1342		0.71	93	6.47	tgccACTACACTgttc	129	1.6
PA1422	*gbuR*	0.74	100	7.64	agcgGCTAGACTtcgc	82	2.3
PA1730		2.32	197	7.66	ctgtTCTAGACTtatc	232	3.0
PA1881		0.71	154	7.66	ttgaTCTAGACTttcg	119	11.4
PA1930		0.93	61	6.99	ccgaTCTACACTggcg	86	16.3
PA2024		1.88	4	6.61	atggGCTATGCTtgtc	28	6.7
PA2072		0.74	57	6.33	ggatGCTTAACTataa	60	4.2
PA2475		0.81	40	7.84	gccaTCTATACTccct	42	3.3
PA2562		0.58	67	6.26	cggtTCTAAGCTatcg	44	1.9

Table 5.3. (Continued)

		ChIP-chip		Revised consensus box 300 bp upstream			Transcriptome
PA number	gene name	log_2-fold enrichment	distance to ATG	weight score	sequence	distance to ATG	fold change[a]
PA2572		1.39	-1	6.10	tcggACTATGCTtgcc	52	13.2
PA2815		0.51	96	6.24	acggGCTAAGCTcgag	44	2.5
PA2816		0.64	68	6.56	attgGCTAGAATcgac	42	2.0
PA3216		0.69	131	6.95	ggatACTAAACTggcc	80	3.3
PA3261		1.74	23	7.82	actgGCTATACTgctg	50	2.6
PA3289		0.75	43	6.17	ctggGCTAGCCTgagg	35	2.1
PA3340		1.65	258	6.56	ttccGCTAGAATcgcc	256	3.6
PA3418	*ldh*	1.80	69	7.13	cctgCCTATACTgaag	69	18.1
PA3451		1.17	5	6.29	cccgCCTACACTgaaa	44	35.7
PA3465		0.99	10	7.64	ggcgGCTAGACTttcc	47	7.7
PA3945		1.07	77	6.47	aaagACTACACTccgg	132	5.9
PA4306	*flp*	1.15	87	7.66	tgaaTCTAGACTcggg	192	76.0
PA4311		1.73	100	6.95	ctttCCTAGACTtgaa	107	3.5
PA4362		0.55	42	6.01	aaggTCTAACCTgaaa	38	9.2
PA4523		1.25	264	6.76	tatcTCTATAATgaat	126	1.8
PA4614	*mscL*	0.63	116	7.48	ttccTCTAAACTtcgt	161	3.1
PA4702		0.83	84	7.84	ctctTCTATACTcacg	39	11.2
PA4703		0.91	169	6.97	ggccGCTACACTtctg	183	15.2
PA4874		0.78	87	7.64	agtcGCTAGACTtcag	53	7.5
PA4875		0.78	308	7.64	cgcgGCTAGACTgacg	275	2.1
PA4915		0.60	51	6.71	accaTCTTTACTctca	35	6.6
PA5196		0.65	76	6.56	ccctGCTAGAATgccg	102	2.8
PA5208		1.22	10	7.13	gtggCCTATACTtttc	37	1.8
PA5424		0.52	96	6.99	ctttTCTACACTgtcc	59	4.0

[a] as described by Schuster *et al.* [136]

6 References

1. Gest H (2004). The discovery of microorganisms by Robert Hooke and Antoni Van Leeuwenhoek, fellows of the Royal Society. *Notes Rec R Soc Lond* 58: 187-201.

2. Berg HC (1975). Chemotaxis in bacteria. *Annu Rev Biophys Bioeng* 4: 119-136.

3. Costerton JW, Lewandowski Z, Caldwell DE, Korber DR, Lappin-Scott HM (1995). Microbial biofilms. *Annu Rev Microbiol* 49: 711-745.

4. Costerton JW, Stewart PS, Greenberg EP (1999). Bacterial biofilms: a common cause of persistent infections. *Science (80-)* 284: 1318-1322.

5. Hall-Stoodley L, Costerton JW, Stoodley P (2004). Bacterial biofilms: from the natural environment to infectious diseases. *Nat Rev Microbiol* 2: 95-108.

6. Høiby N, Bjarnsholt T, Givskov M, Molin S, Ciofu O (2010). Antibiotic resistance of bacterial biofilms. *Int J Antimicrob Agents* 35: 322-332.

7. Bodey GP, Bolivar R, Fainstein V, Jadeja L (1983). Infections caused by *Pseudomonas aeruginosa*. *Rev Infect Dis* 5: 279-313.

8. Lyczak JB, Cannon CL, Pier GB (2000). Establishment of *Pseudomonas aeruginosa* infection: lessons from a versatile opportunist. *Microbes Infect* 2: 1051-1060.

9. Parsek MR, Singh PK (2003). Bacterial biofilms: an emerging link to disease pathogenesis. *Annu Rev Microbiol* 57: 677-701.

10. Costerton JW (2001). Cystic fibrosis pathogenesis and the role of biofilms in persistent infection. *Trends Microbiol* 9: 50-52.

11. Stover CK, Pham XQ, Erwin AL, Mizoguchi SD, Warrener P, Hickey MJ, Brinkman FS, Hufnagle WO, Kowalik DJ, Lagrou M, Garber RL, Goltry L, Tolentino E, Westbrock-Wadman S, Yuan Y, Brody LL, Coulter SN, Folger KR, Kas A, Larbig K, Lim R, Smith K, Spencer D, Wong GK, Wu Z, Paulsen IT, Reizer J, Saier MH, Hancock RE, Lory S, Olson MV (2000). Complete genome sequence of *Pseudomonas aeruginosa* PAO1, an opportunistic pathogen. *Nature* 406: 959-964.

12. Bradley DE (1980). A function of *Pseudomonas aeruginosa* PAO polar pili: twitching motility. *Can J Microbiol* 26: 146-154.

13. Mattick JS (2002). Type IV pili and twitching motility. *Annu Rev Microbiol* 56: 289-314.

14. Köhler T, Curty LK, Barja F, van Delden C, Pechère JC (2000). Swarming of *Pseudomonas aeruginosa* is dependent on cell-to-cell signaling and requires flagella and pili. *J Bacteriol* 182: 5990-5996.

15. Kearns DB (2010). A field guide to bacterial swarming motility. *Nat Rev Microbiol* 8: 634-644.

16. Armitage JP, Evans MC (1983). The motile and tactic behaviour of *Pseudomonas aeruginosa* in anaerobic environments. *FEBS Lett* 156: 113-118.

17. Taylor BL, Koshland DEJ (1974). Reversal of flagellar rotation in monotrichous and peritrichous bacteria: generation of changes in direction. *J Bacteriol* 119: 640-642.

18. Blair DF (1995). How bacteria sense and swim. *Annu Rev Microbiol* 49: 489-522.

19. Bourret RB, Stock AM (2002). Molecular information processing: lessons from bacterial chemotaxis. *J Biol Chem* 277: 9625-9628.

20. Sourjik V, Berg HC (2002). Binding of the *Escherichia coli* response regulator CheY to its target measured in vivo by fluorescence resonance energy transfer. *Proc Natl Acad Sci U S A* 99: 12669-12674.

21. Alon U, Camarena L, Surette MG, Aguera y Arcas B, Liu Y, Leibler S, Stock JB (1998). Response regulator output in bacterial chemotaxis. *EMBO J* 17: 4238-4248.

22. Springer WR, Koshland DEJ (1977). Identification of a protein methyltransferase as the *cheR* gene product in the bacterial sensing system. *Proc Natl Acad Sci U S A* 74: 533-537.

23. Stock JB, Koshland DEJ (1978). A protein methylesterase involved in bacterial sensing. *Proc Natl Acad Sci U S A* 75: 3659-3663.

24. Lupas A, Stock J (1989). Phosphorylation of an N-terminal regulatory domain activates the CheB methylesterase in bacterial chemotaxis. *J Biol Chem* 264: 17337-17342.

25. Kirby JR (2009). Chemotaxis-like regulatory systems: unique roles in diverse bacteria. *Annu Rev Microbiol* 63: 45-59.

26. Rao CV, Ordal GW (2009). The molecular basis of excitation and adaptation during chemotactic sensory transduction in bacteria. *Contrib Microbiol* 16: 33-64.

27. Zusman DR, Scott AE, Yang Z, Kirby JR (2007). Chemosensory pathways, motility and development in *Myxococcus xanthus*. *Nat Rev Microbiol* 5: 862-872.

28. Szurmant H, Ordal GW (2004). Diversity in chemotaxis mechanisms among the bacteria and archaea. *Microbiol Mol Biol Rev* 68: 301-319.

29. Boin MA, Austin MJ, Häse CC (2004). Chemotaxis in *Vibrio cholerae*. *FEMS Microbiol Lett* 239: 1-8.

30. Armitage JP, Schmitt R (1997). Bacterial chemotaxis: *Rhodobacter sphaeroides* and *Sinorhizobium meliloti*--variations on a theme?. *Microbiology* 143 (Pt 12): 3671-3682.

31. Wuichet K, Alexander RP, Zhulin IB (2007). Comparative genomic and protein sequence analyses of a complex system controlling bacterial chemotaxis. *Methods Enzymol* 422: 1-31.

32. Güvener ZT, Tifrea DF, Harwood CS (2006). Two different *Pseudomonas aeruginosa* chemosensory signal transduction complexes localize to cell poles and form and remould in stationary phase. *Mol Microbiol* 61: 106-118.

33. Ferrández A, Hawkins AC, Summerfield DT, Harwood CS (2002). Cluster II *che* genes from *Pseudomonas aeruginosa* are required for an optimal chemotactic response. *J Bacteriol* 184: 4374-4383.

34. Kato J, Nakamura T, Kuroda A, Ohtake H (1999). Cloning and characterization of chemotaxis genes in *Pseudomonas aeruginosa*. *Biosci Biotechnol Biochem* 63: 155-161.

35. Masduki A, Nakamura J, Ohga T, Umezaki R, Kato J, Ohtake H (1995). Isolation and characterization of chemotaxis mutants and genes of *Pseudomonas aeruginosa*. *J Bacteriol* 177: 948-952.

36. Fulcher NB, Holliday PM, Klem E, Cann MJ, Wolfgang MC (2010). The *Pseudomonas aeruginosa* Chp chemosensory system regulates intracellular cAMP levels by modulating adenylate cyclase activity. *Mol Microbiol* 76: 889-904.

37. Whitchurch CB, Leech AJ, Young MD, Kennedy D, Sargent JL, Bertrand JJ, Semmler ABT, Mellick AS, Martin PR, Alm RA, Hobbs M, Beatson SA, Huang B, Nguyen L, Commolli JC, Engel JN, Darzins A, Mattick JS (2004). Characterization of a complex chemosensory signal transduction system which controls twitching motility in *Pseudomonas aeruginosa*. *Mol Microbiol* 52: 873-893.

38. Darzins A (1994). Characterization of a *Pseudomonas aeruginosa* gene cluster involved in pilus biosynthesis and twitching motility: sequence similarity to the chemotaxis proteins of enterics and the gliding bacterium *Myxococcus xanthus*. *Mol Microbiol* 11: 137-153.

39. Hickman JW, Tifrea DF, Harwood CS (2005). A chemosensory system that regulates biofilm formation through modulation of cyclic diguanylate levels. *Proc Natl Acad Sci U S A* 102: 14422-14427.

40. D'Argenio DA, Calfee MW, Rainey PB, Pesci EC (2002). Autolysis and autoaggregation in *Pseudomonas aeruginosa* colony morphology mutants. *J Bacteriol* 184: 6481-6489.

41. Kato J, Kim H, Takiguchi N, Kuroda A, Ohtake H (2008). *Pseudomonas aeruginosa* as a model microorganism for investigation of chemotactic behaviors in ecosystem. *J Biosci Bioeng* 106: 1-7.

42. DeLange PA, Collins TL, Pierce GE, Robinson JB (2007). PilJ localizes to cell poles and is required for type IV pilus extension in *Pseudomonas aeruginosa*. *Curr Microbiol* 55: 389-395.

43. Morgan R, Kohn S, Hwang S, Hassett DJ, Sauer K (2006). BdlA, a chemotaxis regulator essential for biofilm dispersion in *Pseudomonas aeruginosa*. *J Bacteriol* 188: 7335-7343.

44. Elasri MO, Miller RV (1999). Study of the response of a biofilm bacterial community to UV radiation. *Appl Environ Microbiol* 65: 2025-2031.

45. Teitzel GM, Parsek MR (2003). Heavy metal resistance of biofilm and planktonic *Pseudomonas aeruginosa*. *Appl Environ Microbiol* 69: 2313-2320.

46. Le Magrex-Debar E, Lemoine J, Gellé MP, Jacquelin LF, Choisy C (2000). Evaluation of biohazards in dehydrated biofilms on foodstuff packaging. *Int J Food Microbiol* 55: 239-243.

47. Mah TF, O'Toole GA (2001). Mechanisms of biofilm resistance to antimicrobial agents. *Trends Microbiol* 9: 34-39.

48. Flemming H, Wingender J (2010). The biofilm matrix. *Nat Rev Microbiol* 8: 623-633.

49. Parsek MR, Tolker-Nielsen T (2008). Pattern formation in *Pseudomonas aeruginosa* biofilms. *Curr Opin Microbiol* 11: 560-566.

50. Stoodley P, Sauer K, Davies DG, Costerton JW (2002). Biofilms as complex differentiated communities. *Annu Rev Microbiol* 56: 187-209.

51. Klausen M, Heydorn A, Ragas P, Lambertsen L, Aaes-Jørgensen A, Molin S, Tolker-Nielsen T (2003). Biofilm formation by *Pseudomonas aeruginosa* wild type, flagella and type IV pili mutants. *Mol Microbiol* 48: 1511-1524.

52. Lemon KP, Higgins DE, Kolter R (2007). Flagellar motility is critical for *Listeria monocytogenes* biofilm formation. *J Bacteriol* 189: 4418-4424.

53. Merritt PM, Danhorn T, Fuqua C (2007). Motility and chemotaxis in *Agrobacterium tumefaciens* surface attachment and biofilm formation. *J Bacteriol* 189: 8005-8014.

54. O'Toole GA, Kolter R (1998). Flagellar and twitching motility are necessary for *Pseudomonas aeruginosa* biofilm development. *Mol Microbiol* 30: 295-304.

55. Pratt LA, Kolter R (1998). Genetic analysis of *Escherichia coli* biofilm formation: roles of flagella, motility, chemotaxis and type I pili. *Mol Microbiol* 30: 285-293.

56. Kirov SM, Castrisios M, Shaw JG (2004). *Aeromonas* flagella (polar and lateral) are enterocyte adhesins that contribute to biofilm formation on surfaces. *Infect Immun* 72: 1939-1945.

57. Moorthy S, Watnick PI (2004). Genetic evidence that the *Vibrio cholerae* monolayer is a distinct stage in biofilm development. *Mol Microbiol* 52: 573-587.

58. Barken KB, Pamp SJ, Yang L, Gjermansen M, Bertrand JJ, Klausen M, Givskov M, Whitchurch CB, Engel JN, Tolker-Nielsen T (2008). Roles of type IV pili, flagellum-

mediated motility and extracellular DNA in the formation of mature multicellular structures in *Pseudomonas aeruginosa* biofilms. *Environ Microbiol* 10: 2331-2343.

59. Hengge R (2009). Principles of c-di-GMP signalling in bacteria. *Nat Rev Microbiol* 7: 263-273.

60. Jenal U, Malone J (2006). Mechanisms of cyclic-di-GMP signaling in bacteria. *Annu Rev Genet* 40: 385-407.

61. Römling U, Amikam D (2006). Cyclic di-GMP as a second messenger. *Curr Opin Microbiol* 9: 218-228.

62. Kulasakara H, Lee V, Brencic A, Liberati N, Urbach J, Miyata S, Lee DG, Neely AN, Hyodo M, Hayakawa Y, Ausubel FM, Lory S (2006). Analysis of *Pseudomonas aeruginosa* diguanylate cyclases and phosphodiesterases reveals a role for bis-(3'-5')-cyclic-GMP in virulence. *Proc Natl Acad Sci U S A* 103: 2839-2844.

63. Ryan RP, Fouhy Y, Lucey JF, Crossman LC, Spiro S, He Y, Zhang L, Heeb S, Cámara M, Williams P, Dow JM (2006). Cell-cell signaling in *Xanthomonas campestris* involves an HD-GYP domain protein that functions in cyclic di-GMP turnover. *Proc Natl Acad Sci U S A* 103: 6712-6717.

64. Ryjenkov DA, Tarutina M, Moskvin OV, Gomelsky M (2005). Cyclic diguanylate is a ubiquitous signaling molecule in bacteria: insights into biochemistry of the GGDEF protein domain. *J Bacteriol* 187: 1792-1798.

65. Schmidt AJ, Ryjenkov DA, Gomelsky M (2005). The ubiquitous protein domain EAL is a cyclic diguanylate-specific phosphodiesterase: enzymatically active and inactive EAL domains. *J Bacteriol* 187: 4774-4781.

66. Simm R, Morr M, Kader A, Nimtz M, Römling U (2004). GGDEF and EAL domains inversely regulate cyclic di-GMP levels and transition from sessility to motility. *Mol Microbiol* 53: 1123-1134.

67. Tal R, Wong HC, Calhoon R, Gelfand D, Fear AL, Volman G, Mayer R, Ross P, Amikam D, Weinhouse H, Cohen A, Sapir S, Ohana P, Benziman M (1998). Three *cdg* operons control cellular turnover of cyclic di-GMP in *Acetobacter xylinum*: genetic organization and occurrence of conserved domains in isoenzymes. *J Bacteriol* 180: 4416-4425.

68. Chan C, Paul R, Samoray D, Amiot NC, Giese B, Jenal U, Schirmer T (2004). Structural basis of activity and allosteric control of diguanylate cyclase. *Proc Natl Acad Sci U S A* 101: 17084-17089.

69. Christen B, Christen M, Paul R, Schmid F, Folcher M, Jenoe P, Meuwly M, Jenal U (2006). Allosteric control of cyclic di-GMP signaling. *J Biol Chem* 281: 32015-32024.

70. Schirmer T, Jenal U (2009). Structural and mechanistic determinants of c-di-GMP signalling. *Nat Rev Microbiol* 7: 724-735.

71. Seshasayee ASN, Fraser GM, Luscombe NM (2010). Comparative genomics of cyclic-di-GMP signalling in bacteria: post-translational regulation and catalytic activity. *Nucleic Acids Res* 38: 5970-5981.

72. Galperin MY, Nikolskaya AN, Koonin EV (2001). Novel domains of the prokaryotic two-component signal transduction systems. *FEMS Microbiol Lett* 203: 11-21.

73. Ponting CP, Aravind L (1997). PAS: a multifunctional domain family comes to light. *Curr Biol* 7: R674-7.

74. Aravind L, Ponting CP (1999). The cytoplasmic helical linker domain of receptor histidine kinase and methyl-accepting proteins is common to many prokaryotic signalling proteins. *FEMS Microbiol Lett* 176: 111-116.

75. Aravind L, Ponting CP (1997). The GAF domain: an evolutionary link between diverse phototransducing proteins. *Trends Biochem Sci* 22: 458-459.

76. Jonas K, Melefors O, Römling U (2009). Regulation of c-di-GMP metabolism in biofilms. *Future Microbiol* 4: 341-358.

77. Amikam D, Galperin MY (2006). PilZ domain is part of the bacterial c-di-GMP binding protein. *Bioinformatics* 22: 3-6.

78. McCarthy Y, Ryan RP, O'Donovan K, He Y, Jiang B, Feng J, Tang J, Dow JM (2008). The role of PilZ domain proteins in the virulence of *Xanthomonas campestris* pv. *campestris*. *Mol Plant Pathol* 9: 819-824.

79. Boehm A, Kaiser M, Li H, Spangler C, Kasper CA, Ackermann M, Kaever V, Sourjik V, Roth V, Jenal U (2010). Second messenger-mediated adjustment of bacterial swimming velocity. *Cell* 141: 107-116.

80. Christen M, Christen B, Allan MG, Folcher M, Jenö P, Grzesiek S, Jenal U (2007). DgrA is a member of a new family of cyclic diguanosine monophosphate receptors and controls flagellar motor function in *Caulobacter crescentus*. *Proc Natl Acad Sci U S A* 104: 4112-4117.

81. Ryjenkov DA, Simm R, Römling U, Gomelsky M (2006). The PilZ domain is a receptor for the second messenger c-di-GMP: the PilZ domain protein YcgR controls motility in enterobacteria. *J Biol Chem* 281: 30310-30314.

82. Merighi M, Lee VT, Hyodo M, Hayakawa Y, Lory S (2007). The second messenger bis-(3'-5')-cyclic-GMP and its PilZ domain-containing receptor Alg44 are required for alginate biosynthesis in *Pseudomonas aeruginosa*. *Mol Microbiol* 65: 876-895.

83. Ross P, Weinhouse H, Aloni Y, Michaeli D, Weinberger-Ohana P, Mayer R, Braun S, de Vroom E, van der Marel GA, van Boom JH, Benziman M (1987). Regulation of cellulose synthesis in *Acetobacter xylinum* by cyclic diguanylic acid. *Nature* 325: 279-281.

84. Duerig A, Abel S, Folcher M, Nicollier M, Schwede T, Amiot N, Giese B, Jenal U (2009). Second messenger-mediated spatiotemporal control of protein degradation regulates bacterial cell cycle progression. *Genes Dev* 23: 93-104.

85. Newell PD, Monds RD, O'Toole GA (2009). LapD is a bis-(3',5')-cyclic dimeric GMP-binding protein that regulates surface attachment by *Pseudomonas fluorescens* Pf0-1. *Proc Natl Acad Sci U S A* 106: 3461-3466.

86. Navarro MVAS, Newell PD, Krasteva PV, Chatterjee D, Madden DR, O'Toole GA, Sondermann H (2011). Structural basis for c-di-GMP-mediated inside-out signaling controlling periplasmic proteolysis. *PLoS Biol* 9: e1000588.

87. Newell PD, Boyd CD, Sondermann H, O'Toole GA (2011). A c-di-GMP effector system controls cell adhesion by inside-out signaling and surface protein cleavage. *PLoS Biol* 9: e1000587.

88. Hickman JW, Harwood CS (2008). Identification of FleQ from *Pseudomonas aeruginosa* as a c-di-GMP-responsive transcription factor. *Mol Microbiol* 69: 376-389.

89. Chin K, Lee Y, Tu Z, Chen C, Tseng Y, Yang J, Ryan RP, McCarthy Y, Dow JM, Wang AH, Chou S (2010). The cAMP receptor-like protein CLP is a novel c-di-GMP receptor linking cell-cell signaling to virulence gene expression in *Xanthomonas campestris*. *J Mol Biol* 396: 646-662.

90. Leduc JL, Roberts GP (2009). Cyclic di-GMP allosterically inhibits the CRP-like protein (Clp) of *Xanthomonas axonopodis* pv. *citri*. *J Bacteriol* 191: 7121-7122.

91. Tao F, He Y, Wu D, Swarup S, Zhang L (2010). The cyclic nucleotide monophosphate domain of *Xanthomonas campestris* global regulator Clp defines a new class of cyclic di-GMP effectors. *J Bacteriol* 192: 1020-1029.

92. Krasteva PV, Fong JCN, Shikuma NJ, Beyhan S, Navarro MVAS, Yildiz FH, Sondermann H (2010). *Vibrio cholerae* VpsT regulates matrix production and motility by directly sensing cyclic di-GMP. *Science (80-)* 327: 866-868.

93. Smith KD, Lipchock SV, Ames TD, Wang J, Breaker RR, Strobel SA (2009). Structural basis of ligand binding by a c-di-GMP riboswitch. *Nat Struct Mol Biol* 16: 1218-1223.

94. Sudarsan N, Lee ER, Weinberg Z, Moy RH, Kim JN, Link KH, Breaker RR (2008). Riboswitches in eubacteria sense the second messenger cyclic di-GMP. *Science (80-)* 321: 411-413.

95. Ryan RP, Lucey J, O'Donovan K, McCarthy Y, Yang L, Tolker-Nielsen T, Dow JM (2009). HD-GYP domain proteins regulate biofilm formation and virulence in *Pseudomonas aeruginosa*. *Environ Microbiol* 11: 1126-1136.

96. Alm RA, Bodero AJ, Free PD, Mattick JS (1996). Identification of a novel gene, *pilZ*, essential for type 4 fimbrial biogenesis in *Pseudomonas aeruginosa*. *J Bacteriol* 178: 46-53.

97. Ramelot TA, Yee A, Cort JR, Semesi A, Arrowsmith CH, Kennedy MA (2007). NMR structure and binding studies confirm that PA4608 from *Pseudomonas aeruginosa* is a PilZ domain and a c-di-GMP binding protein. *Proteins* 66: 266-271.

98. Lee VT, Matewish JM, Kessler JL, Hyodo M, Hayakawa Y, Lory S (2007). A cyclic-di-GMP receptor required for bacterial exopolysaccharide production. *Mol Microbiol* 65: 1474-1484.

99. Navarro MVAS, De N, Bae N, Wang Q, Sondermann H (2009). Structural analysis of the GGDEF-EAL domain-containing c-di-GMP receptor FimX. *Structure* 17: 1104-1116.

100. Weber H, Pesavento C, Possling A, Tischendorf G, Hengge R (2006). Cyclic-di-GMP-mediated signalling within the sigma network of *Escherichia coli*. *Mol Microbiol* 62: 1014-1034.

101. Jacobs MA, Alwood A, Thaipisuttikul I, Spencer D, Haugen E, Ernst S, Will O, Kaul R, Raymond C, Levy R, Chun-Rong L, Guenthner D, Bovee D, Olson MV, Manoil C (2003). Comprehensive transposon mutant library of *Pseudomonas aeruginosa*. *Proc Natl Acad Sci U S A* 100: 14339-14344.

102. Liberati NT, Urbach JM, Miyata S, Lee DG, Drenkard E, Wu G, Villanueva J, Wei T, Ausubel FM (2006). An ordered, nonredundant library of *Pseudomonas aeruginosa* strain PA14 transposon insertion mutants. *Proc Natl Acad Sci U S A* 103: 2833-2838.

103. Klockgether J, Munder A, Neugebauer J, Davenport CF, Stanke F, Larbig KD, Heeb S, Schöck U, Pohl TM, Wiehlmann L, Tümmler B (2010). Genome diversity of *Pseudomonas aeruginosa* PAO1 laboratory strains. *J Bacteriol* 192: 1113-1121.

104. Dötsch A, Pommerenke C, Bredenbruch F, Geffers R, Häussler S (2009). Evaluation of a microarray-hybridization based method applicable for discovery of single nucleotide polymorphisms (SNPs) in the *Pseudomonas aeruginosa* genome. *BMC Genomics* 10: 29.

105. Lewenza S, Falsafi RK, Winsor G, Gooderham WJ, McPhee JB, Brinkman FSL, Hancock REW (2005). Construction of a mini-Tn5-luxCDABE mutant library in *Pseudomonas aeruginosa* PAO1: a tool for identifying differentially regulated genes. *Genome Res* 15: 583-589.

106. Woodcock DM, Crowther PJ, Doherty J, Jefferson S, DeCruz E, Noyer-Weidner M, Smith SS, Michael MZ, Graham MW (1989). Quantitative evaluation of *Escherichia coli* host strains for tolerance to cytosine methylation in plasmid and phage recombinants. *Nucleic Acids Res* 17: 3469-3478.

107. Simon R, Priefer U, Pühler A (1983). A broad host range mobilization system for in vivo genetic engineering: Transposon mutagenesis in gram negative bacteria. *Biotechnology* 1: 784-790.

108. Wolfe AJ, Conley MP, Berg HC (1988). Acetyladenylate plays a role in controlling the direction of flagellar rotation. *Proc Natl Acad Sci U S A* 85: 6711-6715.

109. Paul R, Weiser S, Amiot NC, Chan C, Schirmer T, Giese B, Jenal U (2004). Cell cycle-dependent dynamic localization of a bacterial response regulator with a novel di-guanylate cyclase output domain. *Genes Dev* 18: 715-727.

110. Kojic M, Venturi V (2001). Regulation of *rpoS* gene expression in *Pseudomonas*: involvement of a TetR family regulator. *J Bacteriol* 183: 3712-3720.

111. West SE, Schweizer HP, Dall C, Sample AK, Runyen-Janecky LJ (1994). Construction of improved *Escherichia-Pseudomonas* shuttle vectors derived from pUC18/19 and sequence of the region required for their replication in *Pseudomonas aeruginosa*. *Gene* 148: 81-86.

112. Güttler A (1998). Entwicklung eines Rekombinationssystems zum Studium des horizontalen Gentransfer auf unbekannte Bakterien sowie die Konstruktion von Transportvektoren mit *gfp* als Markergen. PhD Thesis. *Technische Universität Braunschweig*.

113. Rice MS, Dahlquist FW (1991). Sites of deamidation and methylation in Tsr, a bacterial chemotaxis sensory transducer. *J Biol Chem* 266: 9746-9753.

114. Lin LN, Li J, Brandts JF, Weis RM (1994). The serine receptor of bacterial chemotaxis exhibits half-site saturation for serine binding. *Biochemistry* 33: 6564-6570.

115. Hoang TT, Karkhoff-Schweizer RR, Kutchma AJ, Schweizer HP (1998). A broad-host-range Flp-FRT recombination system for site-specific excision of chromosomally-located DNA sequences: application for isolation of unmarked *Pseudomonas aeruginosa* mutants. *Gene* 212: 77-86.

116. Horton RM, Hunt HD, Ho SN, Pullen JK, Pease LR (1989). Engineering hybrid genes without the use of restriction enzymes: gene splicing by overlap extension. *Gene* 77: 61-68.

117. Hayakawa Y, Nagata R, Hirata A, Hyodo M, Kawai R (2003). A facile synthesis of cyclic bis(3′-5′)diguanylic acid. *Tetrahedron.* 59: 6465-6471.

118. Moll D, Prinz A, Gesellchen F, Drewianka S, Zimmermann B, Herberg FW (2006). Biomolecular interaction analysis in functional proteomics. *J Neural Transm* 113: 1015-1032.

119. Zimmermann B, Hahnefeld C, Herberg FW (2002). Applications of biomolecular interaction analysis in drug development. *TARGETS* 1: 66-73.

120. Perez E, West AH, Stock AM, Djordjevic S (2004). Discrimination between different methylation states of chemotaxis receptor Tar by receptor methyltransferase CheR. *Biochemistry* 43: 953-961.

121. Simms SA, Stock AM, Stock JB (1987). Purification and characterization of the S-adenosylmethionine:glutamyl methyltransferase that modifies membrane chemoreceptor proteins in bacteria. *J Biol Chem* 262: 8537-8543.

122. Christen M, Christen B, Folcher M, Schauerte A, Jenal U (2005). Identification and characterization of a cyclic di-GMP-specific phosphodiesterase and its allosteric control by GTP. *J Biol Chem* 280: 30829-30837.

123. Yeung ATY, Torfs ECW, Jamshidi F, Bains M, Wiegand I, Hancock REW, Overhage J (2009). Swarming of *Pseudomonas aeruginosa* is controlled by a broad spectrum of transcriptional regulators, including MetR. *J Bacteriol* 191: 5592-5602.

124. O'Toole GA, Kolter R (1998). Initiation of biofilm formation in *Pseudomonas fluorescens* WCS365 proceeds via multiple, convergent signalling pathways: a genetic analysis. *Mol Microbiol* 28: 449-461.

125. Müsken M, Di Fiore S, Dötsch A, Fischer R, Häussler S (2010). Genetic determinants of *Pseudomonas aeruginosa* biofilm establishment. *Microbiology* 156: 431-441.

126. Meissner A, Wild V, Simm R, Rohde M, Erck C, Bredenbruch F, Morr M, Römling U, Häussler S (2007). *Pseudomonas aeruginosa cupA*-encoded fimbriae expression is regulated by a GGDEF and EAL domain-dependent modulation of the intracellular level of cyclic diguanylate. *Environ Microbiol* 9: 2475-2485.

127. Martins TJ, Mumby MC, Beavo JA (1982). Purification and characterization of a cyclic GMP-stimulated cyclic nucleotide phosphodiesterase from bovine tissues. *J Biol Chem* 257: 1973-1979.

128. Wessel D, Flügge UI (1984). A method for the quantitative recovery of protein in dilute solution in the presence of detergents and lipids. *Anal Biochem* 138: 141-143.

129. Keller A, Nesvizhskii AI, Kolker E, Aebersold R (2002). Empirical statistical model to estimate the accuracy of peptide identifications made by MS/MS and database search. *Anal Chem* 74: 5383-5392.

130. Nesvizhskii AI, Keller A, Kolker E, Aebersold R (2003). A statistical model for identifying proteins by tandem mass spectrometry. *Anal Chem* 75: 4646-4658.

131. Wade JT, Reppas NB, Church GM, Struhl K (2005). Genomic analysis of LexA binding reveals the permissive nature of the *Escherichia coli* genome and identifies unconventional target sites. *Genes Dev* 19: 2619-2630.

132. Herring CD, Raffaelle M, Allen TE, Kanin EI, Landick R, Ansari AZ, Palsson BØ (2005). Immobilization of *Escherichia coli* RNA polymerase and location of binding sites by use of chromatin immunoprecipitation and microarrays. *J Bacteriol* 187: 6166-6174.

133. Chromatin immunoprecipitation assay protocol. http://media.affymetrix.com/support/downloads/manuals/chromatin_immun_ChIP.pdf.

134. Winsor GL, Van Rossum T, Lo R, Khaira B, Whiteside MD, Hancock REW, Brinkman FSL (2009). *Pseudomonas* Genome Database: facilitating user-friendly, comprehensive comparisons of microbial genomes. *Nucleic Acids Res* 37: D483-8.

135. Hertz GZ, Stormo GD (1999). Identifying DNA and protein patterns with statistically significant alignments of multiple sequences. *Bioinformatics* 15: 563-577.

136. Schuster M, Hawkins AC, Harwood CS, Greenberg EP (2004). The *Pseudomonas aeruginosa* RpoS regulon and its relationship to quorum sensing. *Mol Microbiol* 51: 973-985.

137. Okumura H, Nishiyama S, Sasaki A, Homma M, Kawagishi I (1998). Chemotactic adaptation is altered by changes in the carboxy-terminal sequence conserved among the major methyl-accepting chemoreceptors. *J Bacteriol* 180: 1862-1868.

138. Wu J, Li J, Li G, Long DG, Weis RM (1996). The receptor binding site for the methyltransferase of bacterial chemotaxis is distinct from the sites of methylation. *Biochemistry* 35: 4984-4993.

139. Winsor GL, Lo R, Sui SJH, Ung KSE, Huang S, Cheng D, Ching WH, Hancock REW, Brinkman FSL (2005). *Pseudomonas aeruginosa* Genome Database and PseudoCAP: facilitating community-based, continually updated, genome annotation. *Nucleic Acids Res* 33: D338-43.

140. Stenberg E, Persson B, Roos H, Urbaniczky C (1991). Quantitative determination of surface concentration of protein with surface plasmon resonance using radiolabeled proteins. *J Colloid Interface Sci* 143(2): 513-526.

141. Kuroda A, Kumano T, Taguchi K, Nikata T, Kato J, Ohtake H (1995). Molecular cloning and characterization of a chemotactic transducer gene in *Pseudomonas aeruginosa*. *J Bacteriol* 177: 7019-7025.

142. Taguchi K, Fukutomi H, Kuroda A, Kato J, Ohtake H (1997). Genetic identification of chemotactic transducers for amino acids in *Pseudomonas aeruginosa*. *Microbiology* 143 (Pt 10): 3223-3229.

143. Rao F, Yang Y, Qi Y, Liang Z (2008). Catalytic mechanism of cyclic di-GMP-specific phosphodiesterase: a study of the EAL domain-containing RocR from *Pseudomonas aeruginosa*. *J Bacteriol* 190: 3622-3631.

144. Rosario MM, Kirby JR, Bochar DA, Ordal GW (1995). Chemotactic methylation and behavior in *Bacillus subtilis*: role of two unique proteins, CheC and CheD. *Biochemistry* 34: 3823-3831.

145. De N, Pirruccello M, Krasteva PV, Bae N, Raghavan RV, Sondermann H (2008). Phosphorylation-independent regulation of the diguanylate cyclase WspR. *PLoS Biol* 6: e67.

146. Frisk A, Jyot J, Arora SK, Ramphal R (2002). Identification and functional characterization of *flgM*, a gene encoding the anti-sigma 28 factor in *Pseudomonas aeruginosa*. *J Bacteriol* 184: 1514-1521.

147. Starnbach MN, Lory S (1992). The *fliA* (*rpoF*) gene of *Pseudomonas aeruginosa* encodes an alternative sigma factor required for flagellin synthesis. *Mol Microbiol* 6: 459-469.

148. Paul K, Nieto V, Carlquist WC, Blair DF, Harshey RM (2010). The c-di-GMP binding protein YcgR controls flagellar motor direction and speed to affect chemotaxis by a "backstop brake" mechanism. *Mol Cell* 38: 128-139.

149. Li Y, Xia H, Bai F, Xu H, Yang L, Yao H, Zhang L, Zhang X, Bai Y, Saris PEJ, Tolker-Nielsen T, Qiao M (2007). Identification of a new gene PA5017 involved in flagella-mediated motility, chemotaxis and biofilm formation in *Pseudomonas aeruginosa*. *FEMS Microbiol Lett* 272: 188-195.

150. Potvin E, Sanschagrin F, Levesque RC (2008). Sigma factors in *Pseudomonas aeruginosa*. *FEMS Microbiol Rev* 32: 38-55.

151. Suh SJ, Silo-Suh L, Woods DE, Hassett DJ, West SE, Ohman DE (1999). Effect of *rpoS* mutation on the stress response and expression of virulence factors in *Pseudomonas aeruginosa*. *J Bacteriol* 181: 3890-3897.

152. Irie Y, Starkey M, Edwards AN, Wozniak DJ, Romeo T, Parsek MR (2010). *Pseudomonas aeruginosa* biofilm matrix polysaccharide Psl is regulated transcriptionally by RpoS and post-transcriptionally by RsmA. *Mol Microbiol* 78: 158-172.

153. Heydorn A, Ersbøll B, Kato J, Hentzer M, Parsek MR, Tolker-Nielsen T, Givskov M, Molin S (2002). Statistical analysis of *Pseudomonas aeruginosa* biofilm development: impact of mutations in genes involved in twitching motility, cell-to-cell signaling, and stationary-phase sigma factor expression. *Appl Environ Microbiol* 68: 2008-2017.

154. Xu KD, Franklin MJ, Park CH, McFeters GA, Stewart PS (2001). Gene expression and protein levels of the stationary phase sigma factor, RpoS, in continuously-fed *Pseudomonas aeruginosa* biofilms. *FEMS Microbiol Lett* 199: 67-71.

155. Hong CS, Kuroda A, Takiguchi N, Ohtake H, Kato J (2005). Expression of *Pseudomonas aeruginosa aer-2*, one of two aerotaxis transducer genes, is controlled by RpoS. *J Bacteriol* 187: 1533-1535.

156. Konyecsni WM, Deretic V (1990). DNA sequence and expression analysis of *algP* and *algQ*, components of the multigene system transcriptionally regulating mucoidy in *Pseudomonas aeruginosa*: *algP* contains multiple direct repeats. *J Bacteriol* 172: 2511-2520.

157. Deretic V, Konyecsni WM (1990). A procaryotic regulatory factor with a histone H1-like carboxy-terminal domain: clonal variation of repeats within *algP*, a gene involved in regulation of mucoidy in *Pseudomonas aeruginosa*. *J Bacteriol* 172: 5544-5554.

158. Friedman L, Kolter R (2004). Two genetic loci produce distinct carbohydrate-rich structural components of the *Pseudomonas aeruginosa* biofilm matrix. *J Bacteriol* 186: 4457-4465.

159. Jackson KD, Starkey M, Kremer S, Parsek MR, Wozniak DJ (2004). Identification of *psl*, a locus encoding a potential exopolysaccharide that is essential for *Pseudomonas aeruginosa* PAO1 biofilm formation. *J Bacteriol* 186: 4466-4475.

160. Matsukawa M, Greenberg EP (2004). Putative exopolysaccharide synthesis genes influence *Pseudomonas aeruginosa* biofilm development. *J Bacteriol* 186: 4449-4456.

161. Caiazza NC, O'Toole GA (2004). SadB is required for the transition from reversible to irreversible attachment during biofilm formation by *Pseudomonas aeruginosa* PA14. *J Bacteriol* 186: 4476-4485.

162. Reimmann C, Beyeler M, Latifi A, Winteler H, Foglino M, Lazdunski A, Haas D (1997). The global activator GacA of *Pseudomonas aeruginosa* PAO positively controls the production of the autoinducer N-butyryl-homoserine lactone and the formation of the virulence factors pyocyanin, cyanide, and lipase. *Mol Microbiol* 24: 309-319.

163. Parkins MD, Ceri H, Storey DG (2001). *Pseudomonas aeruginosa* GacA, a factor in multihost virulence, is also essential for biofilm formation. *Mol Microbiol* 40: 1215-1226.

164. Brencic A, McFarland KA, McManus HR, Castang S, Mogno I, Dove SL, Lory S (2009). The GacS/GacA signal transduction system of *Pseudomonas aeruginosa* acts exclusively through its control over the transcription of the RsmY and RsmZ regulatory small RNAs. *Mol Microbiol* 73: 434-445.

165. Kay E, Humair B, Dénervaud V, Riedel K, Spahr S, Eberl L, Valverde C, Haas D (2006). Two GacA-dependent small RNAs modulate the quorum-sensing response in *Pseudomonas aeruginosa*. *J Bacteriol* 188: 6026-6033.

166. Heurlier K, Williams F, Heeb S, Dormond C, Pessi G, Singer D, Cámara M, Williams P, Haas D (2004). Positive control of swarming, rhamnolipid synthesis, and lipase production by the posttranscriptional RsmA/RsmZ system in *Pseudomonas aeruginosa* PAO1. *J Bacteriol* 186: 2936-2945.

167. Pessi G, Williams F, Hindle Z, Heurlier K, Holden MT, Cámara M, Haas D, Williams P (2001). The global posttranscriptional regulator RsmA modulates production of virulence determinants and N-acylhomoserine lactones in *Pseudomonas aeruginosa*. *J Bacteriol* 183: 6676-6683.

168. Brencic A, Lory S (2009). Determination of the regulon and identification of novel mRNA targets of *Pseudomonas aeruginosa* RsmA. *Mol Microbiol* 72: 612-632.

169. Burrowes E, Baysse C, Adams C, O'Gara F (2006). Influence of the regulatory protein RsmA on cellular functions in *Pseudomonas aeruginosa* PAO1, as revealed by transcriptome analysis. *Microbiology* 152: 405-418.

170. Goodman AL, Kulasekara B, Rietsch A, Boyd D, Smith RS, Lory S (2004). A signaling network reciprocally regulates genes associated with acute infection and chronic persistence in *Pseudomonas aeruginosa*. *Dev Cell* 7: 745-754.

171. Ventre I, Goodman AL, Vallet-Gely I, Vasseur P, Soscia C, Molin S, Bleves S, Lazdunski A, Lory S, Filloux A (2006). Multiple sensors control reciprocal expression of *Pseudomonas aeruginosa* regulatory RNA and virulence genes. *Proc Natl Acad Sci U S A* 103: 171-176.

172. Lee SJ, Gralla JD (2001). Sigma38 (rpoS) RNA polymerase promoter engagement via -10 region nucleotides. *J Biol Chem* 276: 30064-30071.

173. Chiang P, Burrows LL (2003). Biofilm formation by hyperpiliated mutants of *Pseudomonas aeruginosa*. *J Bacteriol* 185: 2374-2378.

174. Klausen M, Aaes-Jørgensen A, Molin S, Tolker-Nielsen T (2003). Involvement of bacterial migration in the development of complex multicellular structures in *Pseudomonas aeruginosa* biofilms. *Mol Microbiol* 50: 61-68.

175. Shrout JD, Chopp DL, Just CL, Hentzer M, Givskov M, Parsek MR (2006). The impact of quorum sensing and swarming motility on *Pseudomonas aeruginosa* biofilm formation is nutritionally conditional. *Mol Microbiol* 62: 1264-1277.

176. Simms SA, Subbaramaiah K (1991). The kinetic mechanism of S-adenosyl-L-methionine: glutamylmethyltransferase from *Salmonella typhimurium*. *J Biol Chem* 266: 12741-12746.

177. Perez E, Stock AM (2007). Characterization of the *Thermotoga maritima* chemotaxis methylation system that lacks pentapeptide-dependent methyltransferase CheR:MCP tethering. *Mol Microbiol* 63: 363-378.

178. Djordjevic S, Stock AM (1998). Chemotaxis receptor recognition by protein methyltransferase CheR. *Nat Struct Biol* 5: 446-450.

179. Shiomi D, Zhulin IB, Homma M, Kawagishi I (2002). Dual recognition of the bacterial chemoreceptor by chemotaxis-specific domains of the CheR methyltransferase. *J Biol Chem* 277: 42325-42333.

180. Pamp SJ, Tolker-Nielsen T (2007). Multiple roles of biosurfactants in structural biofilm development by *Pseudomonas aeruginosa*. *J Bacteriol* 189: 2531-2539.

181. Tolker-Nielsen T, Brinch UC, Ragas PC, Andersen JB, Jacobsen CS, Molin S (2000). Development and dynamics of *Pseudomonas* sp. biofilms. *J Bacteriol* 182: 6482-6489.

182. Rix U, Superti-Furga G (2009). Target profiling of small molecules by chemical proteomics. *Nat Chem Biol* 5: 616-624.

183. Bertinetti D, Schweinsberg S, Hanke SE, Schwede F, Bertinetti O, Drewianka S, Genieser H, Herberg FW (2009). Chemical tools selectively target components of the PKA system. *BMC Chem Biol* 9: 3.

184. Scholten A, Poh MK, van Veen TAB, van Breukelen B, Vos MA, Heck AJR (2006). Analysis of the cGMP/cAMP interactome using a chemical proteomics approach in mammalian heart tissue validates sphingosine kinase type 1-interacting protein as a genuine and highly abundant AKAP. *J Proteome Res* 5: 1435-1447.

185. Benach J, Swaminathan SS, Tamayo R, Handelman SK, Folta-Stogniew E, Ramos JE, Forouhar F, Neely H, Seetharaman J, Camilli A, Hunt JF (2007). The structural basis of cyclic diguanylate signal transduction by PilZ domains. *EMBO J* 26: 5153-5166.

186. Ko J, Ryu K, Kim H, Shin J, Lee J, Cheong C, Choi B (2010). Structure of PP4397 reveals the molecular basis for different c-di-GMP binding modes by Pilz domain proteins. *J Mol Biol* 398: 97-110.

187. Wassmann P, Chan C, Paul R, Beck A, Heerklotz H, Jenal U, Schirmer T (2007). Structure of BeF3- -modified response regulator PleD: implications for diguanylate cyclase activation, catalysis, and feedback inhibition. *Structure* 15: 915-927.

188. Trinkle-Mulcahy L, Boulon S, Lam YW, Urcia R, Boisvert F, Vandermoere F, Morrice NA, Swift S, Rothbauer U, Leonhardt H, Lamond A (2008). Identifying specific protein interaction partners using quantitative mass spectrometry and bead proteomes. *J Cell Biol* 183: 223-239.

189. Dasgupta N, Wolfgang MC, Goodman AL, Arora SK, Jyot J, Lory S, Ramphal R (2003). A four-tiered transcriptional regulatory circuit controls flagellar biogenesis in *Pseudomonas aeruginosa*. *Mol Microbiol* 50: 809-824.

190. Hahn HP (1997). The type-4 pilus is the major virulence-associated adhesin of *Pseudomonas aeruginosa*--a review. *Gene* 192: 99-108.

191. Feldman M, Bryan R, Rajan S, Scheffler L, Brunnert S, Tang H, Prince A (1998). Role of flagella in pathogenesis of *Pseudomonas aeruginosa* pulmonary infection. *Infect Immun* 66: 43-51.

192. Zolfaghar I, Evans DJ, Fleiszig SMJ (2003). Twitching motility contributes to the role of pili in corneal infection caused by *Pseudomonas aeruginosa*. *Infect Immun* 71: 5389-5393.

193. Kang PJ, Hauser AR, Apodaca G, Fleiszig SM, Wiener-Kronish J, Mostov K, Engel JN (1997). Identification of *Pseudomonas aeruginosa* genes required for epithelial cell injury. *Mol Microbiol* 24: 1249-1262.

194. Cochran WL, Suh SJ, McFeters GA, Stewart PS (2000). Role of RpoS and AlgT in *Pseudomonas aeruginosa* biofilm resistance to hydrogen peroxide and monochloramine. *J Appl Microbiol* 88: 546-553.

195. Jørgensen F, Bally M, Chapon-Herve V, Michel G, Lazdunski A, Williams P, Stewart GS (1999). RpoS-dependent stress tolerance in *Pseudomonas aeruginosa*. *Microbiology* 145 (Pt 4): 835-844.

196. Manganelli R, Voskuil MI, Schoolnik GK, Smith I (2001). The *Mycobacterium tuberculosis* ECF sigma factor sigmaE: role in global gene expression and survival in macrophages. *Mol Microbiol* 41: 423-437.

197. Cao M, Salzberg L, Tsai CS, Mascher T, Bonilla C, Wang T, Ye RW, Márquez-Magaña L, Helmann JD (2003). Regulation of the *Bacillus subtilis* extracytoplasmic function protein sigma(Y) and its target promoters. *J Bacteriol* 185: 4883-4890.

198. Larisch C, Nakunst D, Hüser AT, Tauch A, Kalinowski J (2007). The alternative sigma factor SigB of *Corynebacterium glutamicum* modulates global gene expression during transition from exponential growth to stationary phase. *BMC Genomics* 8: 4.

199. Raengpradub S, Wiedmann M, Boor KJ (2008). Comparative analysis of the sigma B-dependent stress responses in *Listeria monocytogenes* and *Listeria innocua* strains exposed to selected stress conditions. *Appl Environ Microbiol* 74: 158-171.

200. Leang C, Krushkal J, Ueki T, Puljic M, Sun J, Juárez K, Núñez C, Reguera G, DiDonato R, Postier B, Adkins RM, Lovley DR (2009). Genome-wide analysis of the RpoN regulon in *Geobacter sulfurreducens*. *BMC Genomics* 10: 331.

201. Dong T, Schellhorn HE (2009). Global effect of RpoS on gene expression in pathogenic *Escherichia coli* O157:H7 strain EDL933. *BMC Genomics* 10: 349.

202. Wade JT, Struhl K, Busby SJW, Grainger DC (2007). Genomic analysis of protein-DNA interactions in bacteria: insights into transcription and chromosome organization. *Mol Microbiol* 65: 21-26.

203. Sala C, Grainger DC, Cole ST (2009). Dissecting regulatory networks in host-pathogen interaction using chIP-on-chip technology. *Cell Host Microbe* 5: 430-437.

204. Wade JT, Struhl K (2004). Association of RNA polymerase with transcribed regions in *Escherichia coli*. *Proc Natl Acad Sci U S A* 101: 17777-17782.

205. Wade JT, Roa DC, Grainger DC, Hurd D, Busby SJW, Struhl K, Nudler E (2006). Extensive functional overlap between sigma factors in *Escherichia coli*. *Nat Struct Mol Biol* 13: 806-814.

206. Rodrigue S, Brodeur J, Jacques P, Gervais AL, Brzezinski R, Gaudreau L (2007). Identification of mycobacterial sigma factor binding sites by chromatin immunoprecipitation assays. *J Bacteriol* 189: 1505-1513.

207. Rhodius VA, Wade JT (2009). Technical considerations in using DNA microarrays to define regulons. *Methods* 47: 63-72.

208. Gooderham WJ, Hancock REW (2009). Regulation of virulence and antibiotic resistance by two-component regulatory systems in *Pseudomonas aeruginosa*. *FEMS Microbiol Rev* 33: 279-294.

209. Goodman AL, Merighi M, Hyodo M, Ventre I, Filloux A, Lory S (2009). Direct interaction between sensor kinase proteins mediates acute and chronic disease phenotypes in a bacterial pathogen. *Genes Dev* 23: 249-259.

210. An S, Wu J, Zhang L (2010). Modulation of *Pseudomonas aeruginosa* biofilm dispersal by a cyclic-Di-GMP phosphodiesterase with a putative hypoxia-sensing domain. *Appl Environ Microbiol* 76: 8160-8173.

211. Zhulin IB, Nikolskaya AN, Galperin MY (2003). Common extracellular sensory domains in transmembrane receptors for diverse signal transduction pathways in bacteria and archaea. *J Bacteriol* 185: 285-294.

212. Ryan RP, Fouhy Y, Lucey JF, Dow JM (2006). Cyclic di-GMP signaling in bacteria: recent advances and new puzzles. *J Bacteriol* 188: 8327-8334.

213. Anantharaman V, Aravind L (2003). Application of comparative genomics in the identification and analysis of novel families of membrane-associated receptors in bacteria. *BMC Genomics* 4: 34.

214. Galperin MY, Gaidenko TA, Mulkidjanian AY, Nakano M, Price CW (2001). MHYT, a new integral membrane sensor domain. *FEMS Microbiol Lett* 205: 17-23.

215. Hay ID, Remminghorst U, Rehm BHA (2009). MucR, a novel membrane-associated regulator of alginate biosynthesis in *Pseudomonas aeruginosa*. *Appl Environ Microbiol* 75: 1110-1120.

216. Klebensberger J, Birkenmaier A, Geffers R, Kjelleberg S, Philipp B (2009). SiaA and SiaD are essential for inducing autoaggregation as a specific response to detergent stress in *Pseudomonas aeruginosa*. *Environ Microbiol* 11: 3073-3086.

217. Merritt JH, Ha D, Cowles KN, Lu W, Morales DK, Rabinowitz J, Gitai Z, O'Toole GA (2010). Specific control of *Pseudomonas aeruginosa* surface-associated behaviors by two c-di-GMP diguanylate cyclases. *MBio* 1: e00183-10.

218. Ueda A, Wood TK (2009). Connecting quorum sensing, c-di-GMP, pel polysaccharide, and biofilm formation in *Pseudomonas aeruginosa* through tyrosine phosphatase TpbA (PA3885). *PLoS Pathog* 5: e1000483.

219. Malone JG, Jaeger T, Spangler C, Ritz D, Spang A, Arrieumerlou C, Kaever V, Landmann R, Jenal U (2010). YfiBNR mediates cyclic di-GMP dependent small colony variant formation and persistence in *Pseudomonas aeruginosa*. *PLoS Pathog* 6: e1000804.

220. Güvener ZT, Harwood CS (2007). Subcellular location characteristics of the *Pseudomonas aeruginosa* GGDEF protein, WspR, indicate that it produces cyclic-di-GMP in response to growth on surfaces. *Mol Microbiol* 66: 1459-1473.

221. Merritt JH, Brothers KM, Kuchma SL, O'Toole GA (2007). SadC reciprocally influences biofilm formation and swarming motility via modulation of exopolysaccharide production and flagellar function. *J Bacteriol* 189: 8154-8164.

222. Haddad A, Jensen V, Becker T, Häussler S (2009). The Pho regulon influences biofilm formation and type three secretion in *Pseudomonas aeruginosa*. *Environ Microbiol Rep* 1: 488-494.

223. Kuchma SL, Brothers KM, Merritt JH, Liberati NT, Ausubel FM, O'Toole GA (2007). BifA, a cyclic-Di-GMP phosphodiesterase, inversely regulates biofilm formation and swarming motility by *Pseudomonas aeruginosa* PA14. *J Bacteriol* 189: 8165-8178.

224. Choy W, Zhou L, Syn CK, Zhang L, Swarup S (2004). MorA defines a new class of regulators affecting flagellar development and biofilm formation in diverse Pseudomonas species. *J Bacteriol* 186: 7221-7228.

225. Kazmierczak BI, Lebron MB, Murray TS (2006). Analysis of FimX, a phosphodiesterase that governs twitching motility in *Pseudomonas aeruginosa*. *Mol Microbiol* 60: 1026-1043.

226. Hoffman LR, D'Argenio DA, MacCoss MJ, Zhang Z, Jones RA, Miller SI (2005). Aminoglycoside antibiotics induce bacterial biofilm formation. *Nature* 436: 1171-1175.

227. Kulasekara HD, Ventre I, Kulasekara BR, Lazdunski A, Filloux A, Lory S (2005). A novel two-component system controls the expression of *Pseudomonas aeruginosa* fimbrial cup genes. *Mol Microbiol* 55: 368-380.

7 Acknowledgment

First of all, I would like to thank my supervisor Prof. Susanne Häußler for the exciting project, for fruitful discussions and for her optimism and patience.

I would like to thank Prof. Jürgen Wehland for the warm welcome in the Devision of Cell Biology, Prof. Kathrin Riedel for being my second supervisor and Prof. Dietmar Schomburg for being member of the examination committee.

My special thanks go to past and present members of the "Pseudomonas" group: Agata, Ahmed, Andrea, Andreas, Andrée, Ariane, Bianka, Caroline, Carsten, Christian, Claudia, Denitsa, Fior, Gesa, Janine, Jörg, Katha, Kathi, Klaus, Lena, Mathias, Piotr, Sebastian B., Sebastian S., Stefan, Tanja, Vanessa, Vera and Yusuf – thank you so much for your help and constant support. It is fun working with you! I also appreciate the time we are spending together outside the lab – be it at badminton, poker, birthdays or other occasions. I am happy to have found good friends. I also thank Janine O. for the final proof-reading of my thesis.

I thank all "Zibbies" for the nice working atmosphere and for discussions concerning science but also daily life. I especially would like to thank Marco for always listening, for cheering me up and providing me with the best drop ever – Dank je wel! Furthermore, I want to thank Sabine and Andreas J. for the nice atmosphere in our office.

I thank the various members of my thesis committees, especially Dr. Lothar Jänsch, Prof. Wolf-Dieter Schubert and Prof. Christiane Ritter, for their interest in my project and for inspiring discussions.

I am very grateful for the exceedingly good co-operation with Dr. Frank Schwede/Biolog Life Science Institute and the group of Prof. Herberg/University of Kassel. I especially would like to thank Dr. Daniela Bertinetti and Stefan Möller for numerous telephone conversations, many good ideas and all the encouraging words.
I would also like to thank Dr. Lothar Jänsch and Dr. Josef Wissing for excellent support concerning mass spectrometry, and Zofia Magnowska for the preparation of *Pseudomonas* membranes.

Ein besonderer Dank gilt meinen Eltern und meiner Schwester - dafür, dass sie immer für mich da sind, mir zuhören und mich unterstützen. Ich freue mich immer euch zu sehen!

Zuletzt möchte ich mich aus tiefsten Herzen bei meinem Freund Marc bedanken – für sein außerordentliches Verständnis, seine Geduld und seine uneingeschränkte Unterstützung. Du bist mein Antrieb und Schwung!

8 Lebenslauf

Persönliche Daten

Name	Juliane Schmidt
Geburtsdatum	26.05.1983
Geburtsort	Zeitz
Staatsangehörigkeit	Deutsch

Ausbildung

09/2007 – 04/2011	Doktorarbeit in der Arbeitsgruppe „Chronische *Pseudomonas* Infektionen“ von Prof. Dr. Susanne Häußler am Helmholtz-Zentrum für Infektionsforschung in Braunschweig
11/2006 – 06/2007	Auslandsaufenthalt: Anfertigung der Masterarbeit am Department of Molecular Biosciences, University of Oslo, Norway Thema der Masterarbeit: “Analysis of the GxxxG Motifs in the Two-Peptide Bacteriocin Lactococcin G by Site-Directed Mutagenesis” Abschluss: Master of Science
10/2005 – 06/2007	Masterstudium der Molecular Sciences an der Friedrich-Alexander-Universität Erlangen-Nürnberg Vertiefungsrichtung: Life Science
10/2002 – 09/2005	Bachelorstudium der Molecular Sciences an der Friedrich-Alexander-Universität Erlangen-Nürnberg Vertiefungsrichtung: Life Science Thema der Bachelorarbeit: „Eignung des Büchi B-585 Ofensystems zur Durchführung von Gefriertrocknungsversuchen“ Abschluss: Bachelor of Science
08/1993-06/2002	Otto-Baensch Gymnasium Zeitz Abschluss: Abitur

Veröffentlichungen

Juliane Schmidt, Mathias Müsken, Tanja Becker, Zofia Magnowska, Daniela Bertinetti, Stefan Möller, Bastian Zimmermann, Friedrich W. Herberg, Lothar Jänsch, Susanne Häussler (2011). The *Pseudomonas aeruginosa* chemotaxis methyltransferase CheR1 impacts on bacterial surface sampling. *PloS ONE 6(3):e18184*.

Camilla Oppegård, **Juliane Schmidt,** Per Eugen Kristiansen, Jon Nissen-Meyer (2008). Mutational analysis of putative helix−helix interacting GxxxG-motifs and tryptophan residues in the two-peptide bacteriocin Lactococcin G. *Biochemistry 47(18):5242-9.*

Tagungsbeiträge

Juliane Schmidt, Daniela Bertinetti, Tanja Becker, Michael Morr, Frank Schwede, Josef Wissing, Zofia Magnowska, Lothar Jänsch, Susanne Häussler. Signal transduction of c-di-GMP in *Pseudomonas aeruginosa*. *Vortrag*. Dritte gemeinsame Tagung der Deutschen Gesellschaft für Hygiene und Mikrobiologie und der Vereinigung für Allgemeine und Angewandte Mikrobiologie, Hannover, 2010.

Juliane Schmidt, Daniela Bertinetti, Michael Morr, Frank Schwede, Josef Wissing, Lothar Jänsch, Susanne Häussler. Isolation and identification of c-di-GMP binding proteins in *Pseudomonas aeruginosa*. *Poster*. 61. Jahrestagung der Deutschen Gesellschaft für Hygiene und Mikrobiologie, Göttingen, 2009.

Juliane Schmidt, Daniela Bertinetti, Michael Morr, Frank Schwede, Josef Wissing, Lothar Jänsch, Susanne Häussler. Isolation and identification of c-di-GMP binding proteins in *Pseudomonas aeruginosa*. *Vortrag*. First European Congress on Microbial Biofilms, Rom, 2009.

Juliane Schmidt, Daniela Bertinetti, Michael Morr, Frank Schwede, Josef Wissing, Lothar Jänsch, Susanne Häussler. Isolation and identification of c-di-GMP binding proteins in *Pseudomonas aeruginosa*. *Poster*. XII. International Conference on *Pseudomonas*, Hannover, 2009.

Juliane Schmidt, Daniela Moll, Michael Morr, Frank Schwede, Josef Wissing, Lothar Jänsch, Susanne Häussler. Isolation and identification of c-di-GMP binding proteins in *Pseudomonas aeruginosa*. *Poster*. 60. Jahrestagung der Deutschen Gesellschaft für Hygiene und Mikrobiologie, Dresden, 2008.